

Hydrogeochemistry of a Petroleum Hydrocarbon Plume in a Sand and Gravel Aquifer

Barnstable, Massachusetts

**Mark Edwin Nelson
Sc.B., Brown University, 1984**

**A thesis submitted to the faculty of the
Oregon Graduate Institute of Science & Technology
in partial fulfillment of the requirements for the degree
Master of Science
in
Environmental Science and Engineering**

January, 1993

The thesis "Hydrogeochemistry of a Petroleum Hydrocarbon Plume in a Sand and Gravel Aquifer - Barnstable, Massachusetts" by Mark E. Nelson has been examined and approved by the following Examination Committee:

Carl D. Palmer, Assistant Professor
Thesis Advisor

William Fish
Associate Professor

Richard L. Johnson
Associate Professor

Acknowledgements

Without the assistance, advice and encouragement of a number of people, this thesis would not have been possible. I would like to thank my advisor Carl Palmer, first for his patience, and also for his constant assistance over the years, often at short notice. I would also like to thank Bill Fish for the use of his laboratory, and Rick Johnson for his advice and suggestions throughout my research and writing. A multitude of fellow students also helped me, especially Mike, Leah, Jay, Karel, John, Paul, Jim, and Patty. Also many thanks to Tom Cambareri and Ed Eichnor of the Cape Cod Commission for the opportunity to use the Fire Training Academy as a research site, and to Jon Witten, Scott Horsley, Steve Roy and Mike Frimpter for their willingness to give me the free time I needed to complete the writing of the document. And thank you to Eric Vierra for the excellent graphics found throughout the thesis. Finally, thank you to my best friend Kristie, and to my family for putting up with me throughout my "1-year program"!

TABLE OF CONTENTS

Acknowledgements	iii
List of Figures	vii
List of Tables	ix
Abstract	x
Introduction	1
Research Objectives	5
Site Description	5
Hydrogeology	9
Geology	9
Regional Setting	9
Site Specific Geology	10
Hydrology	13
Climate	13
Regional Hydrologic Setting	13
Site Hydrology	14
Use of Production Wells	15
Water Table Mapping	15
Water Table Fluctuations	22
Variations in Groundwater Flow Directions	22
Groundwater Flow Rates	25
Determination of Aquifer Hydraulic Properties	25
Methods	25
Production Well Pump Tests	25
Monitoring Well Pump Tests	25
Monitoring Well Slug Tests	26
Results	26
Production Well Pump Tests	26
Monitoring Well Pump Tests	29
Monitoring Well Slug Tests	29
Production Well Zones of Contribution	30

Hydrocarbon Contamination in the Unsaturated Zone	34
Methods of Sampling and Analysis	34
Results	36
Estimate of Hydrocarbon Source Strength	36
Hydrocarbon Contamination in the Saturated Zone	41
Methods of Sampling and Analysis	41
Results of TPH Analysis	42
Results of VOC Analysis	44
Theory on Plume Development at the Barnstable Site	54
Geochemistry	59
Introduction	59
Methods	59
Solid Phase Analysis	59
Mineralogy	59
Total Organic Carbon Analysis	60
Extractable Iron, Manganese, and Aluminum Analyses	60
Groundwater Sampling	60
Groundwater Analysis	62
Results	62
Solid Phase Chemistry	62
Groundwater Chemistry	63
Dissolved Oxygen	65
pH, Eh, and Temperature	71
Alkalinity	71
Calcium, Potassium, Magnesium, Sodium and Chloride	73
Iron, Manganese and Sulfate	73
Nitrate and Ammonia	76
Aluminum and Silica	76
Discussion	76
Reduction Processes Within Plume	76
Impacts of Iron and Manganese Dissolution	78
Aluminosilicate Weathering	82
Allophane as Controlling Secondary Mineral	89
Comparison to Northwest Florida Aquifer	92

Mass Balance Modeling	92
Development of Feasible Weathering Reactions	94
Unsaturated Zone Reactions	97
Plume Reactions	100
Aluminosilicate Weathering Rates	103
Conclusions	104
References	106
Appendix A: Hydrocarbon Plume Development in Unconfined Aquifers Receiving Constant or Periodic Recharge	112
Plume Development With Constant Recharge	113
Variable Recharge Effects at Plume Source	122
Variable Recharge Effects Downgradient of Plume Source	125
Summary	127
Appendix B: X-Ray Diffraction Pattern for Sediment Sample B-25	128
Biographical Sketch	129

List of Figures

Figure 1:	Locus Map	6
Figure 2:	Site Plan	7
Figure 3:	Monitoring Well Locations	11
Figure 4:	Hydrogeologic Cross Section	12
Figure 5:	Water Withdrawal from Production Wells MD-3 and MD-4, 1987-1988	16
Figure 6:	Water-Table Map, 30 October 1990	17
Figure 7:	Water-Table Map, 16 March 1990	18
Figure 8:	Water-Table Map, 23 August 1989	19
Figure 9:	Water-Table Map, 28 October 1989	20
Figure 10:	Comparison of Regional and Site Specific Water Table Fluctuations	23
Figure 11:	Potential Range of Groundwater Fluctuations From Measurement Errors	24
Figure 12:	Zones of Contribution for Production Wells MD-3 and MD-4 Pumping Separately	32
Figure 13:	Zones of Contribution for Production Wells MD-3 and MD-4 Pumping Together	33
Figure 14:	On-Site Monitoring Well and Soil Boring Locations	35
Figure 15:	Total Petroleum Hydrocarbons in the Unsaturated Zone, September 1989	37
Figure 16:	Total Petroleum Hydrocarbons in the Unsaturated Zone - Cross Section, September 1989	38
Figure 17:	Total Petroleum Hydrocarbons in Groundwater, July 1989	43
Figure 18:	Volatile Organic Compounds in Groundwater, July 1989	46
Figure 19:	Volatile Organic Compounds in Groundwater, Fall 1989	47
Figure 20:	Volatile Organic Compounds in Groundwater -Cross Section, July 1989, and Fall 1989	49

Figure 21:	Composition of Volatile Organics in Hydrocarbon Plume	51
Figure 22:	Comparison of Volatile Organic Concentrations to Water Level Fluctuations	55
Figure 23:	Dissolved Oxygen In Groundwater, July 1989	68
Figure 24:	Dissolved Oxygen In Groundwater, September 1990	69
Figure 25:	Dissolved Oxygen In Groundwater - Cross Section, July 1989 and September 1990	70
Figure 26:	pH, Eh, Temperature and Alkalinity Longitudinally Through Plume	72
Figure 27:	Calcium, Potassium, Magnesium and Sodium Concentrations Longitudinally Through Plume	74
Figure 28:	Iron, Manganese, Sulfate and Chloride Concentrations Longitudinally Through Plume	75
Figure 29:	Nitrate, Ammonia, Aluminum and Silica Concentrations Longitudinally Through Plume	77
Figure 30:	Saturation Indices of Iron and Manganese Minerals Longitudinally Through Plume	80
Figure 31:	Saturation Indices of Silica Minerals and Albite Weathering Products Longitudinally Through Plume	83
Figure 32:	Saturation Indices of Anorthite and Muscovite Weathering Products Longitudinally Through Plume	85
Figure 33:	Stability Relationships for Sodium, Calcium and Potassium Minerals With Water Quality Data From Barnstable Site	86
Figure 34:	Stability Relationships for Potassium Minerals Showing Data From Northwest Florida Alluvial Aquifer	93
Figure A-1:	Three dimensional Groundwater Flow in an Unconfined Aquifer Receiving Constant Recharge	114
Figure A-2:	Comparison Of Plume Development With Varying Source Locations	117
Figure A-3:	Well Placement Relative to Plume Location - Plume A	118
Figure A-4:	Well Placement Relative to Plume Location - Plume B	119
Figure A-5:	Well Placement Relative to Plume Location - Plume C	120
Figure A-6:	Changes In Measured Concentrations with Varied Screen Length, Plume B	121

Figure A-7:	Fluctuations in Plume Thickness and Measured Concentration at Source, Unconfined Aquifer with Periodic Changes in Recharge Rate	123
Figure A-8:	Development of Plume B at High and Low Recharge Rates	126

List of Tables

Table 1	Summary of Aquifer Properties	27
Table 2:	Input Values for Production Well Zone of Contribution Modeling	30
Table 3:	Estimate of TPH Mass In Unsaturated Zone Sediments	40
Table 4:	Estimate of TPH Mass in Groundwater	45
Table 5:	Retardation Coefficients for BTEX Compounds	50
Table 6:	Estimate of VOC's in Groundwater (1989 and 1990)	52
Table 7:	Results of Extractable Iron, Manganese and Aluminum Analyses	64
Table 8:	Results of Inorganic Analyses	66
Table 9:	Comparison of Calculated and Measured $[H_4SiO_4]$	91
Table 10:	Reactions Used in BALANCE Modeling	95
Table 11:	Mass Balance Reactions Within Residually Contaminated Unsaturated Zone	98
Table 12:	Mass Balance Reactions Within Plume	101

ABSTRACT

Mineral weathering caused by a hydrocarbon plume in an unconfined, sandy, silicate aquifer was examined at a site in Barnstable, Massachusetts. The site was used for over thirty years as a fire training academy, where #2 heating oil was ignited in shallow concrete pits and extinguished by firefighting personnel. Leaks from the pits, and from an underground storage tank and leach pit used to collect waste oil formed a zone of contamination in the unsaturated zone. A dissolved hydrocarbon plume extends downgradient from the site, and flows toward two production wells used by the town of Barnstable. Dissolved oxygen concentrations in groundwater decrease below detectable levels within the plume, and concentrations of iron and manganese are elevated because of the reducing conditions caused by the degradation of the hydrocarbons. Concentrations of major cations are also elevated in the plume, although silica concentrations are constant inside, and outside, the plume.

Weathering of silicate minerals is accelerated in the plume relative to background areas. The inorganic chemistry of the groundwater indicates that a secondary mineral other than kaolinite is being formed which controls the amount of dissolved silica within the plume. Thermodynamic data suggests that allophane could be the secondary mineral. This theory is supported by literature descriptions at similar sites. Further analyses of the aquifer sediments are needed to confirm its presence. A mass balance model using albite, anorthite, muscovite, gibbsite, chlorite and allophane, along with CO₂ exchange, naphthalene and benzoic acid degradation provides a reasonable representation of the mineral/water interactions in the unsaturated zone that are responsible for producing the observed groundwater chemistry near the source of the plume. The same model indicates that 50-90% less weathering occurs within a stream tube moving downgradient from the plume source. In the plume analysis, sodium/magnesium exchange added to the model to balance the observed silicate chemistry and O₂ exchange is substituted for naphthalene degradation to better simulate the expected groundwater reactions.

Weathering rates for anorthite (2.5×10^{-19} M/cm²/s) and potassium feldspar (2.8×10^{-19} M/cm²/s) were calculated based on the observed ground water chemistry within the plume, and compare well with reported field and laboratory measurements.

The development and movement of the hydrocarbon plume is controlled by the location of the source relative to recharge and discharge areas of the aquifer, and by the amount of precipitation recharging the aquifer. Varying recharge rates also cause changes in contaminant concentrations measured in samples from monitoring wells by changing the location of the plume. At the plume source, contaminant concentrations are found to correlate well with water-level fluctuations. Interpretations of monitoring well sample data must consider the location of the source in the aquifer, and recharge induced water-level fluctuations.

In summary, properly defined mass balance calculations, including the precipitation of allophane, provide a reasonable simulation of major hydrogeochemical changes in this oil-contaminated aquifer. The results can be misinterpreted, however, if recharge and water-level fluctuations are not explicitly considered.

INTRODUCTION

Petroleum hydrocarbon releases to the subsurface environment are an ongoing threat to groundwater quality. Sources of hydrocarbons include all types of automotive fuels, aviation fuels, fuel oils, lubricants, and crude oil. Releases can occur from accidental spills, above ground and underground storage tank leaks, landfills, surface impoundments, pipeline leaks and illegal dumping. In New Jersey, 85 percent of hazardous waste sites are contaminated with hydrocarbons, and 50 percent of public supply wells experiencing water quality problems are threatened or affected by hydrocarbons (Pye et al, 1983).

Releases from underground storage tanks (USTs) may account for the highest number of reported cases of groundwater contamination by hydrocarbons. The US Environmental Protection Agency (EPA) estimates that between 2.4 and 4.8 million USTs are in use throughout the United States (EPA, 1987). Of the known tanks, it is estimated that hundreds of thousands are leaking (EPA, 1987). In California, 13,270 UST leaks had been reported as of January 1990 (Daugherty, 1991). These estimates of the number of leaking tanks may be low, as it is likely that many spills are not yet detected or reported.

It does not take a large hydrocarbon spill to contaminate groundwater above drinking water standards. For example, benzene, a known human carcinogen (Pye et al 1983), has a maximum contaminant level for drinking water of 5 µg/l set by the EPA. An evaluation of 6 typical gasoline products showed benzene concentrations of 9.6-28.7 g/L (Potter, 1991). Therefore, one liter of gasoline can contaminate 2-6 billion gallons of groundwater if dissolved and mixed completely. For several of the largest dissolved plumes in the United States, the estimated volume of dissolved contaminant is 208 liters (55 gal) or less (Mackay and Cherry, 1989).

Not only are the threats from hydrocarbon releases serious, the costs of remediation can be high. It is estimated UST remediation costs could be as high as \$48 billion over the next 30 years (Ludvigsen *et al*, 1991). In Truro, Massachusetts, A UST leak at a neighborhood service station released approximately 8,000 L of gasoline into groundwater

near a public supply well. After 15 years, the spill is still being cleaned up, and the cost has reached \$7 million (Comm. of Massachusetts, 1986).

Because of the threats involved and the costs of remediation, numerous field and laboratory investigations have been conducted in an attempt to accurately understand the processes controlling hydrocarbon migration in unconsolidated subsurface sediments. Research initially focused on hydrocarbon transport and attenuation in the saturated zone, while, more recently the complicated three phase interactions involved with hydrocarbon migration in the unsaturated zone have received more attention. In both cases, however, the direction of the research was to understand the processes affecting the movement of the hydrocarbons in order to design more efficient remediation systems.

The effects of hydrocarbon biodegradation on the surrounding sediments and general groundwater quality are not usually investigated to the same level of detail as the hydrocarbon transport processes. However, the reactions involved with the degradation of the hydrocarbons affect the overall geochemistry of the groundwater. They include a complex series of interactions among groundwater, the aquifer sediments and the hydrocarbons.

Laboratory experiments have shown that weathering of aluminosilicate sediments found at many contamination sites is accelerated by the presence of organic acids. In Bemidjii, Minnesota, quartz weathering was accelerated by the presence of a crude oil plume (Bennett, 1987, Bennett and Siegel, 1987). Laboratory experiments showed that organic acids formed by the degradation of the petroleum compounds caused the accelerated weathering. Organic acid degradation products have also been used to explain weathering reactions at a creosote spill site in Pensacola, Florida (Cozzarelli *et al*, 1987).

An extensive body of literature describes the weathering reactions in unconsolidated, typically aluminosilicate, aquifer systems (Kenoyer and Bowser, 1992a, 1992b; Katz and Choquette, 1991; Paces, 1973; Freeze and Cherry, 1979; Hem, 1989; Drever, 1982). While the complex processes involved in natural weathering are generally understood, the types of weathering reactions, and extent of weathering caused by hydrocarbon degradation have not been extensively investigated. If hydrocarbon degradation causes accelerated weathering of the surrounding aquifer sediments, the

potential exists for the buildup of secondary minerals that could affect the movement and remediation of hydrocarbon plumes. The precipitation of secondary minerals could clog pore spaces in the aquifer, slowing the rate of groundwater flow and hydrocarbon transport. If secondary minerals precipitate as particles small enough to migrate through the pore spaces, but become coated with hydrocarbons or organic acids, they may facilitate increased adsorption of other hydrocarbon compounds, and increase their transport through the aquifer. The particles could also clog well screens used to pump contaminants out of the aquifer. Again, the extent of these processes is a function of the rate of weathering.

In addition to the potential acceleration of aluminosilicate weathering, the biodegradation of hydrocarbons will cause the reductive dissolution of iron and manganese available in the aquifer sediments, causing elevated metals concentrations in groundwater (Siegel, 1987, Cozzarelli, *et al*, 1987). The reduced iron and manganese can cause problems with groundwater remediation by precipitating out of solution on recovery well screens, in air stripping towers, or in other portions of a treatment system where the contaminated water becomes oxygenated.

Once dissolved into the plume, the metals will travel within the plume until they meet oxygenated waters and precipitate out of solution. The dissolved metals could potentially migrate farther than the hydrocarbons, which will be attenuated both by adsorption to the aquifer sediments and by biodegradation. The hydrocarbon degradation will form a dissolved oxygen "hole" in the aquifer, which will move in the direction of groundwater flow. The iron will remain dissolved in the flow tube of deoxygenated water which will flow downgradient further than the hydrocarbons.

While metal precipitation onto pumping wells often used in remedial systems has been investigated (Applin and Zhao, 1989), the effects of iron and manganese transport within the aquifer are not usually addressed. If a pumping well intercepts this water, the iron will precipitate over time, causing an incrustation of the well screen. Aesthetic and water quality issues also arise if the well is used for drinking water purposes. While a hydrocarbon plume may not reach a drinking water well, the metals introduced into solution by the plume may travel farther, and cause water quality problems on their own.

There is a finite amount of solid phase iron and manganese that can dissolve into a contaminant plume. If a plume consistently moves through only one section of an aquifer it will eventually strip the available iron from the aquifer minerals. However, if the plume movement is not constant, it will migrate through varying sections of the aquifer, increasing the supply of iron and manganese available for dissolution. Knowledge of the movement of the plume, and the total areas of the aquifer it affects, is needed to predict the extent of metals dissolution.

Field studies of hydrocarbon releases have also shown that compounds remaining in the unsaturated zone often comprise the largest component of a hydrocarbon spill. This is especially true for the heavier fuel oils. At an aviation fuel spill in Traverse City, Michigan, the greatest mass of contaminants remains in the sediments above the water table (Ostendorf and Kambell, 1991). Fuel oil in the unsaturated zone accounts for the largest hydrocarbon mass resulting from a pipeline leak in Bemidji, Minnesota (Hult, 1987). The residual hydrocarbons in the unsaturated zone can remain as a continuing source of groundwater contamination, and can control the size and strength of the dissolved plume.

In the saturated zone, inputs of precipitation recharge can affect plume strength and migration. Contaminant plumes have been shown to plunge below the water table as a result of the input of overlying recharge water (LeBlanc, 1984). Recharge water also provides a pathway to bring more contamination into groundwater from the overlying unsaturated zone source. Fluctuations of the water table caused by the recharge inputs can affect contaminant concentrations in groundwater by exposing more of the unsaturated zone source to the groundwater system.

These hydrologic processes are not always considered as part of monitoring well design. When petroleum product releases are investigated, wells are often constructed with screens placed at the water table, and no thought is given to how the plume may plunge into the aquifer. Screens also are usually long relative to the thickness of the plume, allowing for mixing of clean and contaminated water. Unless these considerations are included in monitoring well design and sample interpretation, misleading decisions can be made in health risk assessments and remedial actions.

Research Objectives

The goal of this research was to investigate the processes controlling mineral weathering within a petroleum hydrocarbon plume in an unconfined sandy aquifer. A study site in Barnstable, Massachusetts was used to conduct field investigations into groundwater chemistry and groundwater/sediment interactions in order to examine the weathering processes. As part of the investigation, the hydrologic processes controlling plume development and migration are examined, and their impacts on interpretation of water quality sampling data are evaluated.

Site Description

The Barnstable County Fire Training Academy is located on Flint Rock Road in Barnstable Massachusetts between Barnstable Village and Hyannis (See Locus Map Figure 1). Activities at the site have included the controlled burning of No. 2 heating oil and other more volatile hydrocarbon compounds. Fires were ignited and then extinguished by firefighters using water, CO₂, and foam.

The Fire Training Academy site comprises approximately 2 ha (five acres). It is bordered on the west by Flintrock Pond, and on the north and south by undeveloped forest land. Approximately 500 m east of the site are two public water supply wells (MD-3 and MD-4) operated by the Barnstable Water Company. The topography on the site is level and most of the site has been cleared of vegetation, although there are scrub pine and oak trees along the property boundaries. There are three small wetlands to the north and northeast of the site.

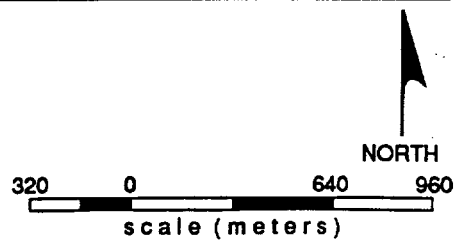
Four concrete fire pits were for fire training purposes. Three have been demolished and buried on site and the fourth has been capped with cement. One above ground storage tank is used to store propane. The site plan (Figure 2) shows the locations of all of these features.

Heating oil was used to ignite and fuel training fires for approximately thirty years at the site. It was stored in an 8,000 gallon underground tank and was pumped to concrete burning pits through an underground distribution system. Once a fire in one of the pits

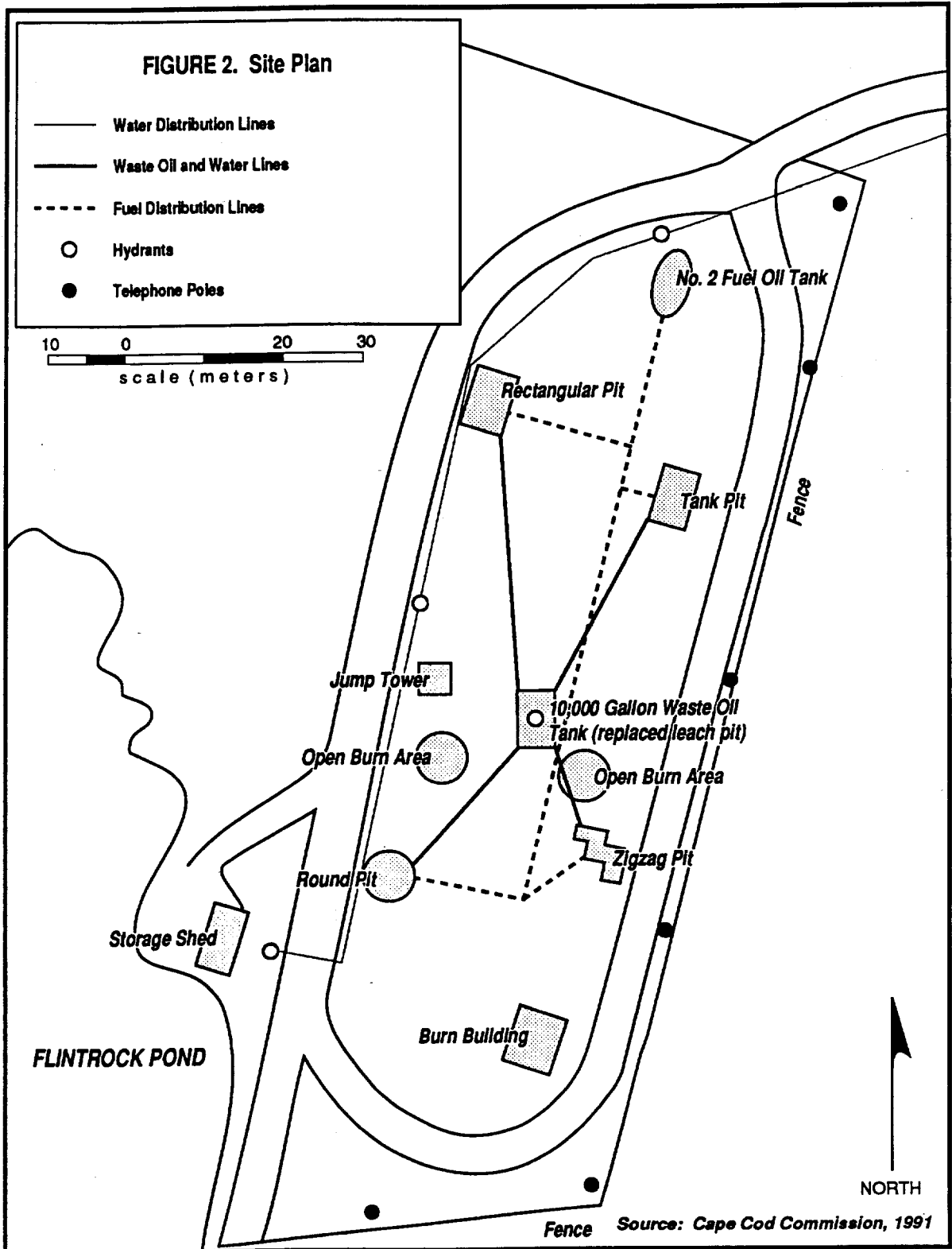


FIGURE 1.
Locus Map - Massachusetts Fire Training Academy

 Site



Source: USGS Quadrangle (Hyannis, 1979)



was extinguished, the excess water and oil was drained into a leaching pit in the center of the site and discharged to the subsurface. In the late 1970's, the leaching pit was replaced with a 10,000 gallon holding tank.

In July 1986, a leak was discovered in the distribution system connecting the underground fuel tank to the concrete burning pits. Investigations of this leak uncovered petroleum hydrocarbon releases in the subsurface soils and groundwater. The sources of these releases included the distribution system leak, and discharges from the leaching pit which collected drainage from the burning pits. Overflow of contaminated water may have occurred from the 10,000 gallon underground tank which replaced the leaching pit. In addition, the use of the burning pits themselves have released petroleum hydrocarbons to the subsurface through cracks in the pits and through spillage of the heating oil when fires were extinguished.

According to people familiar with past activities at the site, including fire chiefs and former cadets, household hazardous wastes such as waste oil, paint thinners and solvents were collected at the site and burned in the fire pits. These practices were discontinued in the late 1970's.

In addition to the burning of petroleum hydrocarbons, and other volatile organic compounds, a two story concrete structure on site is used to simulate the smoke and fire conditions in a burning building. Straw is ignited in the building and firefighters practice extinguishing this fire using water. The burnt straw is then dumped on the ground outside the building. Fires are also created on site using propane as a fuel source, and automobiles are used to practice both firefighting and rescue techniques.

HYDROGEOLOGY

GEOLOGY

Regional Setting

The site is located on glacially deposited, sands and gravels mapped as part of the Barnstable Outwash Plain by the U.S. Geological Survey (USGS, Oldale, 1974). The outwash sediments consist of well sorted medium to coarse sands with gravel and boulders up to one ft in diameter. Throughout the outwash deposits are lenses of sandy till, silt and clay.

The outwash sediments were deposited during the late Wisconsin glacial episode in the Pleistocene Epoch, approximately 15,000 years before present. The ice sheet which covered the Cape Cod area consisted of three lobes, the Buzzards Bay lobe, the Cape Cod Bay lobe and the South Channel lobe. Approximately 26,000 years before present, the ice lobes extended beyond Cape Cod, as far south as Marthas Vineyard and Nantucket (Oldale, 1984). As the ice sheet retreated, it remained stationary for a period of time in a position approximately 460 m (1500 ft) north of the site, in the area mapped as part of the Sandwich Moraine. Sediments were washed away from the edge of the glacier by meltwater streams, forming the outwash deposits.

According to radiocarbon dating conducted by Kaye (1964), glacial deposition was still occurring over Cape Cod 15,000 years ago. The deposition of marine clays in the Boston, Massachusetts area that occurred after the retreat of the ice has been dated at 14,000 years before present (Oldale, 1984). This implies that the retreat of the ice from Cape Cod to the north occurred in approximately 1,000 years. The deposition of the outwash plains and moraine sediments that formed the surficial features of Cape Cod happened during this time.

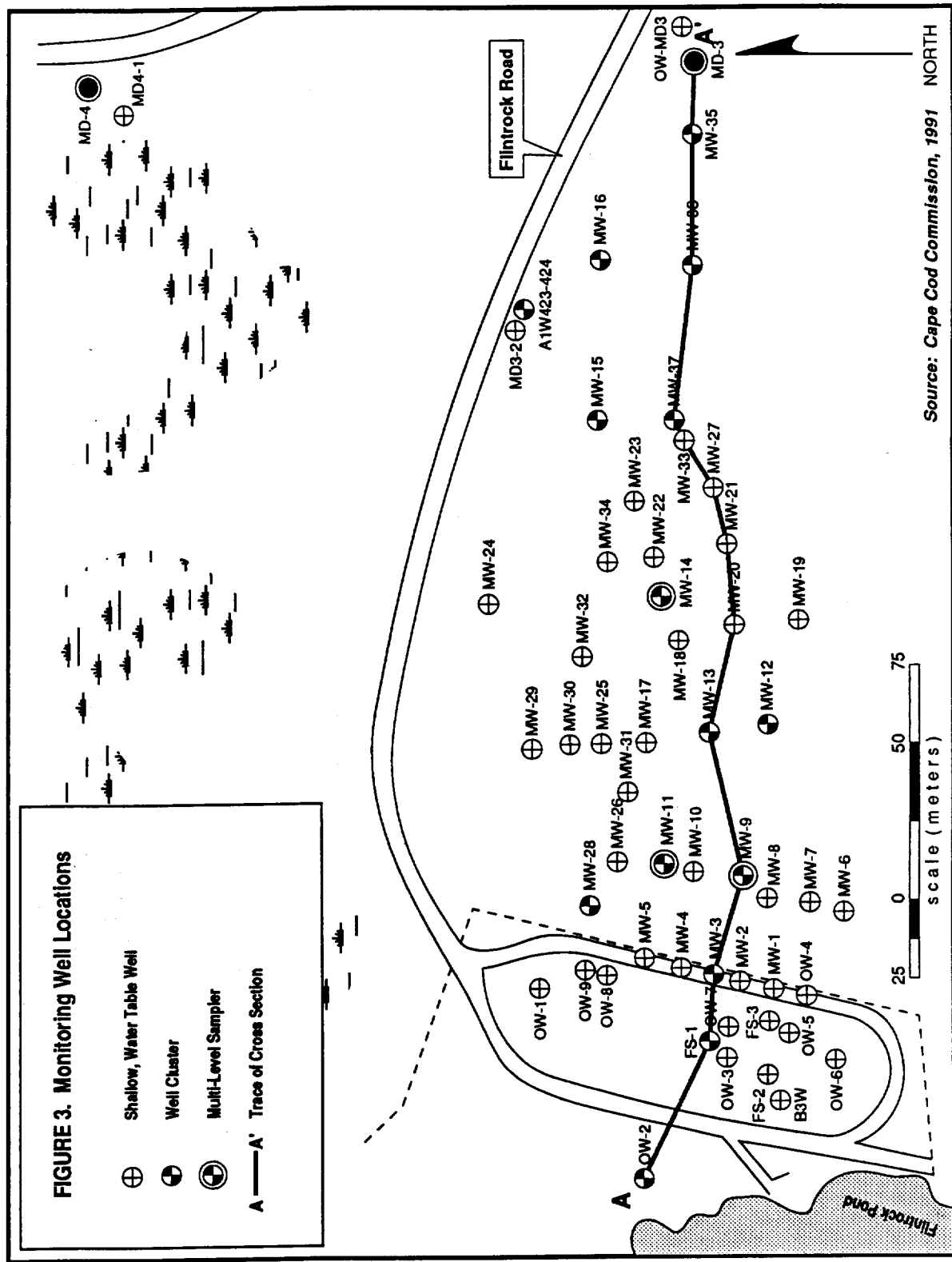
Below the outwash is a relatively continuous layer of blue-grey silt and clay of varying thickness that dips southward from the area of the site towards Nantucket Sound (Cambareri, 1986; Oldale, 1974; Horsley Witten Hegemann, Inc. 1991). The outwash deposits overlying this clay layer also dip to the south (Oldale, 1974). The underlying silt and clay deposits are thought to be older glacial lacustrine sediments deposited in deeper water environments than the coarser outwash deposits. Bedrock is located approximately 107 m (350 ft) below grade (Oldale, 1974).

Site Specific Geology

Eighty one geologic borings have been constructed on the site and the surrounding area for the investigation (Figure 3; Cape Cod Commission, 1991). Twenty-five of the borings extend just to the water table (4.6 to 6 m below grade), and were constructed to determine the extent of on-site soil contamination. The remaining 56 borings were formed during monitoring well installation. In addition, 8 test pits were excavated on the site in the early stages of the investigation to determine geologic conditions and gauge the extent of contamination around the concrete fire pits. The boring logs for the two production wells downgradient of the site have also been used to evaluate the area geology (Coffin and Richardson, 1975).

The borings encountered a thin (10 to 30 cm thick) soil layer followed by medium to coarse, well sorted sands with some fine gravel. A cobble layer was found at a depth of approximately 3 m in the borings on site and in many of the off site borings. This layer was approximately one foot thick, and consisted of one to three inch diameter cobbles.

While most borings were shallow, eighteen extended beyond the water table, ranging up to 30 m below grade. These deep borings indicate that the surficial sand and gravel deposits are approximately 12 to 15 m thick, and are underlain by increasingly fine silts and clays (Figure 4). The boring log for the production well MD-3 shows a fining downward sequence in the sands and gravels, with coarse sands near the ground surface, and finer sands in the vicinity of the well screen on top of the silt/clay layer. The boring for well AIW-423 encountered a lens of sand and gravel between silt and clay deposits at a depth of 15 m. The sediments observed on and near the site correlate well with the regional mapping conducted by the USGS.



Source: Cape Cod Commission, 1991

Horizontal Scale:
1" = 30m

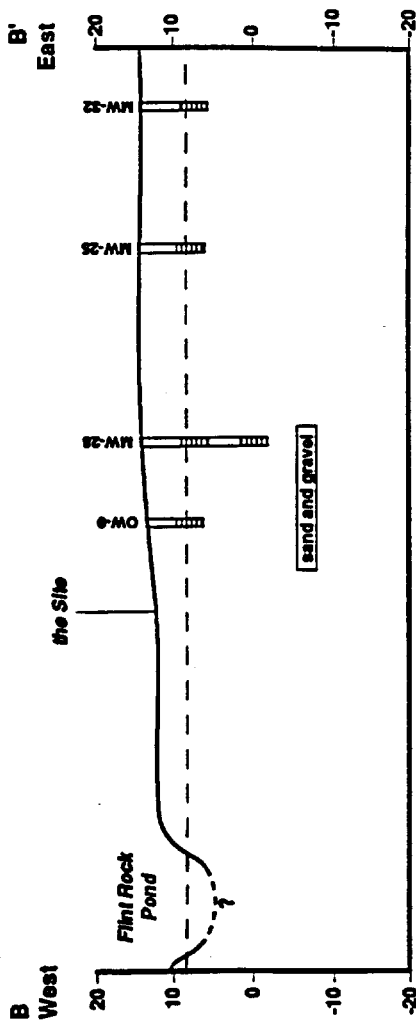
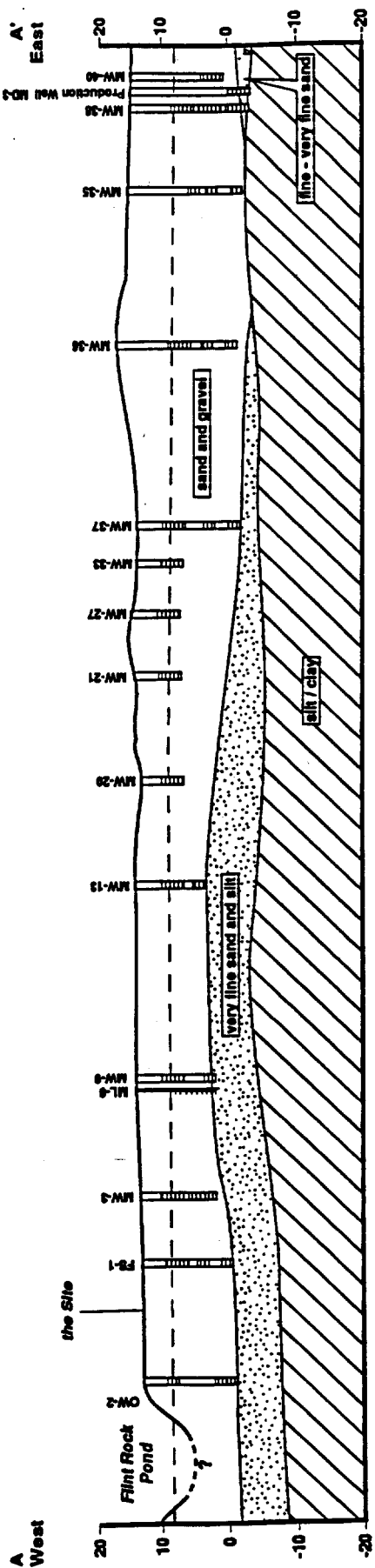






FIGURE 4. Hydrogeologic Cross Section

A - A' , B - B'

-  Sand and Gravel
-  Very Fine Sand and Silt
-  Silt and Clay
-  Very Fine Sand

HYDROLOGY

Climate

Cape Cod lies in a sub-humid setting along with the rest of southern New England. Average precipitation ranges between 1.0 to 1.2 m per year (LeBlanc *et al* 1986; Palmer, 1977). The average temperature of groundwater in the region is 10 to 12 °C (Todd, 1980).

Evapotranspiration rates at several stations across Cape Cod have been estimated at approximately 64 cm/yr using the Thornthwaite method (Thornthwaite and Mather, 1957) which takes into account air temperature and latitude (LeBlanc *et al*, 1986; Palmer 1977).

Regional Hydrologic Setting

The site lies within a regional, unconfined aquifer known as the Sagamore lens, which extends across the western portion of Cape Cod from Buzzards Bay and the Cape Cod Canal on the west to Bass River on the east. The water table elevation is highest in the center of the lens at a height of approximately 18 m. Groundwater flows radially from this high point towards Nantucket Sound, Cape Cod Bay or Bass River (LeBlanc *et al*, 1986).

The Sagamore lens, and the rest of the Cape Cod aquifer system has been designated a Sole Source Aquifer by the U.S. Environmental Protection Agency. (USEPA, 1982). The designation is the result of the fact that the population of Cape Cod receives all its drinking water from groundwater; there are no outside water supplies servicing the area (Ryan, 1979).

The only source of water replenishing the aquifer is recharge from precipitation. The recharge rates for the area of Cape Cod around the Barnstable Fire Training Academy have been estimated at approximately 48 cm per year based on precipitation rates and estimated runoff and evapotranspiration rates (LeBlanc *et al*, 1986). This recharge rate is within the range of those estimated by Palmer (1977) in Falmouth, Massachusetts (43 - 53 cm/yr), based on calculations using Thornthwaite's method, chloride balances and flow net analyses. On Nantucket, the USGS measured recharge rates by determining the profile of

tritium concentrations with depth in the aquifer. Rates of 43 - 66 cm/yr. were determined, equaling between 44 and 68 % of average annual precipitation (Knott and Olympio, 1986). These values may represent the upper boundary of recharge for Southeastern Massachusetts because runoff rates are extremely low on Nantucket (2 % of water balance, Knott and Olympio, 1986). Recharge rates of 41 to 46 cm/yr have been used in hydrogeologic investigations of the Cape Cod aquifer system (CCPEDC, 1979; Guswa and LeBlanc, 1985; Nelson *et al*, 1988)

Site Hydrology

Since 1986, 41 single and 16 clustered monitoring wells have been installed on site and in the surrounding area; a total of 84 wells. The wells on site have been labeled as OW wells, while those off site have been labeled as MW wells. Not all the wells that are on the site now were in place at the time the majority of the field work for this project occurred (June-October 1989). Wells were installed since then by Cape Cod Commission site investigators to continue investigating the movement of contamination toward the public supply wells (Cape Cod Commission, 1991). Some of these new wells have been used in subsequent water table and water quality mapping to verify the results from the summer of 1989. In addition to the monitoring wells, three multi-level samplers were constructed at the locations for wells MW-9, MW-11 and MW-14. These devices have sampling ports at 60 cm intervals extending 6.1 m (20 ft) into the aquifer.

The monitoring wells were constructed with 2" interior diameter threaded PVC casings, with 1.5 - 3.0 m (5 to 10 ft), 0.010 slot PVC screens. The annulus of each boring has been sealed with bentonite clay and the top of each well is protected with a cast iron curb box cemented in place flush or almost flush with the ground. The multi-level samplers were constructed with 0.25" Tygon tubing with nylon screens over the end of each tube. The individual tubes extended up to the ground surface within 5 cm, threaded PVC casing that was sealed and encased in the same way as the regular monitoring wells.

Most of the wells are screened across the water table with approximately 2 m of the screen located in the aquifer. Deeper wells installed at FS-1, OW-2, MW-3, MW-9, MW-12, MW-13, MW-14, MW-15 and MW-16 were used to determine vertical hydraulic gradients and to delineate the vertical extent of the contaminant plume.

Use of Production Wells

The pumping schedules of the two production wells located downgradient of the site (MD-3 and MD-4) were examined to aid in interpreting the water table maps. Well MD-4 is pumped year round, on an as needed basis, at a rate of 1730 L/min (450 gpm) an average of 14 hours per day in the summer and 6-12 hours per day in the winter. Well MD-3 has historically been used only during the peak demand months in the summer as extended usage may cause drawdown of the water table below the elevation of the screen (Coffin and Richardson, 1975). The well pumps at an average rate of 1700 L/min (450 gpm). Its use was curtailed when the contamination was discovered at the site in 1986, and has been used only in times of extreme demand or for sampling purposes since then. Average monthly water usage for both wells for the period of January 1987 through December 1990 is shown in Figure 5.

The water use records were examined in detail for the days immediately preceding the water table measurements. Well MD-3 was not pumped during the months measurements were taken any of the four water table maps. Its influence on groundwater flow conditions has therefore not been observed in the field. The pumping of well MD-4 has been observed to shift the groundwater flow towards the north near the well.

Water Table Mapping

The elevation of all the 5 cm diameter observation wells were surveyed relative to each other using a level transit. The elevation of well OW-1 was set at an arbitrary value of 12.50 m. Depth to water measurements were taken on four different occasions; 23 August 1989, 28 October 1989, 16 March 1990 and 30 October 1990. They were made using a steel measuring tape, with chalk to mark the penetration of the tape into the water.

From these measurements two water table maps were prepared showing groundwater flow directions under static, or non-pumping conditions (Figures 6 and 7) and with production well MD-4 pumping at approximately 1700 L/min (450 gpm) for 6 to 8 h prior to the measurements (Figures 8 and 9).

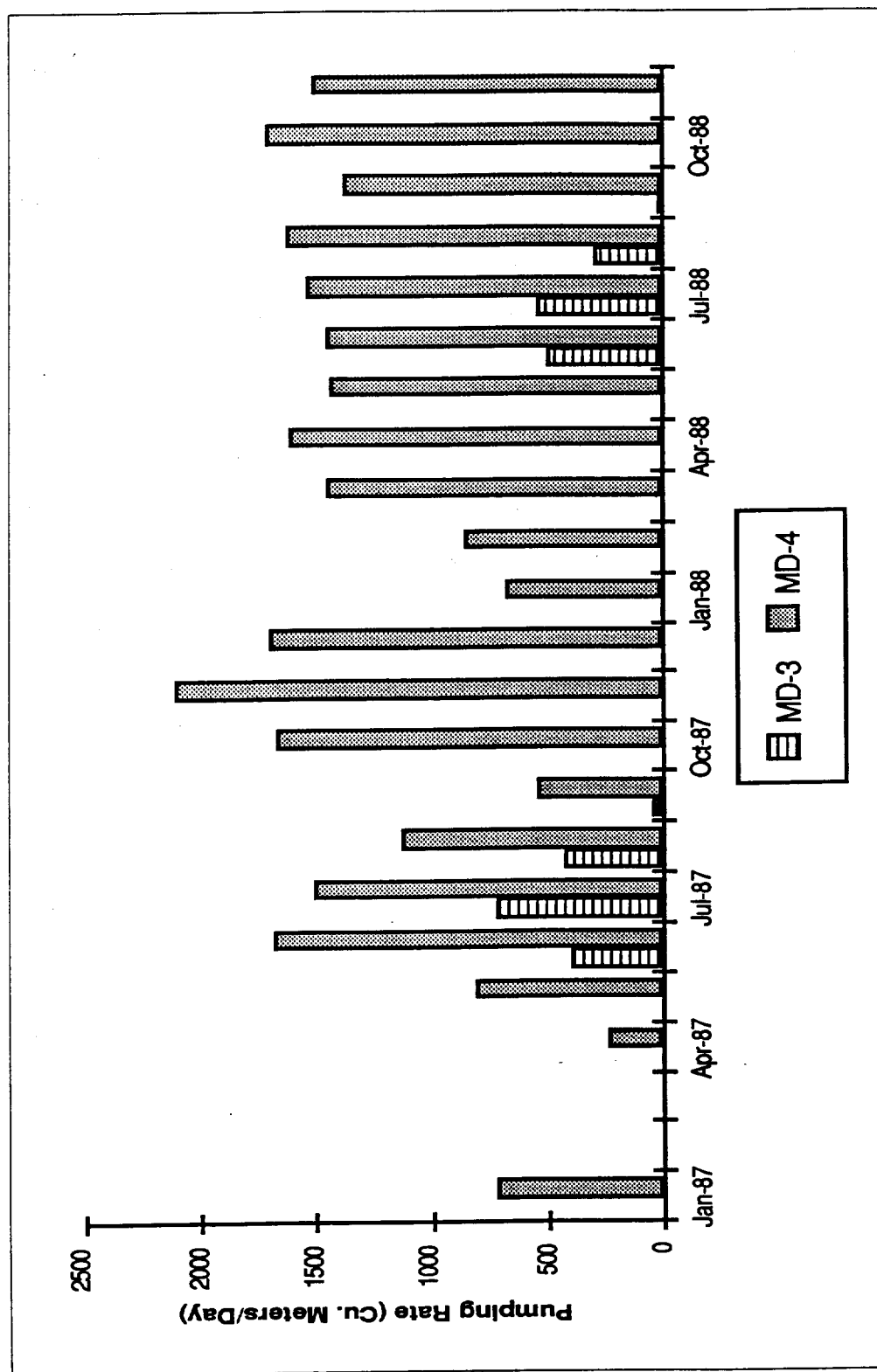
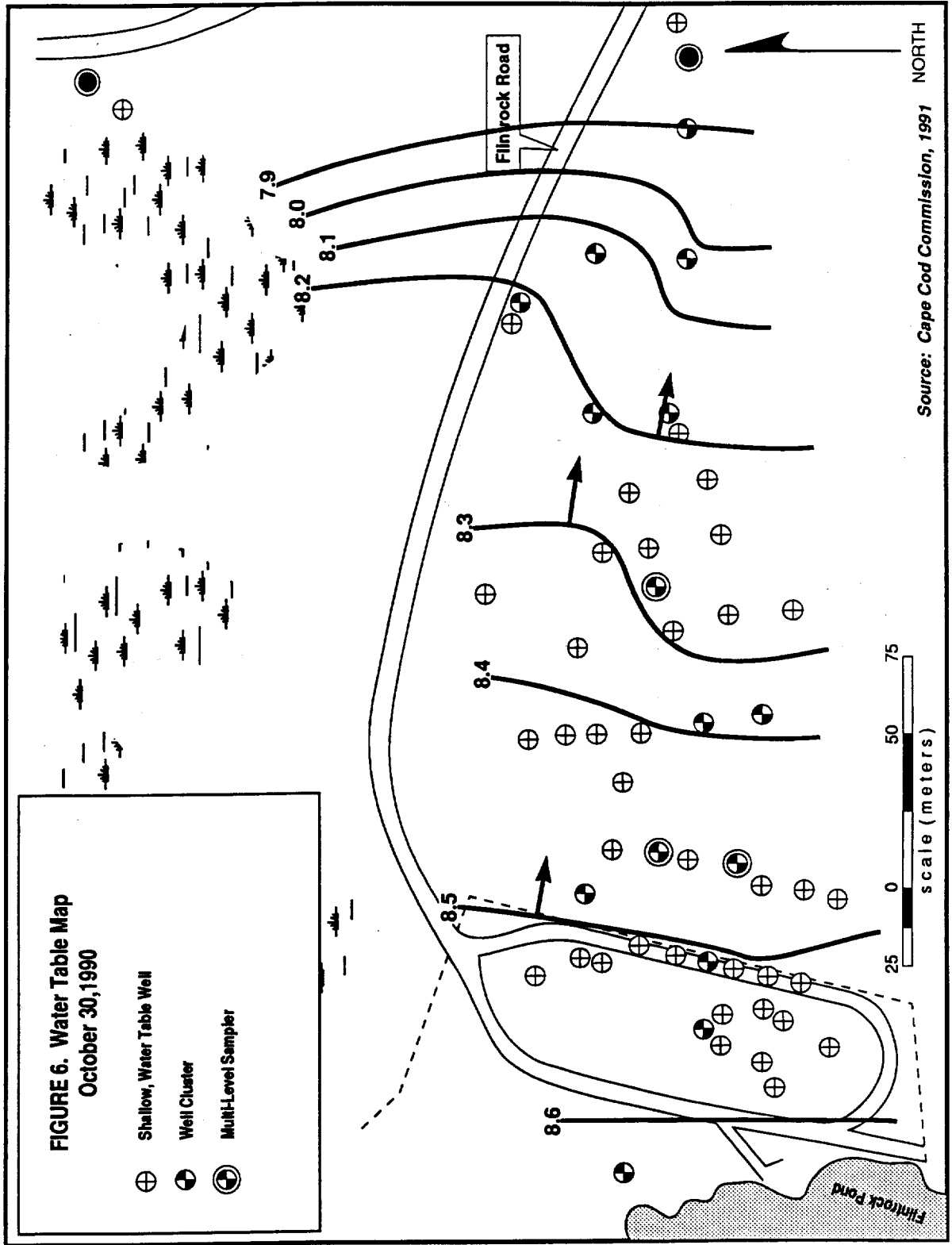
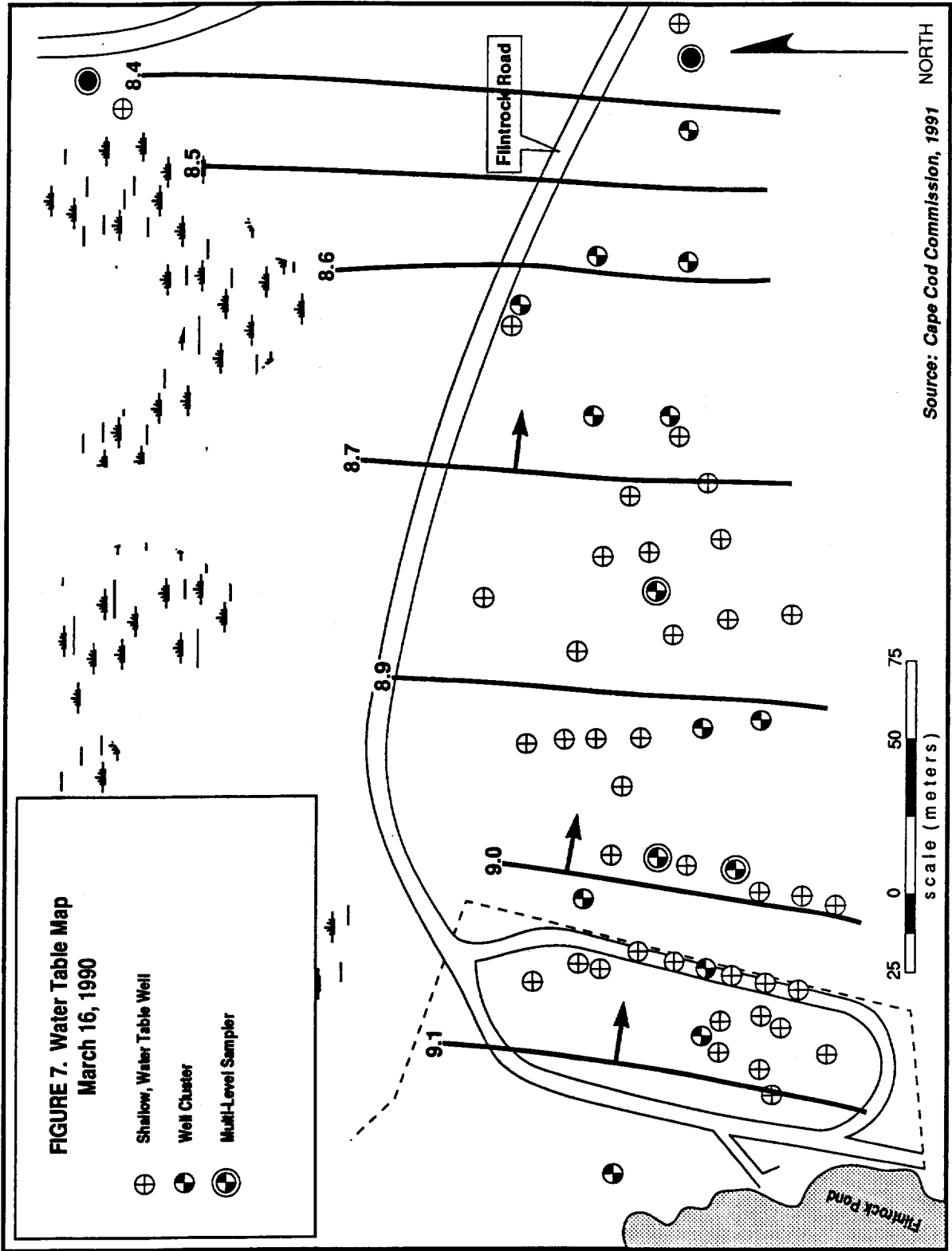


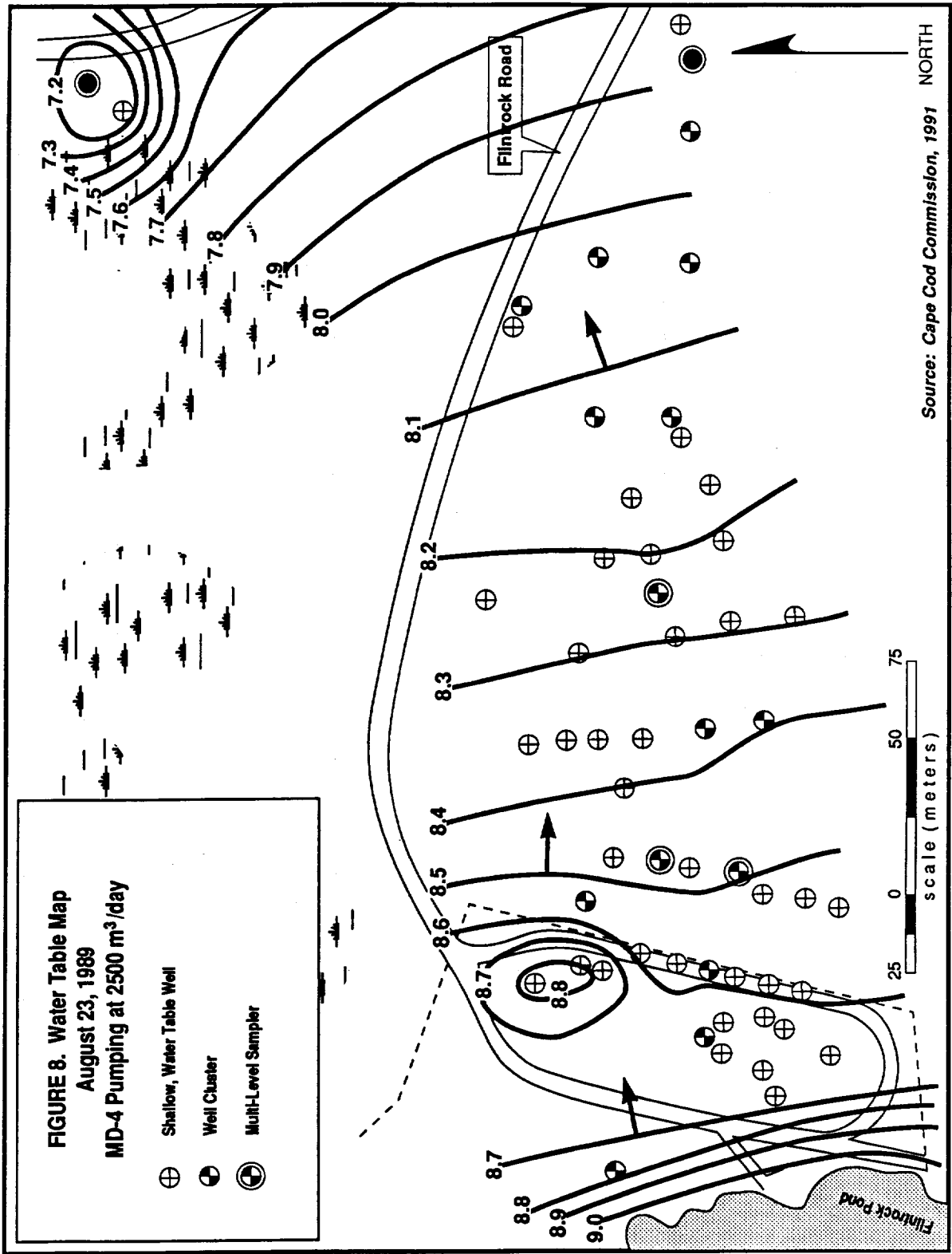
Figure 5: Water Withdrawal from Production Wells MD-3 and MD-4, 1987-1988

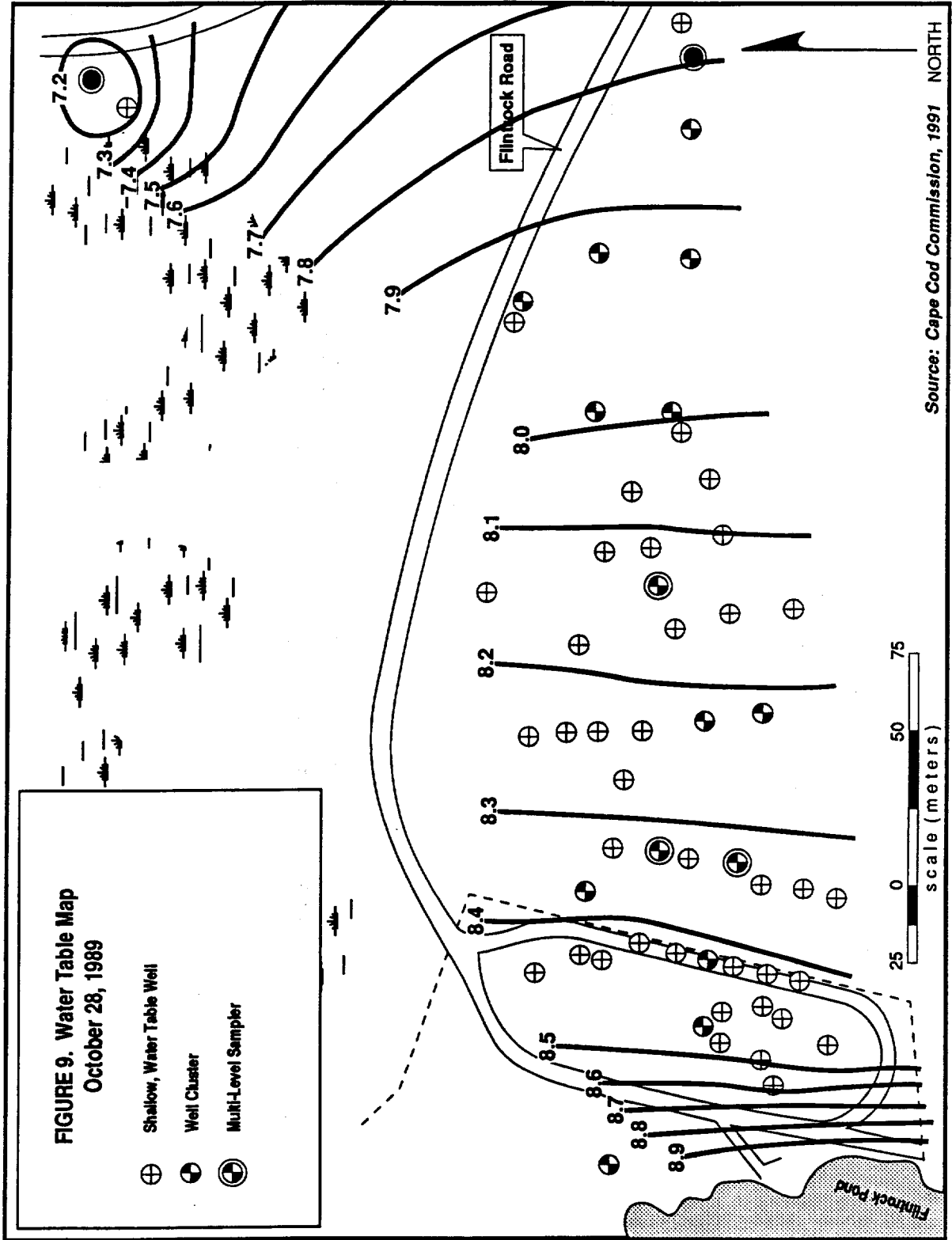


Source: Cape Cod Commission, 1991

NORTH







The water table contours under non-pumping conditions show a west to east direction of groundwater flow. The gradient is steeper east of the site near the production wells. The hydraulic gradient on and adjacent to the site is 0.0016, but increases to 0.0032 in the area the production wells. The elevation of the water in Flintrock Pond west of the site was always slightly higher than groundwater on the site, indicating that water flows from the pond into the aquifer underneath the site.

To estimate contour intervals in the vicinity of the pumping well (MD-4), drawdowns were calculated using the Theis equation (Theis, 1935). The radial distance of drawdowns were calculated based on the known pumping rate of the well and aquifer thickness, hydraulic conductivity and specific storage values estimated from pump test information for well MD-3. These drawdown values were subtracted from estimated static water table contours based on the water table configuration outside the influence of the pumping well. The resultant elevations were used to contour the water table around the pumping well.

The two water table maps from measurements with MD-4 pumping show a northerly shift in groundwater flow directions, especially in the vicinity of the pumping well. In Figure 8 the increased northerly orientation begins at or near the site, while in Figure 9, the west to east flow is seen across the site and the northerly orientation does not begin until well AIW-423, three quarters of the way from the site to the production well. This difference in flow directions may be the result of more regular pumping of the production well in the summer months compared to intermittent pumping in the fall.

Water table gradients immediately adjacent to the site with MD-4 pumping are similar to the static water table maps. The gradient on the site is 0.013 using 28 October 1989 water table measurements (Figure 9). Downgradient (west) of the site the magnitude of the hydraulic gradient is 0.002. Similar hydraulic gradients were observed in August 1989 (Figure 8).

In August 1989, a small groundwater mound was observed in the area of well OW-1 and OW-8 (Figure 8). These variations may be due to substantial discharges of water from the fire training activities at the site. A hydrant next to well OW-1 is a source of imported water used at the site.

Water-Table Fluctuations

Water-table elevations in well MW-5 have varied a total of 2.0 m (6.34 ft) during the 5 y period of investigation at the site (Figure 10). A longer period of observation is available for a USGS monitoring well located 1 km north of the site in a similar hydrogeologic environment. Water-level fluctuations in this well have varied 2.0 m (6.5 ft) between 1978 and 1991. The highest water levels were measured in the summer of 1987, when the highest water levels were measured on the site. Water levels in the fall and winter of 1991 almost match the record lows observed in the fall of 1981. The four water table maps presented above represent conditions approximately half way between the record high and low water table fluctuations.

Variations in Groundwater Flow Directions

The variations in groundwater flow directions from potential measurement errors were determined for the site based on a projected error of ± 1.2 cm (0.04 ft) for the surveying and water level measurements. As the gradations of the surveying rod and the steel tape used in water level measurements are both 0.3 cm, a combined error of ± 1.2 cm is conservative yet reasonable.

Errors in measured groundwater flow directions were determined for three groups of three wells that each formed a triangular pattern (Figure 11). The flow directions were estimated by varying individual head measurements in the three wells in each group by the assumed error or ± 1.2 cm. The maximum range of groundwater flow directions was then interpolated. The errors were calculated for a series of 3 to 5 measurement rounds taken in the wells since the investigations began at site in 1986.

In general, the measured flow directions are to the east and slightly southeast. Variations in flow directions over time for each of the well groups are a function of natural changes in flow directions from changing recharge and pumping patterns, and errors in the measurements. For the three well group of MW-3, MW-6 and MW-13, measured groundwater flow directions range from 48° to 122° . Because of the shallow slope of the

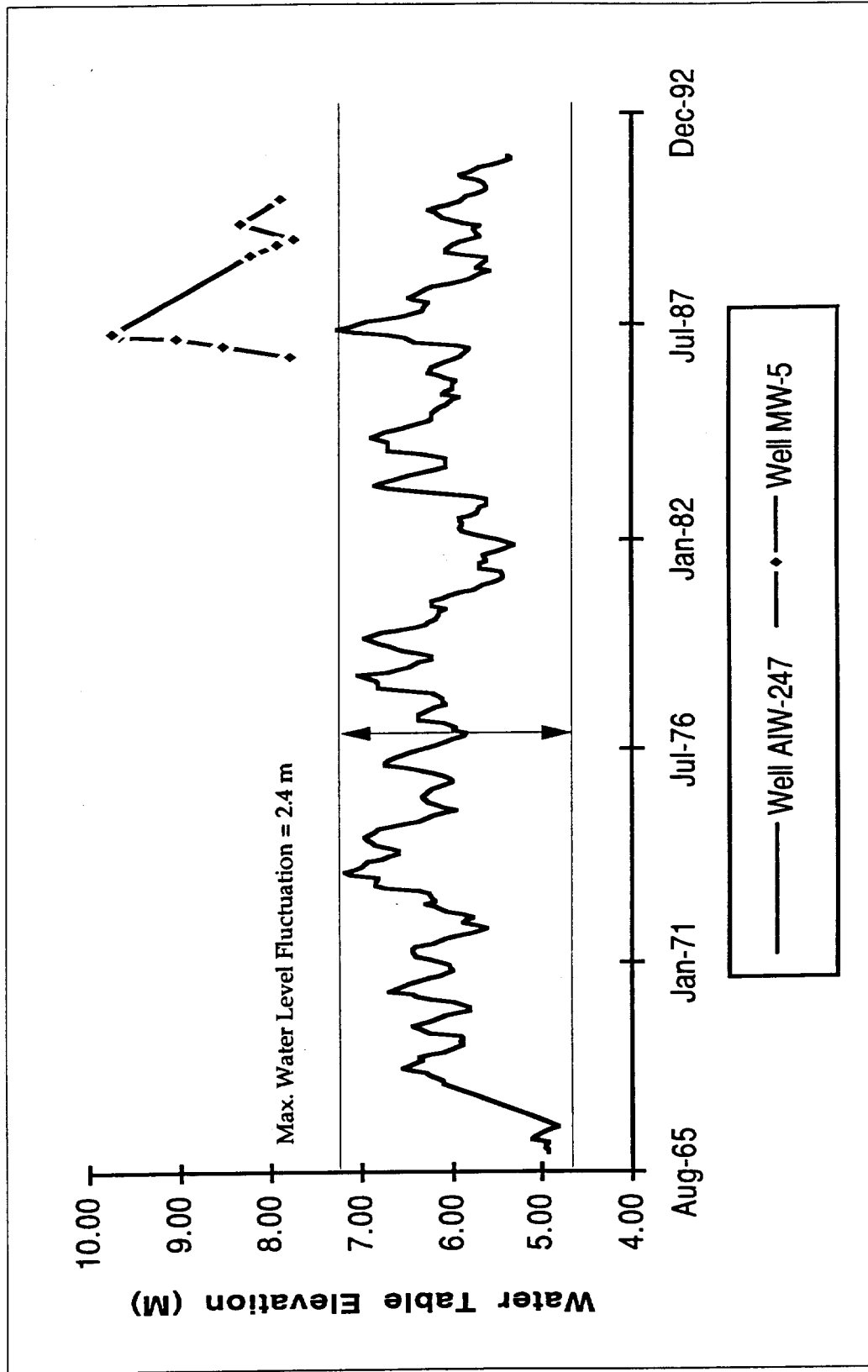
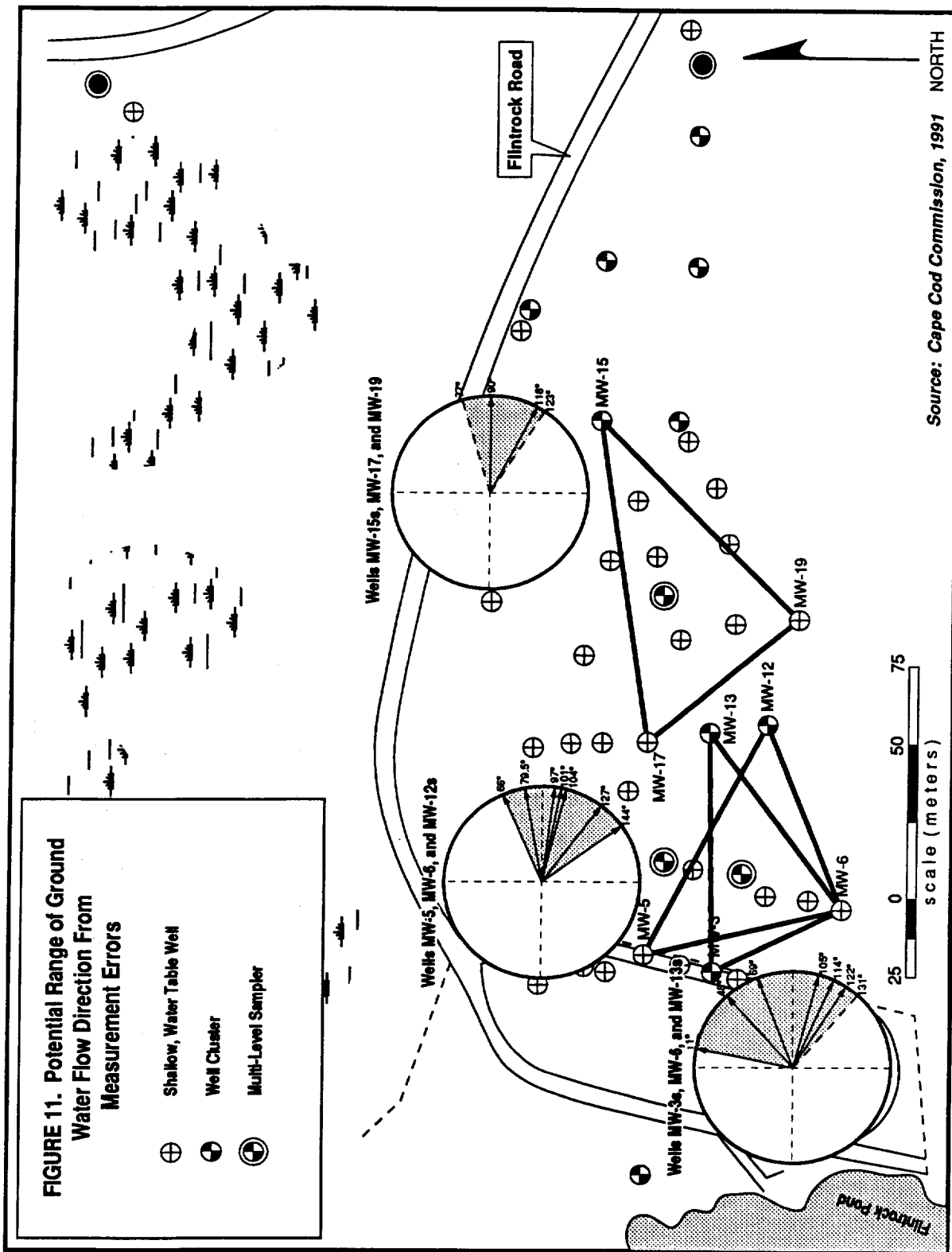


Figure 10: Comparison of Regional and Site Specific Water Table Fluctuations



Source: Cape Cod Commission, 1991

water table in this vicinity, slight changes in water table elevation from changes in recharge or from measurement errors can significantly alter mapped flow directions.

Groundwater Flow Rates

Groundwater velocities of 0.32 to 0.64 m/d were calculated for the site using a hydraulic conductivity of 60 m/d, a porosity of 0.3 and hydraulic gradients of 0.0016 and 0.0032 measured on the non-pumping water table maps. Groundwater velocities appear to be slower on the site and increase off-site, consistent with the changing groundwater gradients.

Determination of Aquifer Hydraulic Properties

The characteristics of the aquifer in the vicinity of the site have been investigated through evaluation of pump tests in production well MD-3, and slug tests and pump tests in monitoring wells across the site. Two pump tests of production well MD-3 were analyzed, and slug and pump tests were conducted in six monitoring wells between the site and the production wells.

Methods

Production Well Tests A 1987 pump test for well MD-3 (conducted by IEP, Inc., 1986) was analyzed using the Thiem, Thiem-Dupuit, Cooper-Jacob and Neuman methods. The test ran for 70 hours at a pumping rate of 2070 m³/d (380 gpm) and drawdown measurements were taken in three wells, OW-MD3, MW-16 and MW-14. During the test production well MD-4 located 195 m north was pumping at 1470 m³/d (270 gpm).

Monitoring Well Pump Tests Short (5-10 min) pump tests were conducted at six monitoring wells. Pump tests were conducted using a gasoline powered pump with a 1" diameter suction hose. The pumping rate was determined for each test from the outflow of the pump. Water level measurements for both types of test were recorded using a data logger and pressure transducer with a sampling interval of 0.2 s, and an approximate error of ± 0.3 cm.

Each well was pumped until drawdowns reached steady state within the well casing. The well configuration, pumping rate, and resultant drawdown was used to calculate hydraulic conductivity using a constant head method developed by Hvorslev (1951).

Monitoring Well Slug Tests Rising and falling head slug tests were conducted using a 1.5 m long, 2.5 cm diameter, weighted PVC slug. The slug was rapidly lowered into the well causing a rise in head. The fall of the water level was then recorded using a pressure transducer and data logger. After the falling head test, the slug was quickly removed from the well, and the rise in water level over time was recorded.

Results

Production Well Tests The Thiem method (Thiem, 1906) was used to calculate the aquifer hydraulic conductivity using late time drawdown data for wells OW-MD3 and MW-16. Steady state drawdown is required for this analysis (Table 1). The drawdown data in well OW-MD3 is closer to steady state than that for MW-16. Because this method is designed for confined aquifers, the calculated conductivity values may be lower than actual values. A modification of this method, the Thiem-Dupuit Method (Kruseman and de Ridder, 1990) was used to correct for the increased drawdowns in the unconfined aquifer at the site. This method yielded slightly higher conductivity values than the Thiem method.

The Cooper-Jacob solution (Kruseman and de Ridder, 1990) was used to calculate a transmissivity and storage coefficient using drawdown data from well OW-MD3, 15 m from the production well. Two slopes were observed in the semi-log plot of the time-drawdown data for the well. One slope was determined for data from the first 60 minutes of the test and provided what appears to be an overly high transmissivity value (4150 m^2/d). The slope calculated from later time values provides a more realistic transmissivity value. Again, this test is designed for confined aquifers, and the calculated transmissivity may be slightly lower than actual value. The storage coefficient of 0.3 is at the high end of the range of specific yield values expected for an unconfined sand and gravel aquifer (Freeze and Cherry, 1979).

Table 1: Summary of Measured Aquifer Characteristics

1987 Pump Test of MD-3

T (sq. m/day)	T (sq. ft/day)	K (m/day) *	K (ft/day) *	Kv (m/day)	Kv (ft/day)	Sy	S	Analysis
590	6300	60	180					Thiem
650	7000	60	200					Thiem-Dupuit
550	5950	50	170			0.3		Cooper Jacob
440	4750	40	140	20	67	0.36	0.008	Neuman (unconfined)
557.5	6000	52.5	172.5			0.33		Averages

1990 Pump Test of MD-3 (Cape Cod Commission, 1991)

T (sq. m/day)	T (sq. ft/day)	K (m/day) *	K (ft/day) *
840	9000	80	260

1989 Monitoring Well Pump Tests (Evaluated using constant head solution Hvorslev, 1951)

	K (m/day)	K (ft/day)
OW-1	80	270
OW-2	90	300
MW-3s	60	200
MW-3i	50	150
MW-5	80	260
MW-9s	60	200
Average	62.5	202.5

1989 Monitoring Well Slug Tests (Evaluated using Hvorslev solution, 1951)

	K (m/day)	K (ft/day)	
OW-2	150	490	Rising Head Test
OW-2	140	425	Falling Head Test
MW-3i	150	450	Rising Head Test #1
MW-3i	150	450	Rising Head Test #2 (early time)
MW-3i	60	190	Rising Head Test #2 (late time)

* Note= Pump test hydraulic conductivity values based on an aquifer thickness of 10.7 m (35 ft.).

The Neuman solution for unconfined aquifers (1975) was also used to evaluate the drawdown data for well MD-3. The transmissivity calculated with this method was slightly lower than the other methods, while the specific yield was slightly higher. There is probably some error in the calculations as the log-log time-drawdown curve was difficult to match to the Neuman type-curves. If the calculations were correct, the Neuman solution should provide a transmissivity value higher than the confined solutions, the opposite of what was observed.

The Neuman solution also provided an estimate of the anisotropy in the aquifer. The vertical conductivity was approximately one-half of the horizontal conductivity (Table 1). The slight layering between sand and gravel layers, and the fining downward sequence seen in the boring logs supports the anisotropy calculated from the pump test data.

The distance between the two production wells is great enough that any interference effects from MD-4 should be negligible for most of the time the wells were pumped. Slight interference (<3 cm) may have occurred in the last 10 - 20 h of the test. If interference did occur, the reported transmissivity and conductivity values may be again be slightly lower than the actual values.

The effects of partial penetration may also be impacting the results calculated from well OW-MD3 located 15 m (50 ft) from the production well. Both of these wells have a 3-m screen in a 10.7-m thick aquifer. The distance (L) within which partial penetration effects need to be considered is :

$$L = 1.5-2b(K_h/K_v)^{1/2} \text{ (Todd, 1980, Kruseman and de Ridder, 1990)}$$

If K_h/K_v is between 1 and 2 then wells within 16-25 m are affected. Well OW-MD-3 is within this distance, so transmissivity values calculated using data from this well may be lower than actual values. Despite the potential interference and partial penetration problems the calculated transmissivity and conductivity values appear reasonable and within the range for the aquifer sediments (Freeze and Cherry, 1979).

The results of the 1987 test of well MD-3 compare reasonably well with a test conducted in 1990 by the Cape Cod Commission (1991). The more recent test was analyzed using the Cooper-Jacob solution, and provided slightly higher transmissivity and hydraulic conductivity values (Table 1)

Monitoring Well Pump Tests The conductivities calculated from the monitoring well pump tests ranged between 50 and 90 m/d, with an average of 62.5 m/d (Table 1). Variations in the conductivity values are a result of local aquifer heterogeneities and slight errors in measurement, especially pumping rate estimates. The values determined from these tests are slightly higher than those determined from the 1987 production well test. The monitoring well tests relate only to a small area around the well screens, which are located at the water table where coarser grained sediments exist. The value for well MW-3i, located approximately 4 m below the water table is slightly lower as would be expected from the finer downward sequence in the aquifer sediments. The monitoring well tests were also not subject to interference from other pumping wells or partial penetration effects which tend to lower calculated transmissivity and conductivity values. Given the differences between the tests, including the interferences in the pumping well tests, the results from both types tests are quite similar.

Monitoring Well Slug Tests Each slug test lasted only 2-5 s in the permeable sands and gravels at the site, and water-level fluctuations were recorded during some of the tests. Results from two wells (OW-2 and MW-3i) were used to calculate hydraulic conductivity using the Hvorslev method (1951) and evaluate the validity of the tests. Rising and falling head tests from OW-2 and a rising head test for MW-3i provided conductivity values of 140 - 150 m/d, higher than the values from the pump tests. These tests all lasted 2 s or less, and it is likely that results reflect groundwater flow only through coarser, disturbed sediments that were placed around the well screen during well construction

One test of MW-3i provided a water level-time graph with two different slopes. A calculation using the later time slope (2-4 s) provided a more reasonable conductivity value (60 m/d). The higher value from the early data may again reflect flow immediately around the well screen. Overall, the slug tests occurred so quickly in the permeable sands and

gravels that they do not appear to provide reliable results that match with the other tests. For these types of sediments, the constant head pumping tests are more useful.

Production Well Zones of Contribution

The zones of contribution (ZOCs) or capture areas to the two downgradient production wells were modeled to determine the interactions between groundwater at the site and the drinking water supply. The ZOCs were modeled using the GPTRAC component of the WHPA computer code developed for the USEPA Office of Groundwater Protection (EPA, March 1991). The GPTRAC model can delineate steady state capture areas for up to 20 wells in confined, unconfined and leaky aquifers. Pathlines can also be determined to show the movement of groundwater through the aquifer to a well over time. For unconfined aquifers such as the one at the site, the model first determines the cone of depression caused by the pumping of each well (assuming a flat water table). The total area of the cone of depression is calculated to be equal to the area within which there is sufficient precipitation recharge to balance the water lost through the well. The model then calculates a final head distribution by superimposing the cone of depression over the non-pumping water table. With these final head values, time related pathlines can be determined showing groundwater flow into the well.

Inputs to the model are shown on Table 2. The model was used to estimate the capture area to MD-3 and MD-4 pumping separately and together. A pumping rate of 1430 m³/d was chosen for each well to simulate the use of each well during summer, or peak pumping conditions where the wells are used for approximately 14 hours each day.

Table 2: Input Values for Production Well Zone of Contribution Modeling

	<u>Well MD-3</u>	<u>Well MD-4</u>
Pumping Rate (m ³ /d)	1430	1430
Hydraulic Conductivity (m/d)	60	60
Aquifer Thickness (m)	15	15
Aquifer Porosity (%)	30	30
Hydraulic Gradient (m/m)	.0025	.0025
Time (yrs)	5	5

When well MD-3 is pumping, its ZOC encompasses all of the fire training site and associated contaminant plume (Figure 12). This is true even when both wells are pumping together (Figure 13). When MD-4 is pumping alone the southern portion of its ZOC includes the site (Figure 12). The effects of MD-4 pumping have been observed in the field as shown on the water table maps, confirming that groundwater flows from the site to the well (Figures 8 and 9). As well MD-3 is directly downgradient from the site, it is not surprising that its ZOC includes the site.

Since well MD-3 has not been used significantly since the contamination was discovered, the ZOC with well MD-4 pumping more closely represents present day conditions. The size of this ZOC is directly related to the pumping rate of the well and the duration of pumping. During times, especially in the winter, that well MD-4 is not used to capacity, groundwater from the site may flow past both production wells and not enter the drinking water supply.

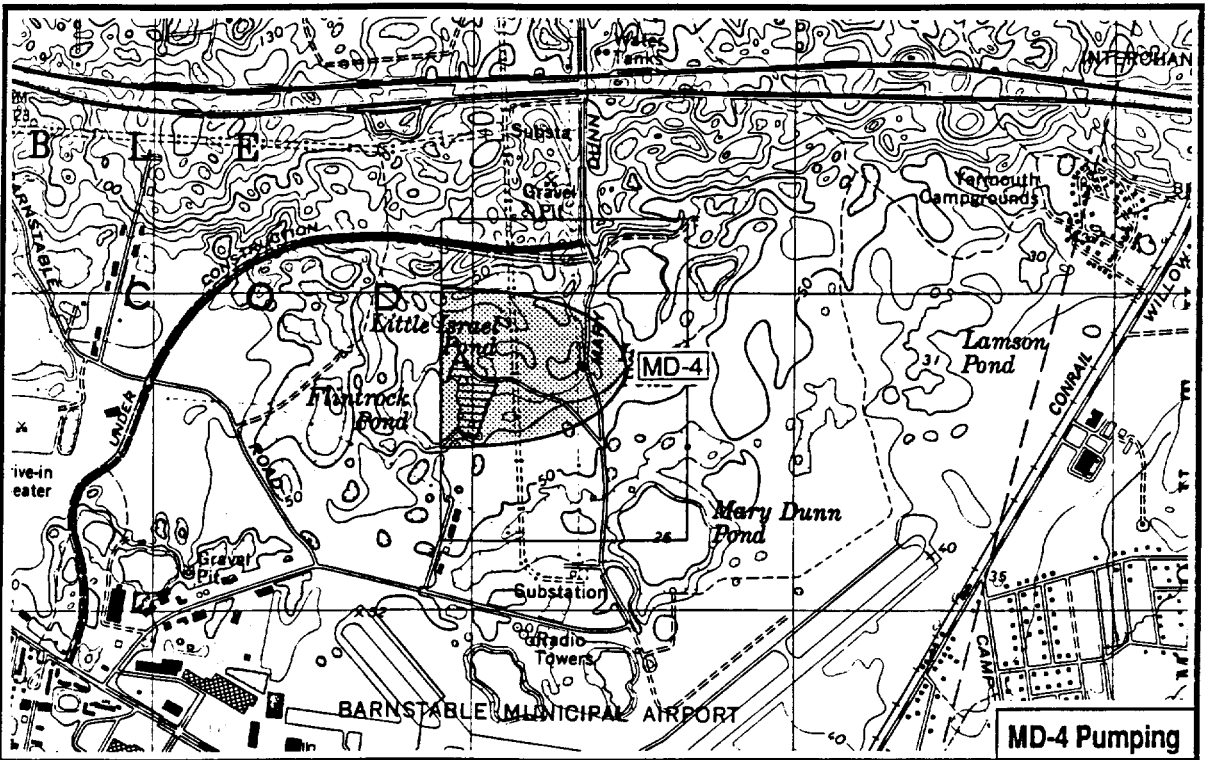
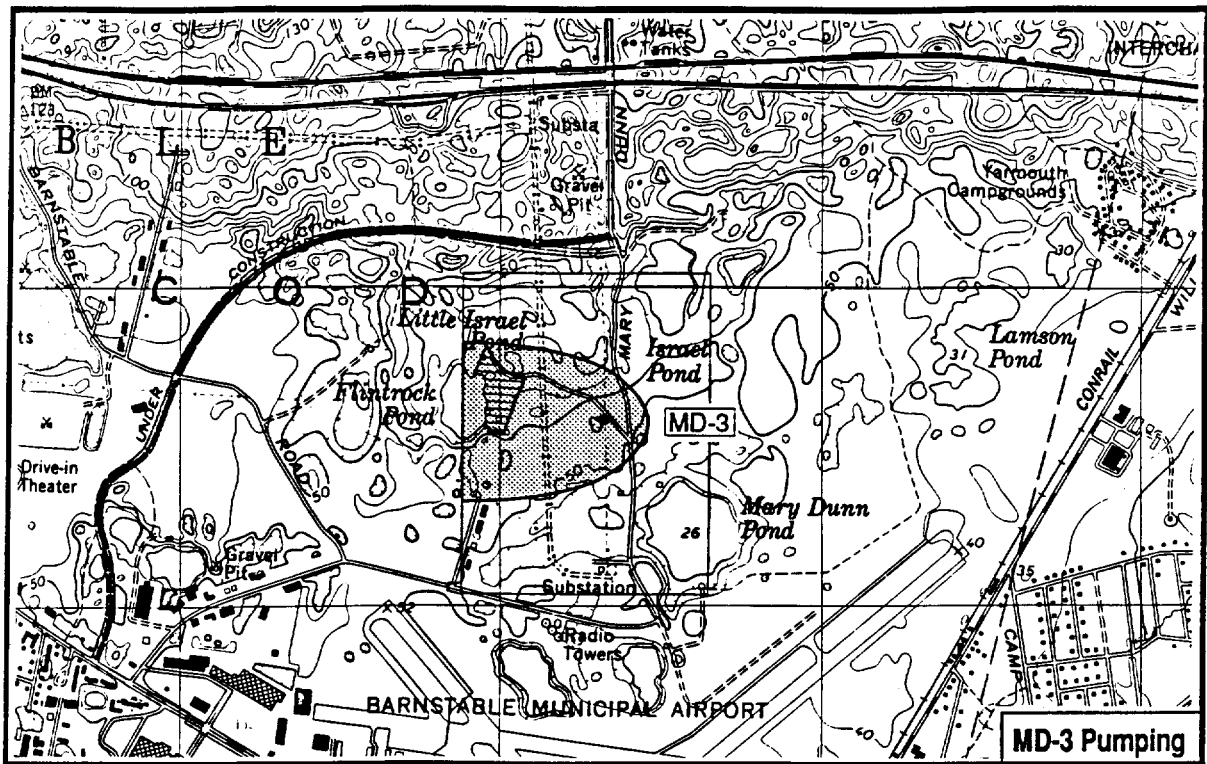
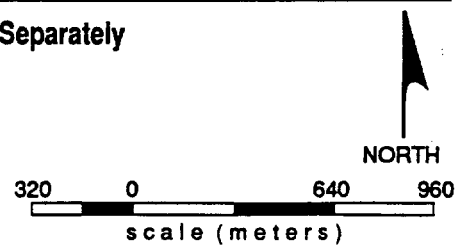


FIGURE 12. Production Well ZOC for MD-3 and MD-4 Pumping Separately

- Public Supply Well
- ▬ Site
- ▨ Zone of Contribution (ZOC)

Source: USGS Quadrangle (Hyannis, 1979)



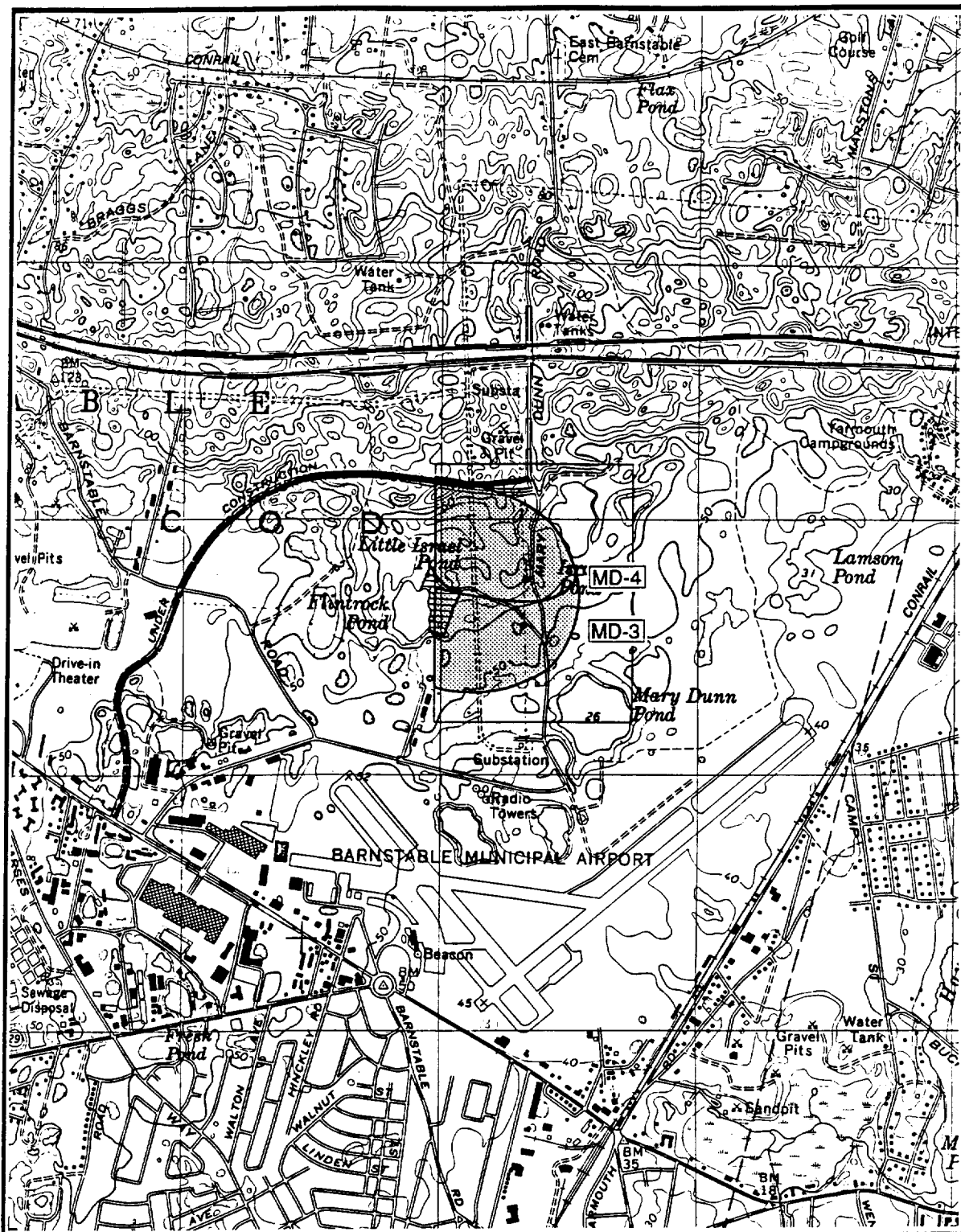
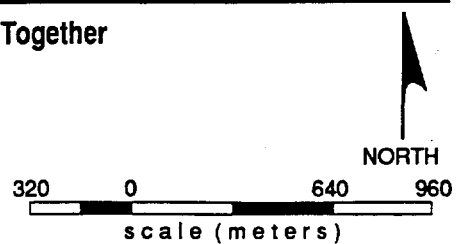


FIGURE 13. Production Well ZOC for MD-3 and MD-4 Pumping Together

- Public Supply Well
- ▨ Site
- ▨ Zone of Contribution (ZOC)

Source: USGS Quadrangle (Hyannis, 1979)



HYDROCARBON CONTAMINATION IN THE UNSATURATED ZONE

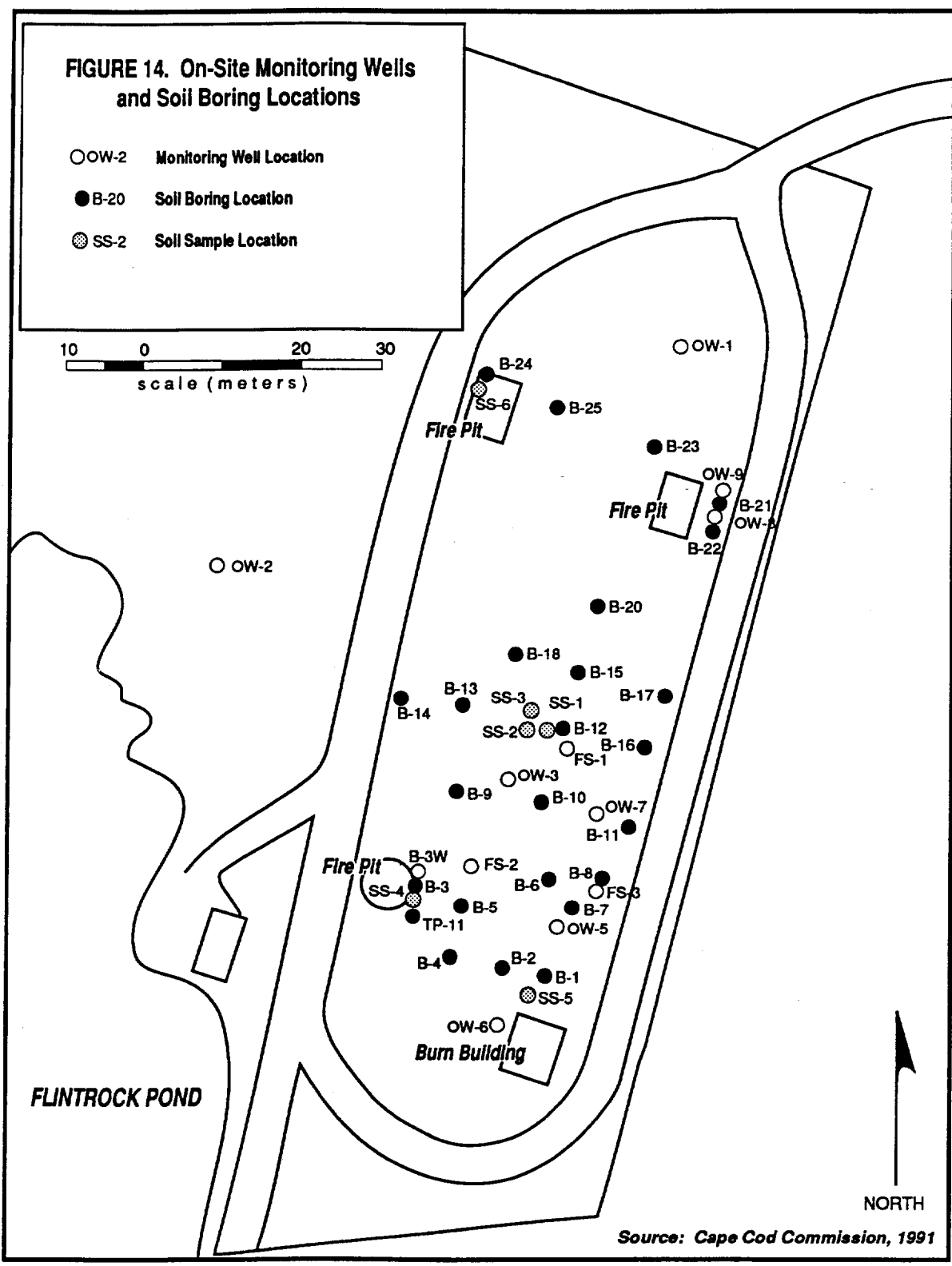
Methods of Sampling and Analysis

The residual contamination remaining in the unsaturated zone at the BFTA site was determined through analysis of soil samples taken from 24 borings across the portions of the site where contamination was suspected (Figure 14). The borings were conducted between 5-7 September 1989 using a hollow stem auger. Split spoon samples were taken at the ground surface and at 4 ft intervals extending down to, or just across the water table. If hydrocarbon contamination was not detected in the surface sample, intermediate samples were skipped and soils at the water table interface were analyzed.

Soil samples were stored in clean glass jars filled to approximately three-quarters of capacity, sealed with a layer of aluminum foil, and capped. An initial qualitative screening of the extent of hydrocarbon contamination was conducted on-site using a portable gas chromatograph coupled with a flame ionization detector (Photovac 10S10). Head space samples from the soil jars were taken using 100, 300 and 500 μL syringes by piercing the foil layer after the jar had been shaken. Volumes of head space sample injected into the gas chromatograph ranged from 20 to 500 μL . The sample volumes and the relative sensitivity of the photoionization detector were adjusted based on the level of contamination observed in the samples before analysis.

Quantitative assessments of unsaturated zone petroleum hydrocarbon concentrations were not made as part of the field screening. Only the presence or absence, and the relative extent of contamination were determined. Head space samples of fuel oil were analyzed throughout the testing period to verify that peaks seen on the chromatograph were the result of petroleum hydrocarbons. Appropriate blank and duplicate samples were also analyzed.

Based on the results of the on-site screening, 20 samples representative of site conditions were sent to ERCO Laboratories of Cambridge, Massachusetts for analysis of total petroleum hydrocarbons (TPH) using an infrared technique (EPA Method 418.1).



Results

Four areas of contamination were identified from the soil analyses (Figure 15). The largest area is centered on the location of the underground storage tank (removed in March, 1990) that captured excess oil and water from the fire pits (Site A in Figure 15). Here TPH concentrations of 11,000 mg/kg were found. This area extends south and east to the zig-zag shaped fire pit, downgradient of the area where the leak in the fuel oil distribution system was found. In cross section, it can be seen that the contamination between the two sites is only found at the water table (Figure 16)

The second area is near the round fire pit on the southwest portion of the site (Site B). TPH concentrations decrease rapidly from 8,100 mg/kg at the surface to 240 mg/kg at the water table. Approximately 15 years ago, this pit was covered with a cement cap after heat cracks in the cement base developed during its use. The cap may be preventing downward migration of dissolved hydrocarbons, as it keeps recharge from percolating through the contaminated sediments underneath the pit. It could also be preventing the vapor phase hydrocarbons from moving into the atmosphere. As a result, the hydrocarbon concentrations remain trapped just below the ground surface.

Near-surface soil contamination is also seen at the site of the rectangle fire pit to the northwest (Site C). As shown in cross section, TPH concentrations decrease quickly with depth. Another small area of contamination was seen on the edge of the northeastern fire pit (Site D). Here TPH concentrations were detected only at the water table.

Estimate of Hydrocarbon Source Strength

An estimate of the volume and mass of TPH remaining in the unsaturated zone was made based on the soil analyses conducted in 1989. Areas of soil contamination were subdivided using the concentration contours in Figure 15. Volumes of contaminated soil were estimated by measuring the areas within each contour interval and estimating a depth of contamination from the cross-sections (Figure 16). The mass of TPH was then calculated for the three contaminated areas on site using the contoured concentrations as estimates of the actual concentration within each contoured area. A particle density of 2630 kg/m³ was used to convert the volume of soil into a mass of soil.

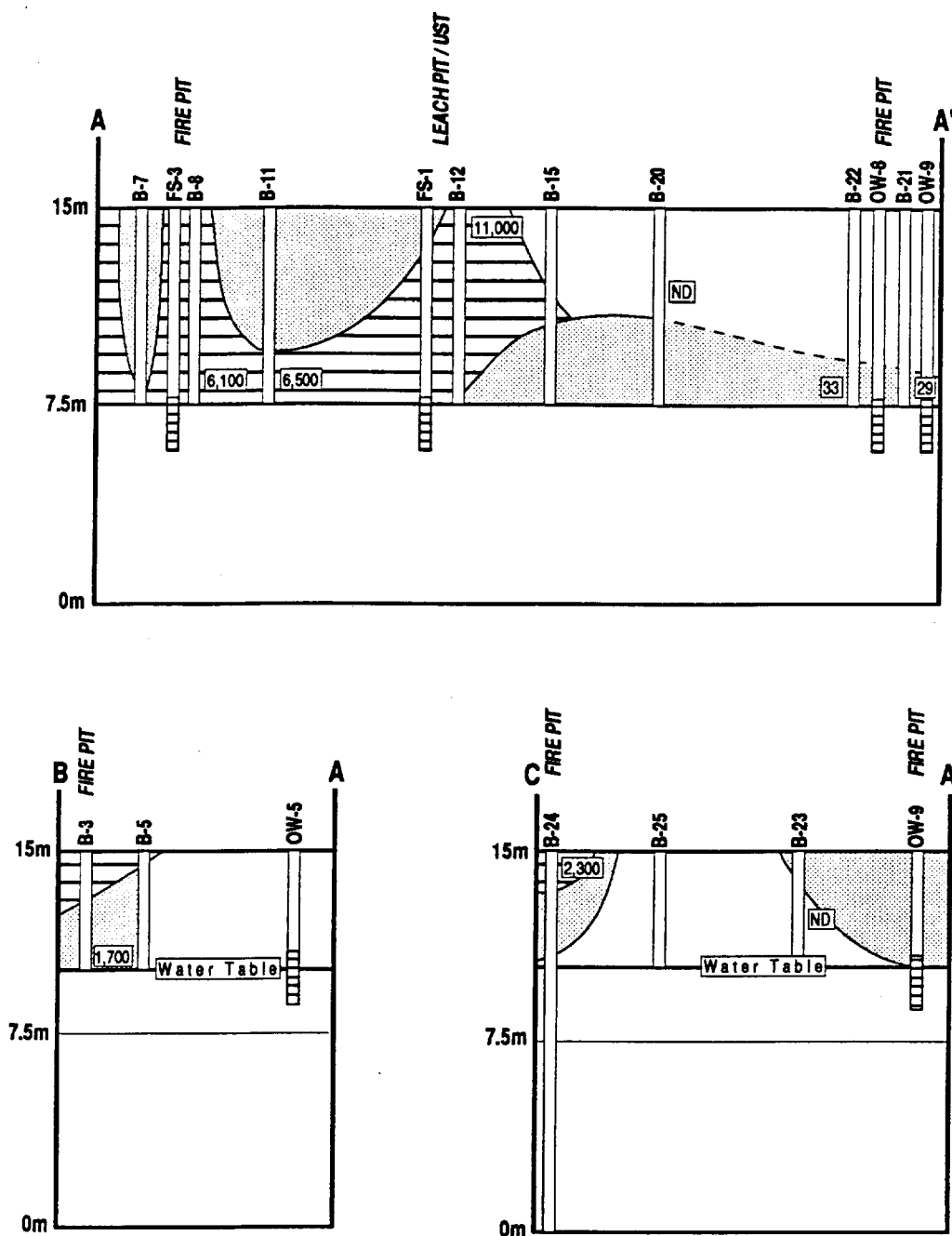

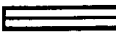

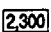


FIGURE 16. Total Petroleum Hydrocarbons in the Unstaurated Zone - Cross Section (Qualitative Field Measurements of TPH)

-  HIGH - High Intensity peaks detected with Field G.C.
-  LOW - Any peaks below high intensity detected with Field G.C.
-  NONE DETECTED
-  Measured TPH Concentration from Laboratory Analysis (mg/kg)

The total mass of TPH in the unsaturated zone is estimated at 6900 kg (Table 3), with the greatest amount in the vicinity of the central underground storage tank and the zig-zag pit. The round pit on the southwest corner of the site is the source of the second highest mass of TPH, followed by northwest the fire pit. As the parent TPH is No. 2 fuel oil, which has a specific gravity of 0.85 (Pamukcu et al, 1990), the volume of oil spilled at the site is at least 8,100 L (2140 gal).

The calculation of TPH mass above the water table should only be considered an order of magnitude estimate because of the number of assumptions and potential for error in the calculations. The main source of error is in the interpolation of TPH concentrations because of the wide horizontal spacing of data points (25-50 ft), the four foot vertical separation between samples, and the relatively few (20) soil samples that were analyzed for TPH concentrations. The estimate should also be considered a lower limit for the total spill volume because it does not account for material that has dissolved to groundwater, volatilized into the atmosphere, or been degraded by microorganisms. In spite of the potential errors, the measurements provide an estimate of the hydrocarbon source remaining in the unsaturated zone, and can be useful in deciding appropriate remedial actions.

Table 3: Estimate of TPH Mass in Unsaturated Zone Sediments

Source	Concentration/ Contour Interval (mg/kg)	Area (m ²)	Thickness (m)	Volume (m ³)	Total Soil Mass (kg)	TPH Mass (kg)	Totals (kg)
Round Pit	5,000	90	1	110	288,785	1,444	
Round Pit	500	62	4	247	648,277	324	1,768
Center System	10,000	28	2	43	112,760	1,128	
Center System	5,000	111	3	305	800,484	4,002	
Center System	500	255	3	777	2,041,587	1,021	6,151
Northwest Pit	1,000	72	2	109	286,552	287	
Northwest Pit	500	72	2	174	458,483	229	516
Total TPH Mass at Site							8,435
Volume of Fuel Oil Spill Assuming Density =0.9							2,476

HYDROCARBON CONTAMINATION IN THE SATURATED ZONE

Since the discovery of fuel oil contamination at the site, over 25 rounds of groundwater samples have been taken from monitoring wells on the site for analyses of total petroleum hydrocarbons and volatile organic compounds. The number of wells sampled in each round varied, but generally increased as the new monitoring wells were installed. Two rounds of sampling conducted in July 1989 and October-November 1990 show the most complete picture of the contaminant plumes at the site. The 1990 sampling was conducted by the Cape Cod Commission (1991).

Methods of Sampling and Analysis

Prior to sampling, each well was purged for 5 to 10 min using a gasoline-powered pump operating at approximately 19 L/min (5 gpm). The purging continued until measurements of specific conductance in the discharge water had stabilized. Sample water was then taken from the well using a decontaminated PVC bailer. Three bailer volumes were removed from the well before the sample was taken. Samples from the two multi-level samplers ML-9 and ML-14 were taken using a peristaltic pump. A dedicated sampling tube connecting the multi-level sampler to the pump was used for each sampling port. The pump was run for 5 minutes at 1-2 L/min (0.25-0.5 gpm) to purge water from the sampling tube prior to a sample being taken.

All the VOC samples were collected in two 40 mL glass containers with teflon caps that were filled completely, leaving no headspace. Samples were delivered, on ice, to the Barnstable County Health and Environmental Laboratory for analysis according to EPA method 502.1/503.

TPH samples taken in the July 1989 sampling round were collected in 1 L, Teflon-capped jars. Twenty-eight samples were analyzed using an infrared technique (EPA Method 418.1) with a detection limit of 0.5 mg/L. Four split samples were analyzed using a hydrocarbon fingerprinting technique (a modification of ASTM Method D3328), which

allowed an examination of the type of hydrocarbon and a lower detection limit for reporting individual hydrocarbons (0.01 mg/L). All TPH analyses were conducted by ERCO Laboratories of Cambridge, Massachusetts.

Estimates of TPH concentrations were made for the fall 1990 samples by determining the areas under the peaks from the chromatograms used to determine individual VOC concentrations. The 502.1/503 methods used in the VOC analyses provide for the detection of many of the heavier, higher boiling point compounds. Their total concentrations were used as an estimate of TPH concentrations (Cape Cod Commission, 1991).

Following the sampling at each well, measurements of dissolved oxygen were taken using a dissolved oxygen meter (YSI model 51B). The meter's probe was placed just above the bottom of the well screen and allowed to equilibrate with the groundwater that had been brought into the well by the purging with the gasoline-powered pump. Details on the dissolved oxygen results are provided in Geochemistry section of this thesis.

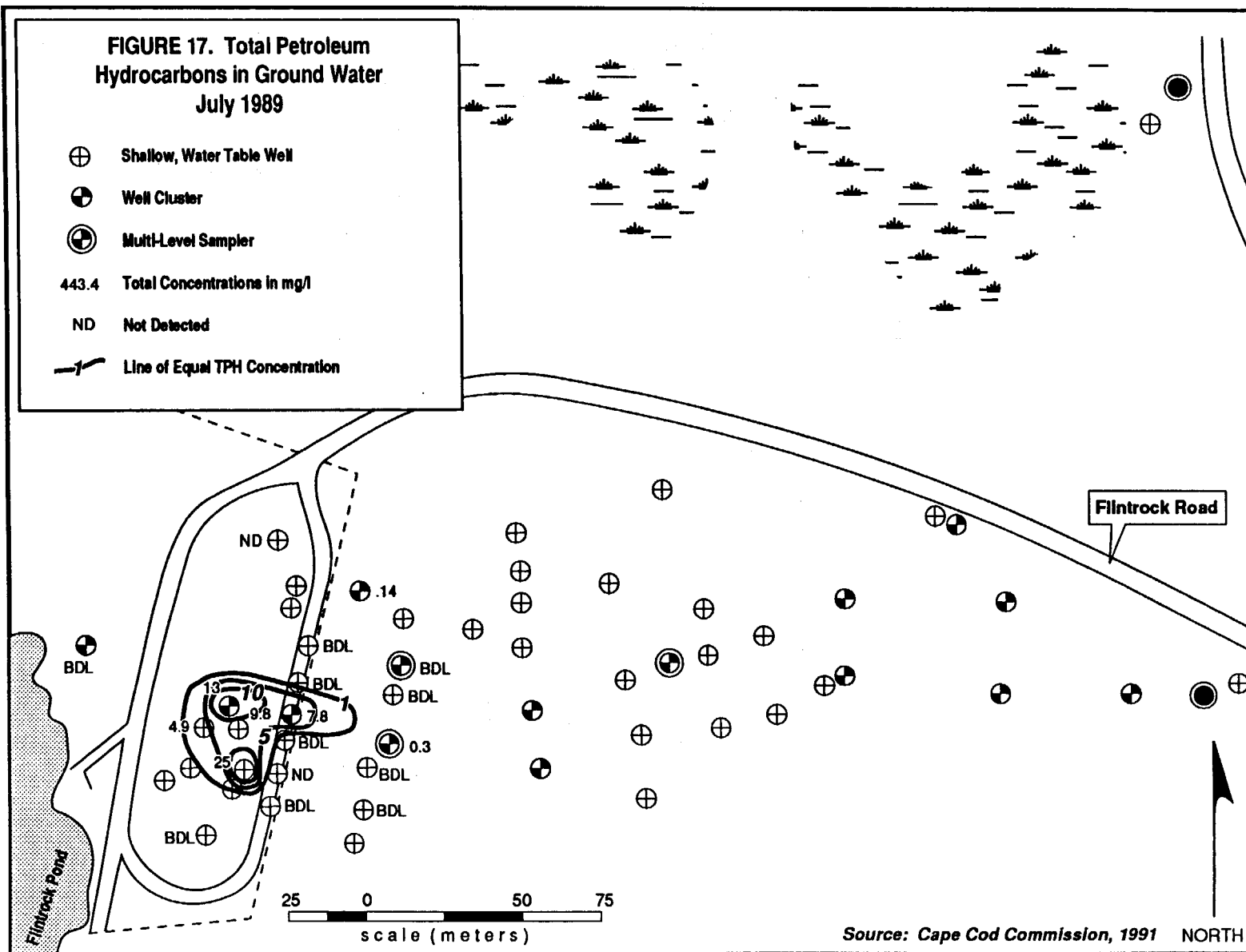
Results of TPH analysis

The highest TPH concentrations among the July 1989 analyses were in samples from wells in areas that correlate with the higher concentrations of soil contamination in the central portion of the site (Figure 17). These ranged as high as 25 mg/L in well FS-3 adjacent to the zig-zag pit where the leak in the fuel line was discovered. TPH concentrations decreased downgradient of the site, to 7.8 mg/L in well MW-3s. It is likely that lower TPH concentrations exist in areas further downgradient of the site that could not be seen because of the relatively high detection limit of the method used in most of the analyses (0.5 mg/L). The GC/FID analyses conducted by ERCO laboratories identified the hydrocarbons as a weathered fuel oil, possibly #2 fuel oil.

The 1990 TPH estimates using the 502.1/503 method show that TPH concentrations below 0.5 mg/L are present in wells downgradient of the site (Cape Cod Commission, 1991). They also indicate that TPH concentrations have decreased in the year between sampling rounds, and since investigations have been conducted at the site.

FIGURE 17. Total Petroleum Hydrocarbons in Ground Water July 1989

- ⊕ Shallow, Water Table Well
- ⊙ Well Cluster
- ⊕ Multi-Level Sampler
- 443.4 Total Concentrations in mg/l
- ND Not Detected
- Line of Equal TPH Concentration



Source: Cape Cod Commission, 1991 NORTH

For example, samples from well FS-1s located near the central underground storage tank decreased in concentration from 44 mg/L in 1986 to 13 mg/L in 1989, and to 2.7 mg/L in 1990.

Calculations show that an estimated 2 kg of TPH is present in groundwater, based on the 1989 analyses (Table 4). These calculations were conducted in the same way as the soil TPH mass calculations, and the same concerns about the accuracy of the estimates apply. Approximately 0.03 percent of the TPH in the unsaturated zone in 1989 was found as dissolved TPH in groundwater at the same time.

Concentrations of individual hydrocarbon compounds in the unsaturated soil can not be compared to those in groundwater samples because of the laboratory methods used in the analyses. Lighter, more soluble components are assumed to dissolve into groundwater while heavier, less soluble components remain in the unsaturated zone.

Results of VOC Analyses

The results of the VOC analyses from both the July 1989 and the fall of 1990 sampling events show two areas of groundwater contamination (Figures 18 and 19). The largest plume begins in the central portion of the site near the site of the former underground storage tank and the leak in the fuel oil distribution line. It also extends back to the round fire pit in the southwest corner of the site. Total VOC concentrations of 1323 µg/L were detected in samples near the central underground storage tank in July 1989.

A smaller area of contamination was also found moving away from the northern part of the site. The source of this contamination is one or both of the northern fire pits. There are no monitoring wells between the two fire pits, so it is not possible to determine if both are a source of the contamination.


The vertical VOC plume thickness was determined to be between 1.2 to 2 m (4 to 6 ft) in the main plume based on analyses of samples from deep monitoring wells and multi-level sampling points (ML-9 and ML-14), and confirmed by the dissolved oxygen measurements (see Geochemistry Section). The only exception are trace concentrations of benzene, toluene and ethylbenzene wells MS-3d and MW-9d screen approximately 7.6 m

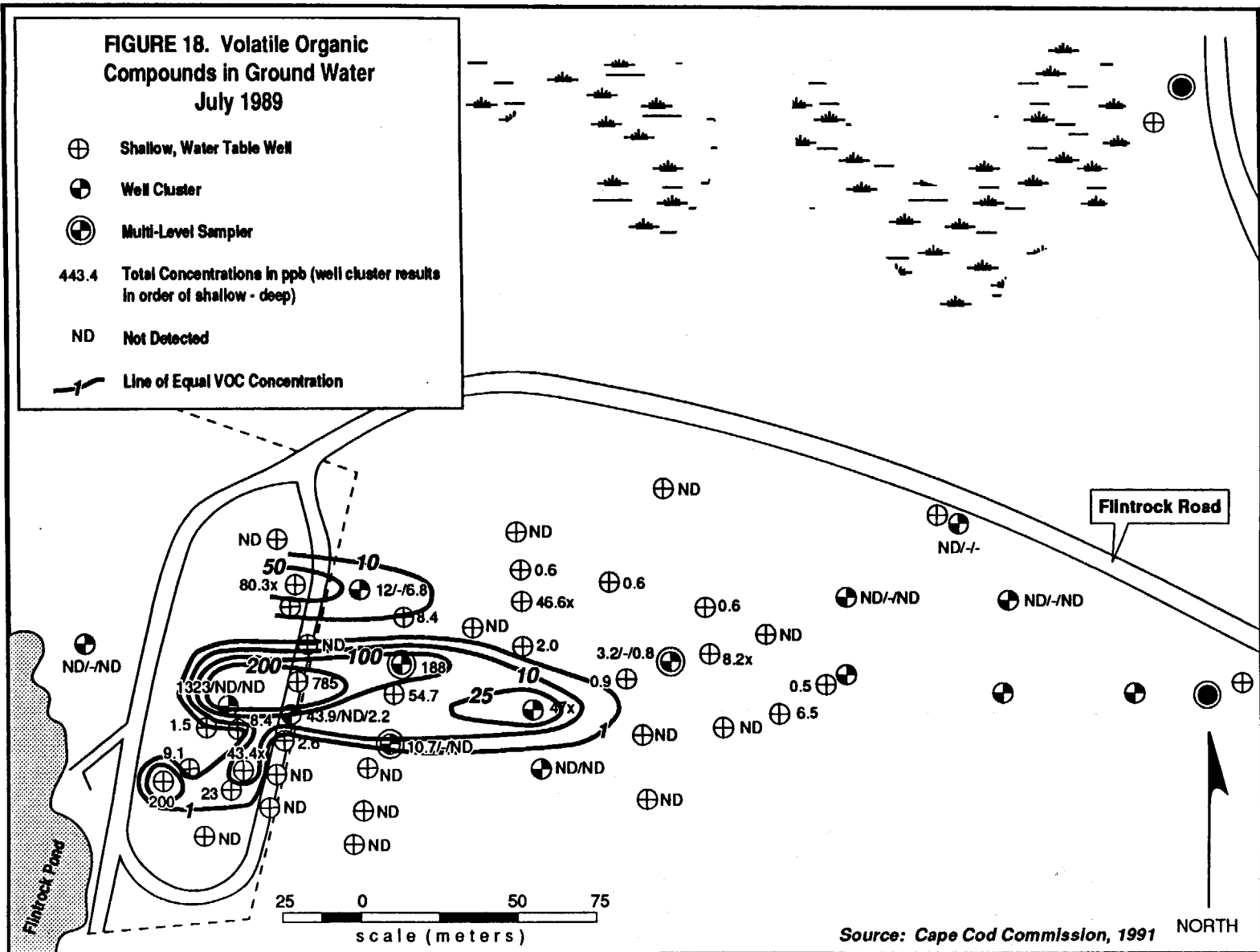
Table 4: Estimates Of TPH Mass In Groundwater

Concentration Contour Interval (mg/l)	Area (ft ²)	Thickness (ft ²)	Volume (Liters)*	TPH Mass (kg)
10	202	2	107,514	1.1
5	470	1	150,510	0.8
1	720	1	230,298	0.2
Total TPH in Groundwater (2.1

*-Assumes aquifer porosity of 0.35

FIGURE 18. Volatile Organic Compounds in Ground Water July 1989

- ⊕ Shallow, Water Table Well
 - ⊗ Well Cluster
 - ⊛ Multi-Level Sampler
- 443.4 Total Concentrations in ppb (well cluster results in order of shallow - deep)
- ND Not Detected
-  Line of Equal VOC Concentration



Source: Cape Cod Commission, 1991

(25 ft) below the water table. Samples taken downgradient from the source show the plume does not plunge below the water table until it has moved approximately 210 m (700 ft) from the site (Figure 20). From here the plume continues to plunge to the depth of the well screen at MD-3. The placement of well screens downgradient for the site are not adequate to accurately determine the plunge of the plume and its thickness as it moves towards well MD-3.

The VOCs in both contaminated areas consist primarily of BTEX compounds (benzene, toluene, ethylbenzene and xylenes), although trace to low concentrations of chlorinated solvents were detected both on site and in downgradient areas. In addition, naphthalene and trimethylbenzene were detected in five and six wells respectively in the 1990 sampling.

Trace levels of chloroform were detected in many of the samples both on and off the site. Chloroform is found in groundwater throughout Cape Cod, including in 93 % of the public drinking water supplies (BCHED 1987). The source of the chloroform is not well understood, and may be the result of reactions between atmospheric chloride or human-disposed chlorine compounds and humic substances in the soils and subsurface sediments (BCHED 1987).

The greatest contamination of soils and groundwater occurs in the vicinity of well FS-1s. This suggests that the source of the BTEX compounds in groundwater is the fuel oil remaining in the unsaturated zone. They dissolve into infiltrating water and are washed into the saturated zone. Fluctuations in the water table may also cause variations in the concentrations of hydrocarbons entering groundwater. In addition to the residual fuel oil, an accidental overflow of contaminated water from one of the underground storage tanks increased soil and groundwater contaminant concentrations.

Total volatile organic concentrations in the main contaminant plume have decreased in the year between sampling, with concentrations in well FS-1s dropping from 1323 $\mu\text{g/L}$ to 843 $\mu\text{g/L}$. At the same time, however, the area of contamination over 100 $\mu\text{g/L}$ has increased and moved further downgradient. While total concentrations are decreasing, the size of the plume is increasing.

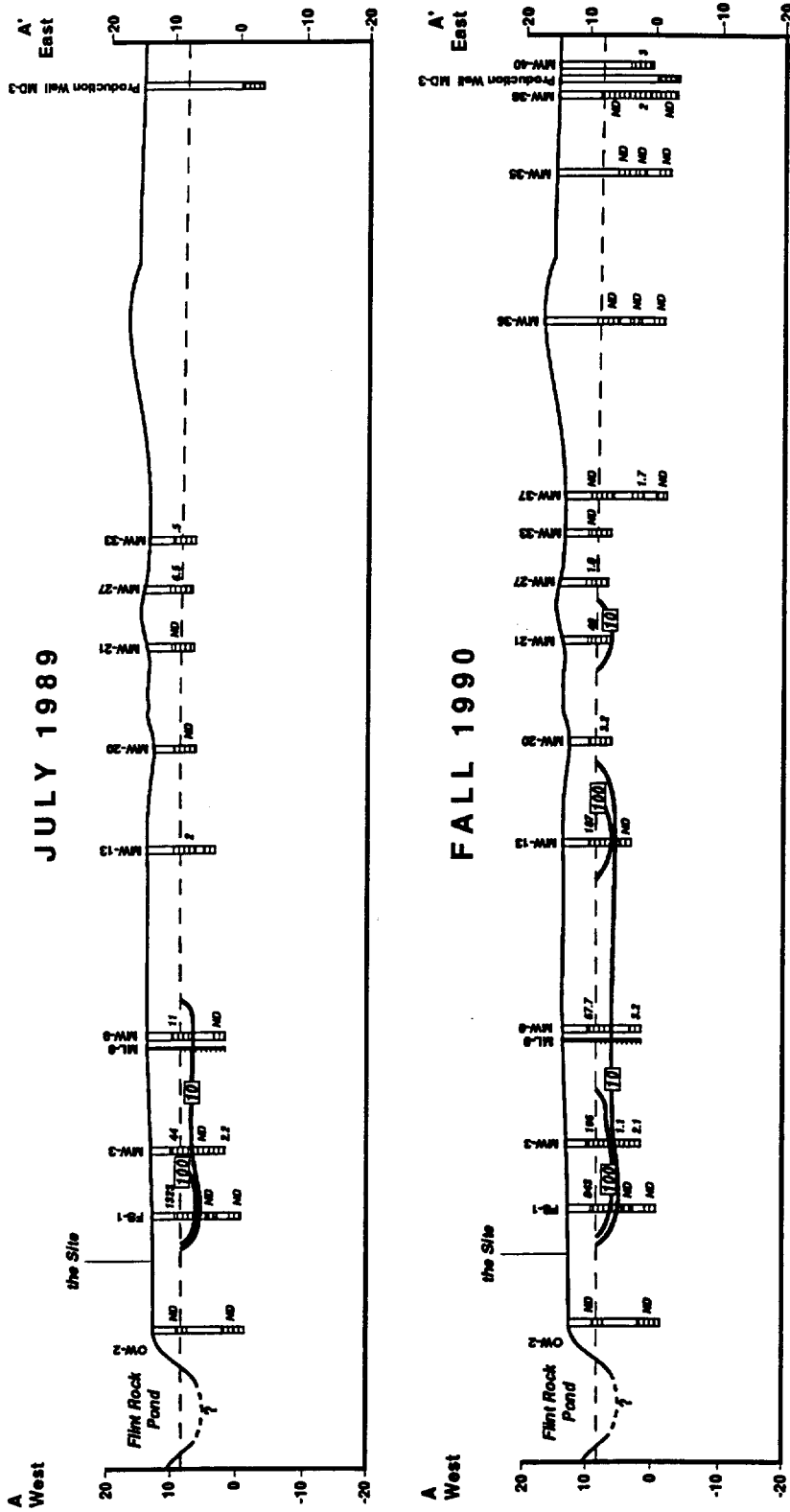


FIGURE 20. Volatile Organic Compounds in Ground Water July 1989 and Fall 1990

Changes in the composition of the main plume occur as it moves downgradient, most likely because of variations in the source strength and composition, and the differences in the retardation coefficients of the individual hydrocarbons. The compound that appears to have moved the farthest at the site is benzene, followed by the other BTEX compounds, toluene, ethylbenzene and xylenes (Figure 21). This fractionation of individual hydrocarbons is relatively consistent with retardation coefficients calculated for the site based on a measured fraction of organic carbon in the sediments ($f_{oc} = .011\%$, see Geochemistry Section), and an average of K_{oc} values for each compound from data summarized by Montgomery and Welkon (1990, Table 5).

Table 5: Calculated Retardation Coefficients for BTEX Compounds

	Retardation Coefficient
Benzene	1.07
Toluene	1.12
Ethylbenzene	1.15
Xylenes	1.39

The only noticeable exception is that xylenes appear to travel further from the site than toluene, even though its retardation coefficient is greater. Concentration variations at the source may be the cause of discrepancies in the relative movement of each compound over time. Discrepancies in the rates of degradation could also be a factor. Slight variations in sampling protocol and screen placement between wells also affect the data and should be considered in any interpretations.

The changes in water quality in the smaller, northern plume are opposite those in the main plume. Concentrations in well OW-9 next to the northeast fire pit have increased from 80 $\mu\text{g/L}$ to 443 $\mu\text{g/L}$ in the year between sampling events. Prior to 1989, no monitoring wells were installed in this area.

The mass of total VOCs in both plumes in 1989 and 1990 was calculated in the same manner as the soil and groundwater TPH estimates (Table 6). In the main plume the VOC mass dropped 16 % between sampling events, from 0.26 to 0.22 kg. Only a small fraction (0.003 percent) of the TPH mass in the unsaturated zone is present as dissolved VOCs. The total VOC mass in the northern plume grew approximately 420 % from 1989

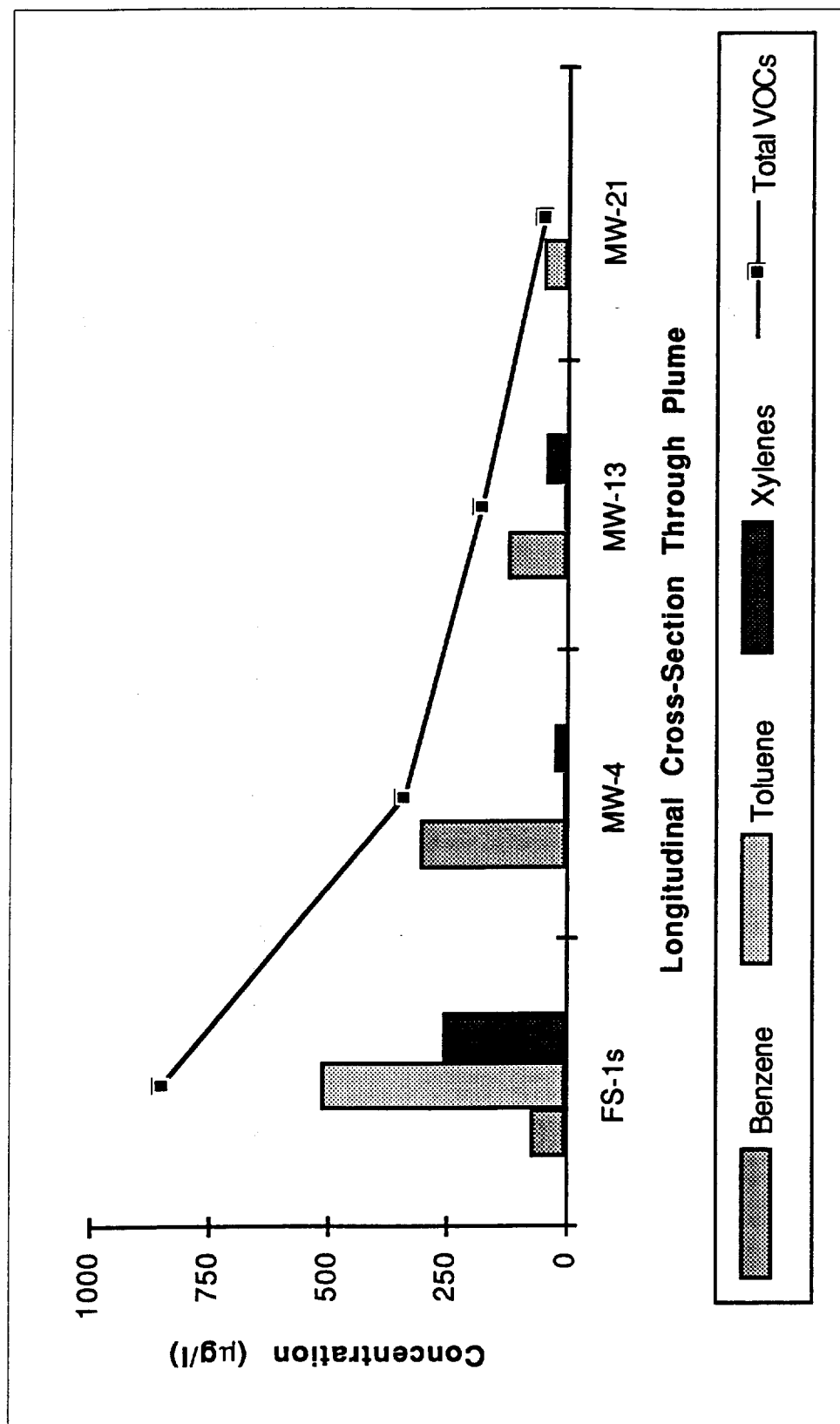


Figure 21: Composition of VOCs Longitudinally Through Plume

Table 6: Estimate of VOC Mass In Groundwater, 1989-1990

1989

Plume	Concentration/ Contour Interval (mg/l)	Area (m ²)	Thickness (m)	Volume (Liters)*	VOC Mass (kg)
#1	1,000	168	2	125,410	.125
#1	500	106	2	78,867	.039
#1	100	1,329	1	567,000	.057
#1	40	1,692	1	721,821	.029
#1	10	1,006	1	429,343	.004
Subtotal Plume #1					.255
#2	50	149	2	111,190	.006
#2	10	359	1	153,314	.002
Subtotal Plume #1					.007
Total VOC in Groundwater - 1989					.262

1990

#1	500	389	2	290,288	.145
#1	100	1,406	1	599,899	.060
#1	40	149	1	63,458	.003
#1	10	1,708	1	728,797	.007
Subtotal Plume #1					.215
#2	100	389	2	290,288	.029
#2	10	168	1	71,663	.001
Subtotal Plume #2					.030
Total VOC in Groundwater - 1990					.245

Percentage Change From 1989-1990

Plume #1	16%
Plume #2	419%

*-Assumes aquifer porosity of 0.35

to 1990, indicating an active discharge of hydrocarbons to groundwater in this area that more than compensates for losses to volatilization and degradation.

The quality of groundwater pumped from production well MD-3 has been analyzed carefully since 1986 and, until 1990, only trace levels of heavier fuel oil hydrocarbons have been detected. In 1990, benzene was detected for four months in 3 samples at concentrations ranging from 1.5 to 11 $\mu\text{g/L}$.

When the benzene was detected, additional monitoring wells were installed and sampled between the production well and the presumed toe of the plume. A thin strip with low concentrations of benzene was detected extending to the production well (See Figure 19). It appears that a small amount of benzene broke away and traveled to the area of the production well, creating a thin flow tube with low dissolved oxygen concentrations (See Geochemistry Section). Subsequent to the detection of the benzene the water quality in the production well improved, although it appears now that a low dissolved oxygen pathway exists for BTEX contamination to migrate from the site to the well.

THEORY ON PLUME DEVELOPMENT AT THE BARNSTABLE SITE

The effects of varying recharge at the Barnstable site, coupled with information on well construction and sampling artifacts were used to develop a hypothesis on the formation of the plume represented by 1990 sampling results. Under steady-state conditions the plume has stable contaminant concentrations. The only source is contamination dissolving into recharge water moving through the unsaturated zone. The maximum extent of hydrocarbon contamination is controlled by the solubility of the individual compounds in water.

As contaminated groundwater moves from the site, it is forced deeper into the aquifer by recharge entering the system from above. If recharge rates are constant over time, the plume will follow a consistent flow path down into the aquifer, similar to that modeled using Strack's solution for an aquifer receiving uniform recharge (Strack 1989). However, recharge rates have varied at the fire training site, and the plunge of the plume has not followed such a consistent path. A more detailed description of plume formation in unconfined aquifers, and the effects of varying recharge rates and the location of the plume source relative to aquifer boundaries is provided in Appendix A.

Two events have caused observed increases in hydrocarbon concentrations in groundwater; high water levels in 1987, and an accidental overflow of oil contaminated water from an underground storage tank in 1990. Flow rates in the aquifer are between 0.3 - 0.6 m/d (1-2 ft/d). Without any retardation, it would take 1.4 to 2.7 years for hydrocarbons to move from the source to the production well. As a result, both the 1987 and 1990 events are detectable in the 1990 sampling rounds (Figure 20).

The hydrocarbons that entered the aquifer in 1987 are the source of the deeper contamination close to the production well. During 1987, water levels rose to record levels causing an increase in plume thickness that was documented by increases in concentrations in samples from a well at the source (Figure 22, Well FS-1s). The record water levels were the result of an excess of 26 cm of precipitation in 1986 and 1987 (HWH, 1992).

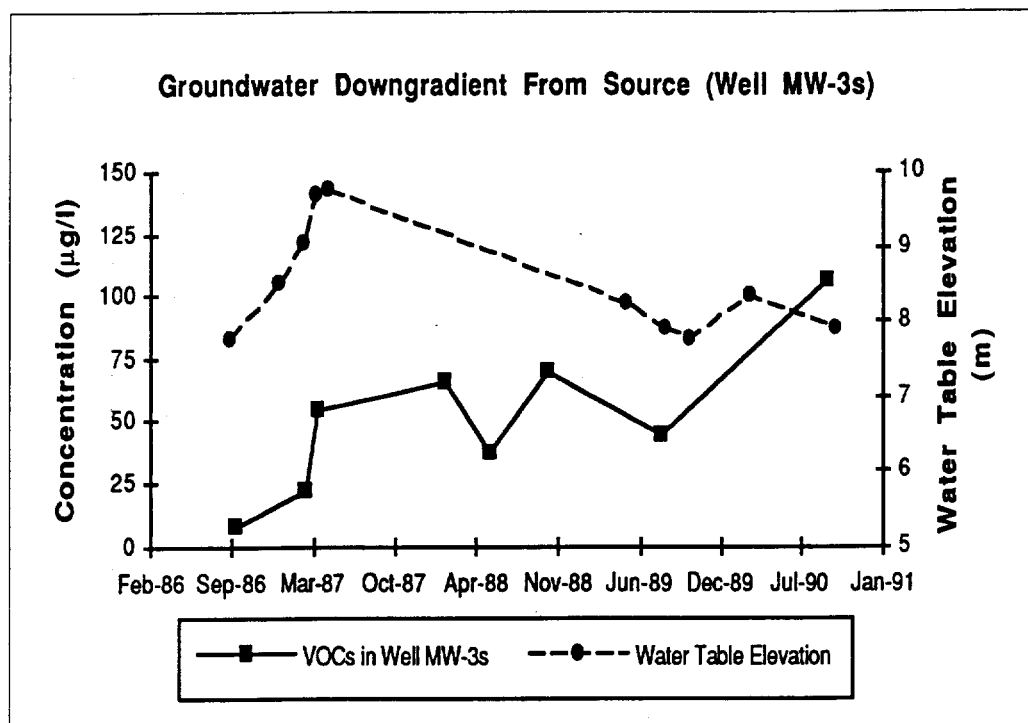
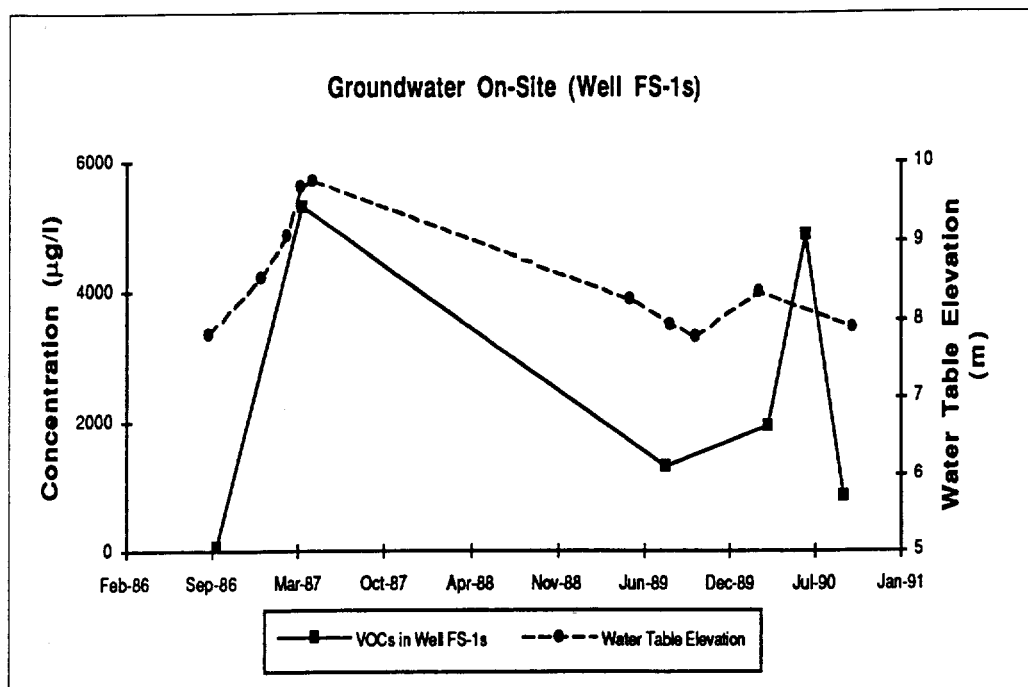


Figure 22: Comparison of VOC Concentrations to Water-Table Fluctuations

A greater percentage of the monitoring well screens near the source were occupied by plume water. As the contaminated water moved from the site, "clean" recharge caused the plume to plunge deeper into the aquifer. The plunge likely occurred near the source during the time the area was subject to high levels of precipitation recharge that caused the record increases in water table elevations throughout the region (Figure 10).

As the 1987 portion of the plume moved downgradient, recharge rates and water level elevations diminished, decreasing the angle of plunge and lowering water-table elevations. Over time, this portion of the plume migrated downgradient to its observed location near production well MD-3. The migration of the plume deeper in the aquifer would explain the occasional detections of hydrocarbons in mid-level well screens below the water table at well MW-14 and other wells downgradient from the site. The plume was moving just below the wells placed across the water table.

At the time of the 1990 tank overflow release, recharge rates and water table elevations had dropped from the peak levels in 1987. Total precipitation dropped 53 cm (20.9 in) below average for the years of 1988-1990. (HWH, 1992), causing a corresponding drop in recharge. The groundwater contamination caused by the 1990 release therefore remained close to the water table immediately downgradient from the site. With less recharge, the recent contamination has not plunged as deeply into the aquifer, resulting in the 4- 5 ft plume measured near the surface in wells ML-9 and ML-14.

Instead of moving through the aquifer with a consistent downward slope, the plume exhibits a stepped plunge caused by variations in the recharge rate. High recharge rates in 1987 caused a steep plunge of the plume. Lower recharge rates since then have allowed the 1987 portion of the plume to remain at a consistent depth in the aquifer, while the newer contamination has remained at the water table. Variations in the thickness of the plume over time have not been well documented at the site because of a lack of multi-level sampling points.

As expected, variations in VOC concentrations in groundwater at the source correlate well with measured water-table fluctuations. VOC concentrations in samples from well MW-3s downgradient from the source did not correlate as closely with water-table fluctuations (Figure 22). Well MW-3s is not located in the source area so groundwater is

not receiving new inputs of contaminants. The observed changes should instead reflect variations in the plume strength or depth relative to the well screen. The concentrations measured in this well have generally increased over time, although they dropped slightly between May 1987 and June 1989; similar to the water-table elevation. Given the lack of samples between 1987 and 1989 in well FS-1s, it is difficult to determine the actual plume strength and thickness at the source that resulted in the measured concentrations in samples from well MW-3s.

If the proposed plume development hypothesis is correct, it highlights the need to pay attention to recent fluctuations in recharge rates and resulting changes in water table elevations. It also shows that determining an average plunge for a plume may be a good initial estimate, but may not represent actual conditions. The relationship between horizontal and vertical groundwater flow rates should also be examined, as they will determine the angle of plume plunge for a given recharge rate. The eventual depth of a plume will not vary with different horizontal flow rates, but the distance from the source at which the plume reaches a particular depth will be different. Again, one needs to accurately understand the hydrologic system to properly determine contaminant flow paths.

This hypothesis still does not explain the hydrocarbon concentrations detected in samples from deep wells MW-9d and MW-3d. The hydrocarbons may have been forced deep into the aquifer by temporary mounding caused by site activities. Mounding was observed in on-site wells in August 1989, at a time when heavy water use for fire training activities was noted. An analysis of water level measurements in well clusters indicates that this mounding created downward vertical gradients in the vicinity of the site. Further downgradient, horizontal flow resumed. The vertical gradients indicate that a route existed for contaminants to migrate to deeper portions of the aquifer, to the depths of wells MW-3d and MW-9d. Like precipitation recharge, the on-site groundwater mounding flushes more water through the contaminated zone and pushes the plume deeper into the aquifer.

The frequency of peak uses at the site that would cause mounding is not known, but they likely occur more often in the summer months. Measurements from May 1987, when the site was not being used, show no measurable vertical gradients across the site.

The hydrocarbons detected here could also have been caused by of cross contamination during sampling or well installation, although this is less likely as concentrations were detected twice over a period of 15 months. If contamination occurred from improper sampling practices, it is not likely to be repeated so similarly. If contamination occurred during well installation it should have moved away from the well, or decreased in concentration between the sampling events.

GEOCHEMISTRY

INTRODUCTION

An analysis of the aquifer sediments and the groundwater was conducted to evaluate the effects of the plume on aquifer geochemistry, including the weathering of parent minerals and the precipitation of secondary products. The sediment composition was analyzed visually using sediment samples from clean areas on the site. The composition was also analyzed using x-ray diffraction spectroscopy. The amounts of total organic carbon (TOC) and extractable iron, manganese and aluminum available in the sediment grains were also determined.

Ground water analyses were conducted using samples from eleven monitoring wells and four multi-level sampling points in order to determine the inorganic chemical composition of groundwater across the site. Sampling locations were chosen to provide information across the plume in three directions, longitudinally in the direction groundwater flow, transverse through the center of the plume and vertically, using multi-level sampling points at MW-9. Wells MW-15s and OW-2 were chosen to provide background information in areas thought to be unaffected by the plume. The methods of sampling and analysis, and the results of the analyses are described below followed by a discussion of aluminosilicate weathering reactions at the site.

Methods

Solid Phase Analyses

Mineralogy The chemical makeup of the subsurface sediments was examined to better understand the nature of solid phase/aqueous phase interactions. A sample of sediment was taken for visual and x-ray diffraction analysis from a depth of 8 feet below grade in Boring B-25, an area on-site with no fuel oil contamination (see Figure 14 for

location). A portion of the sample was crushed and ground using a mechanical mortar and pestle. It was analyzed using a Nicolet I2 x-ray diffractometer to determine the bulk mineral composition of the sediments.

Total Organic Carbon Analysis A portion of the sample used in the x-ray diffraction analysis was also examined to determine the amount of total organic carbon available for use by micro-organisms and for retardation reactions with the hydrocarbon contaminants. The TOC was determined using a chromium reduction technique modified from a procedure developed by Walkley and Black (1934). The sediment sample was mixed with potassium dichromate ($K_2Cr_2O_7$) and sulfuric acid. After sitting for 30 minutes the sample was centrifuged to remove particulate matter, and the amount of Cr(VI) reduced by the organic carbon and remaining Cr(VI) was determined by comparison with standards using the diphenylcarbazide method (APHA, 1989). The amount of hexavalent chromium reduced by the sediment sample was used to calculate the percentage of organic carbon.

Extractable Iron, Manganese and Aluminum Analysis The amount of solid phase iron, manganese and aluminum that is readily available to dissolve into groundwater was determined using oxalate and dithionate-citrate-bicarbonate (DCB) extractions. The oxalate extraction removes the amorphous materials coating the sediments that will dissolve in the weak acid solution. The DCB extractions are harsher, and are designed to extract the crystalline oxide components of the compounds that can dissolve into the aqueous phase under more extreme chemical conditions. The extractions were conducted sequentially using two sediment samples taken from 2.5 m and 4 m depths in a boring located in an uncontaminated portion of the site (samples B25-2 and B25-3). Oxalate extractions of the sediment were followed by the DCB extractions.

Groundwater Sampling

Sampling was conducted from 22-27 October 1989. The weather throughout the sampling period was sunny and dry, with temperatures of 13° to 18 °C. Each monitoring well included in the sampling program was pumped for approximately five minutes at approximately 19 L/min (5 gpm) using a gasoline powered pump to evacuate water in, and around the well casing. The pump was run for 5 to 15 minutes, depending on the depth of

the well, such that approximately 10 to 15 well volumes were removed. Water for sampling was then taken using a peristaltic pump with dedicated polyethylene tubing used for each well. The multi-level sampling points were evacuated and sampled using the peristaltic pump.

Water drawn by the peristaltic pump was discharged directly into a clear PVC flow cell in which probes were installed to measure pH, Eh, temperature and dissolved oxygen before the groundwater was exposed to the atmosphere. Groundwater was pumped through the flow cell for 10 to 20 minutes until measurements of pH, Eh, temperature and dissolved oxygen stabilized to $\pm 5\%$. Intermediate and final measurements were recorded. Samples were then taken from the discharge point of the flow cell for analysis of total concentrations of Fe, Mn, Mg, NO_3 , NH_3 , Cl, SO_4 , Al, Ca, K, Na, and SiO_2 . Duplicate samples were taken for each, with one filtered through $0.45 \mu\text{m}$ GFC glass fiber filter. Samples for metals analysis were preserved at pH 2 using nitric acid. Ammonia samples were preserved using sulfuric acid. Silicate samples were preserved at pH 12 using sodium hydroxide.

Field alkalinity titrations were conducted on both filtered and unfiltered samples. The titrations were conducted using 0.146 M nitric acid that was added in 25 to 100 μl volumes until the sample pH fell below the alkalinity end point of approximately 4.3. The acid was pipetted into a 250 ml plastic bottle containing 100 ml of sample using an automatic pipette. The sample was shaken between acid injections and the pH was recorded. Alkalinity was computed from the amount of acid needed to reach the end point pH.

Between sampling stations the pH meter was calibrated using pH 4 and pH 7 buffer solutions. The Eh probe was calibrated to ZoBell's solution with the appropriate reading determined based on temperature corrections (Nordstrom, *et al* 1990). The dissolved oxygen meter was calibrated according to temperature by inserting the probe in a small plastic bottle containing water saturated with atmospheric oxygen.

Along with the measurements taken during the October 1989 sampling round, dissolved oxygen concentrations were also measured during the volatile organic sampling rounds in July 1989 and the fall of 1990. In both of these sampling rounds, measurements

were taken by inserting the dissolved oxygen probe to the bottom of the monitoring well after it had been pumped and sampled.

Groundwater Analyses

Trace metals and cations were analyzed using Atomic Adsorption Spectroscopy using an air-acetylene flame. Samples were compared against laboratory standards to determine concentrations. If concentrations were outside the linear range of the spectrometer, as indicated by the standard, they were diluted and reanalyzed. Chloride and sulfate concentrations were determined using a Hewlett Packard ion chromatograph. Laboratory standards and the groundwater samples were run through the machine using a parahydroxybenzoic acid (PHBA) eluent buffered at pH 9.5.

Silicate concentrations were determined using a molybdosilicate method (AHPA, 1989) with a detection limit of approximately 1 mg/L. In the method, ammonium molybdate, $(\text{NH}_4)_6\text{Mo}_7\text{O}_{24}\cdot\text{H}_2\text{O}$, is added to the sample where it reacts with both silicate and phosphate to form an acid. Oxalic acid is added to break down the molybdophosphoric acid, leaving the yellow colored molybdosilicic acid. The molybdosilicic acid concentration is determined using a spectrophotometer at a wavelength of 410 nm by comparing to standard silica solutions prepared with the ammonium molybdate and oxalic acid. Nitrate and ammonia samples were analyzed by the Barnstable County Health and Environmental Laboratory using standard methods (AHPA, 1989).

RESULTS

Solid Phase Chemistry

Grains of quartz, plagioclase and potassium feldspar and muscovite were observed in the sediment samples. Quartz was the dominant mineral, comprising over 90% of the sediments. Traces of darker, more mafic mineral, including magnetite were also seen. The minerals observed in samples from the Barnstable site are consistent with those found at the US Geological Survey research site located approximately 30 km away near Otis Air Force Base in Falmouth, Massachusetts. At the USGS site, quartz, plagioclase and orthoclase were the dominant minerals comprising 90% of the sediments (Barber *et al*, 1992). The

remaining 10% of the sediments consisted of 21 different accessory minerals including biotite, chlorite, glauconite, magnetite and muscovite.

Results of the diffraction analysis show that the majority of the sediment consists of quartz grains, with a small percentage of sodium rich feldspar, possibly albite (See Appendix B for diffraction pattern). The average TOC content was 0.011 %, based on the average of two samples analyzed at different times.

The results of the oxalate and DCB extractions are shown in Table 7. Iron readily dissolves in the oxalate extractions indicating it is present in the amorphous form on the sand grains. An even greater amount of iron is dissolved in the DCB extraction. Only trace amounts of manganese are removed in the oxalate extraction, with slightly higher concentrations observed in the DCB extractions. The relative difference between the iron and manganese concentrations are similar to the differences in measured groundwater concentrations. Iron concentrations were much higher than manganese concentrations in all groundwater samples.

The results for sample B25-3 (4 m depth) are twice as high as for B25-2 (2.5 m depth) for all the minerals. This sample could possibly be from a more concentrated layer of iron and manganese. It was taken from near the water table, and may have been periodically below the water table. The changing chemical conditions caused by the water table fluctuations could allow more precipitation of iron and manganese through differences in the amount of dissolved oxygen present between the aquifer and the unsaturated zone. The ratios of oxalate to DCB extraction concentrations for the iron were similar for both samples, indicating that, while there is more total iron in sample B25-3, the solid phase supplying the iron is similar in both samples.

Groundwater Chemistry

The sampling locations provided a good representation of changes in groundwater chemistry longitudinally through the main plume. The spacing of the wells chosen to provide a cross-sectional picture of the contaminant plumes (wells MW-6, 7, 8, 9, 10 and 11) did not extend across the full width of both plumes as additional wells north of well MW-11 were not available when sampling took place.

Table 7: Results of Extractable Iron, Manganese and Aluminum Analyses

	Iron		Manganese		Aluminum	
	B25-2	B25-3	B25-2	B25-3	B25-2	B25-3
Mass of Oxalate Extraction (mg/g)	0.033	0.067	Trace	Trace	0.031	0.110
Mass of DCB Extraction (mg/g)	0.240	0.520	0.002	0.003	0.042	
Oxalate/DCB	0.138	0.129			0.738	

Filtering of the samples appears to have had little effect on the analytical results (Table 8). The filters removed the larger sediment grains and particulates, but were not small enough to filter the smaller particulates or colloids that may be influencing the results of the dissolved species analysis. A comparison of the results of filtered versus unfiltered samples does provide a check on the precision of the sampling and analytical methods.

Charge balance errors, an indication of the completeness and accuracy of the water quality data, were below 13 percent for all fourteen samples used in the model runs. All but three of the samples (MW-11, -13%; ML-92, - 9% and FS-1s, - 8.6%) contained errors below 5 percent. Errors were calculated using the aqueous speciation program WATEQ4F (Plummer, *et al*, 1978).

Dissolved Oxygen

Background dissolved oxygen concentrations were approximately 0.2 mM (6.3 mg/L, well MW-15s), and decreased to almost zero in the center of the contaminant plume for the October 1989 analyses (Table 8). Background concentrations from July 1989 and September 1990 extended up to 10 mg/L in water table wells across the site (Figures 23 and 24). These readings may be high, because the sampling technique allowed the water in the well to be in contact with the atmosphere when the reading was taken.

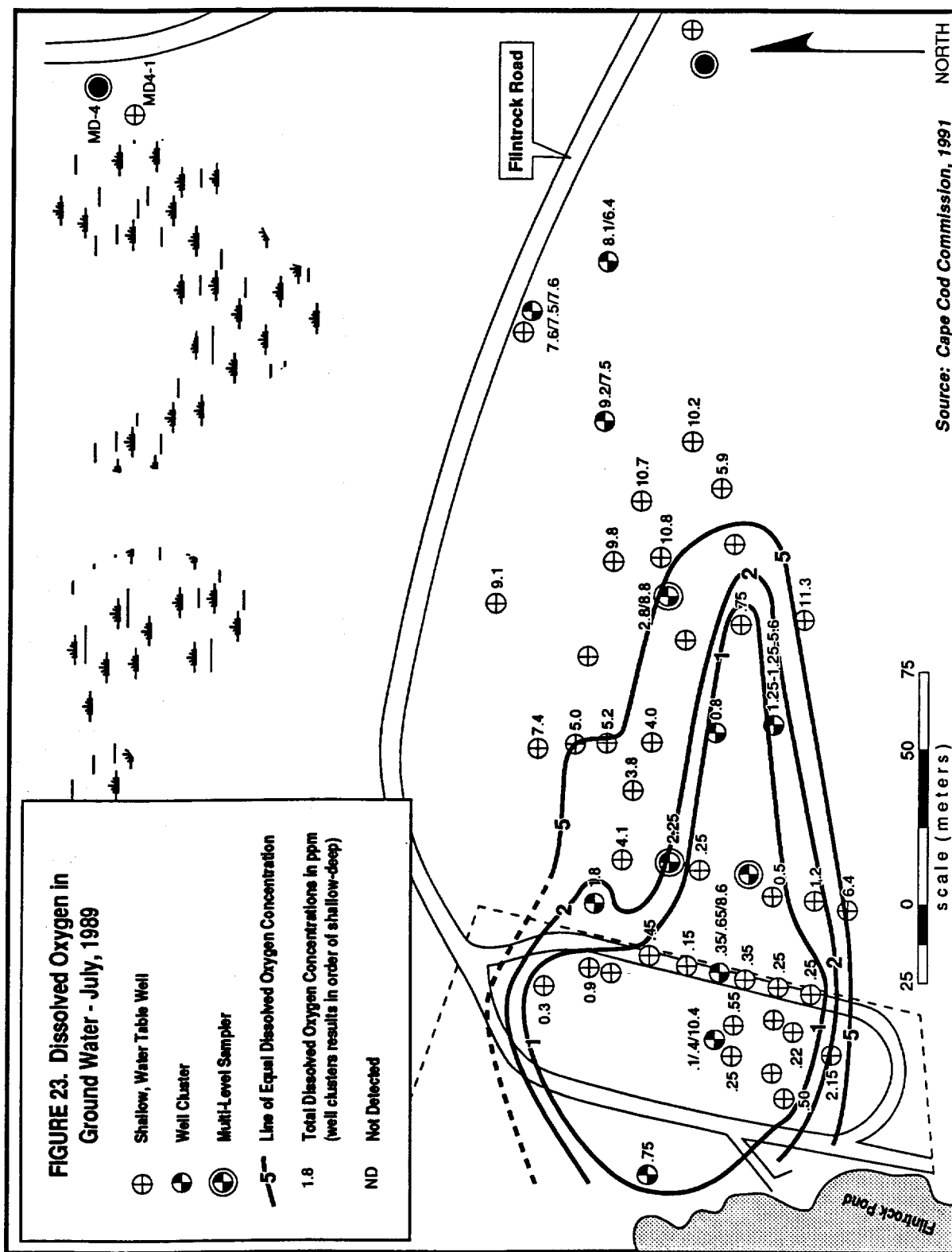
The concentration of dissolved oxygen drops to below 1 mg/L within the contaminant plume. Samples with concentrations below 1 mg/L are considered to have no dissolved oxygen present, as low oxygen readings are most likely because of oxygen remaining on the probe from prior to when the reading was taken.

The thickness of the dissolved oxygen plume corresponds to the hydrocarbon plume (Figure 25). The September 1990 measurements show a dissolved oxygen "hole" that extends from the site beyond production well MD-3. Like the hydrocarbon plume it remains at the surface of the aquifer up to 700 feet from the site before it dips down towards the production well screen. Dissolved oxygen concentrations are depleted in the upgradient well on the site where no contamination has been detected (OW-2). This well is directly downgradient from Flintrock Pond, and may be receiving groundwater that has migrated through the silt/muck pond bottom where oxygen was removed.

TABLE 8: RESULTS OF INORGANIC CHEMISTRY FIELD AND LABORATORY ANALYSIS											
WELL	TEMP	pH	Eh (mV)	ALK UNF. (EQ./L)	ALK FIL. (EQ./L)	DISS. OXY. (mg/l)	FE UNF. (mg/l)	FE FIL. (mg/l)	MN UNF. (mg/l)	MN FIL. (mg/l)	CA UNF. (mg/l)
OW-2	14.6	5.54	210	1.50E-04	1.30E-04	0.50	2.78	2.49	0.00	0.00	0.51
MW-6	12.1	6.15	450	2.90E-03	2.75E-03	1.60	0.81	0.06	0.00	0.00	11.72
MW-7	12.1	5.52	210	4.80E-04	4.20E-04	1.50	2.03	1.33	0.00	0.00	1.24
MW-8	12.1	6.03	280	1.78E-03	1.97E-03	0.75	18.74		0.69	0.68	1.39
ML-92	13.1	6.19	180	1.48E-03		0.30	33.08	37.12	1.11	1.08	1.87
ML-94	11.8	5.97	110	5.78E-04	5.90E-04	0.25	12.51	11.30	0.11	0.12	1.00
ML-96	11.5	5.65	120	2.00E-04	2.00E-04	0.25	4.63	4.80	0.00	0.00	0.43
MW-10	11.8	5.81	170	1.19E-03	1.10E-03	0.20	19.28		1.02	1.02	0.91
MW-11	12	6.03	350	1.90E-03	1.88E-03	0.75	9.69	12.11	2.36	2.24	1.20
MW-14S	13	5.70	370	2.40E-04			0.00	0.00	0.00	0.00	0.90
ML-143	13	5.64	530	6.10E-04			0.02	0.18	0.75	0.72	0.35
MW-15S	11.2	5.30	540	1.40E-04	1.20E-04	6.30	0.00	0.00	0.00	0.00	0.24
MW-17	12	6.05	480	6.57E-04	5.28E-04	5.80	0.00	0.00	0.00	0.00	0.14
FS-1S	15.4	5.93	140	1.58E-03	1.58E-03	0.05	16.55	12.51	0.45	0.43	0.97
WELL	TEMP	pH	Eh (mV)	ALK UNF. (EQ./L)	ALK FIL. (EQ./L)	DISS. OXY. (mM)	FE UNF. (mM)	FE FIL. (mM)	MN UNF. (mM)	MN FIL. (mM)	CA UNF. (mM)
OW-2	14.6	5.54	210	1.50E-04	1.30E-04	1.6E-02	5.0E-02	4.5E-02	0.0E+00	0.0E+00	1.3E-02
MW-6	12.1	6.15	450	2.90E-03	2.75E-03	5.0E-02	1.5E-02	1.1E-03	0.0E+00	0.0E+00	2.9E-01
MW-7	12.1	5.52	210	4.80E-04	4.20E-04	4.7E-02	3.6E-02	2.4E-02	0.0E+00	0.0E+00	3.1E-02
MW-8	12.1	6.03	280	1.78E-03	1.97E-03	2.3E-02	3.4E-01		1.3E-02	1.2E-02	3.5E-02
ML-92	13.1	6.19	180	1.48E-03		9.4E-03	5.9E-01	6.7E-01	2.0E-02	2.0E-02	4.7E-02
ML-94	11.8	5.97	110	5.78E-04	5.90E-04	7.8E-03	2.2E-01	2.0E-01	2.0E-03	2.2E-03	2.5E-02
ML-96	11.5	5.65	120	2.00E-04	2.00E-04	7.8E-03	8.3E-02	8.6E-02	0.0E+00	0.0E+00	1.1E-02
MW-10	11.8	5.81	170	1.19E-03	1.10E-03	6.3E-03	3.5E-01		1.9E-02	1.9E-02	2.3E-02
MW-11	12	6.03	350	1.90E-03	1.88E-03	2.3E-02	1.7E-01	2.2E-01	4.3E-02	4.1E-02	3.0E-02
MW-14S	13	5.70	370	2.40E-04			3.6E-05	3.6E-05	0.0E+00	0.0E+00	2.3E-02
ML-143	13	5.64	530	6.10E-04			3.6E-04	3.1E-03	1.4E-02	1.3E-02	8.8E-03
MW-15S	11.2	5.30	540	1.40E-04	1.20E-04	2.0E-01	3.6E-05	3.6E-05	0.0E+00	0.0E+00	5.9E-03
MW-17	12	6.05	480	6.57E-04	5.28E-04	1.8E-01	3.6E-05	3.6E-05	0.0E+00	0.0E+00	3.5E-03
FS-1S	15.4	5.93	140	1.58E-03	1.58E-03	1.6E-03	3.0E-01	2.2E-01	8.2E-03	7.8E-03	2.4E-02

TABLE 8: RESULTS OF INORGANIC CHEMISTRY FIELD AND LABORATORY ANALYSIS Cont.

WELL	CA FIL. (mg/l)	MG UNF. (mg/l)	MG FIL. (mg/l)	K UNF. (mg/l)	NA UNF. (mg/l)	CL UNF. (mg/l)	SO4 UNF. (mg/l)	SI UNF. (mg/l)	NO3 UNF. (mg/l)	NH3 UNF. (mg/l)	AL UNF. (mg/l)
OW-2	0.31	2.74	2.60	0.72	9.67	18.66	7.14	8.29	<.1	0.39	0.32
MW-6	10.77	5.24	5.18	88.72	23.95	34.48	36.05	6.56	1.40	<.01	0.11
MW-7	1.12	1.44	1.40	20.33	20.65	38.76	16.18	6.18	1.00	0.05	0.04
MW-8	1.35	2.88	3.77	3.59	21.60	5.70	10.75	6.56	<.1	2.43	0.03
ML-92	1.89	3.67	4.56	4.40	15.73	11.58	6.53	5.14	0.30	0.79	0.03
ML-94	1.00	2.88	2.86	1.39	11.30	25.35	TR	4.38	<.1	0.02	0.09
ML-96	0.45	2.79	2.41	1.12	10.35	22.74	6.26	7.88	<.1	0.69	0.03
MW-10	0.91	2.85	3.02	1.97	16.67	24.61	TR	6.22	0.20	0.50	0.05
MW-11	1.23	3.30	3.20	1.97	22.59	17.83	4.77	7.23	0.80	0.22	0.03
MW-14S	1.16	1.28	1.17	1.06	16.54	16.78	5.96	5.44	0.20	<.01	0.02
ML-143	0.35	1.27	1.22	1.14	15.73	14.07	TR	6.35	0.30	<.01	0.53
MW-15S	0.22	0.58	0.58	0.66	11.07	11.70	5.17	4.56	0.10	<.01	0.03
MW-17	0.08	0.55	0.50	0.70	18.44	12.17	6.58	6.68	0.30	<.01	0.01
FS-1S	0.81	1.90	1.92	1.63	19.88	15.20	3.13	6.14	1.20	0.77	0.05
WELL	CA FIL. (mM)	MG UNF. (mM)	MG FIL. (mM)	K UNF. (mM)	NA UNF. (mM)	CL UNF. (mM)	SO4 UNF. (mM)	SI UNF. (mM)	NO3 UNF. (mM)	NH3 UNF. (mM)	AL UNF. (mM)
OW-2	7.7E-03	1.1E-01	1.1E-01	1.8E-02	4.2E-01	5.3E-01	7.4E-02	1.4E-01	BDL	2.3E-02	1.2E-02
MW-6	2.7E-01	2.2E-01	2.1E-01	2.3E+00	1.0E+00	9.7E-01	3.8E-01	1.1E-01	2.3E-02	BDL	4.1E-03
MW-7	2.8E-02	5.9E-02	5.8E-02	5.2E-01	9.0E-01	1.1E+00	1.7E-01	1.0E-01	1.6E-02	2.9E-03	1.5E-03
MW-8	3.4E-02	1.2E-01	1.6E-01	9.2E-02	9.4E-01	1.6E-01	1.1E-01	1.1E-01	BDL	1.4E-01	1.1E-03
ML-92	4.7E-02	1.5E-01	1.9E-01	1.1E-01	6.8E-01	3.3E-01	6.8E-02	8.6E-02	4.8E-03	4.6E-02	1.0E-03
ML-94	2.5E-02	1.2E-01	1.2E-01	3.5E-02	4.9E-01	7.2E-01	TR	7.3E-02	BDL	1.2E-03	3.3E-03
ML-96	1.1E-02	1.1E-01	9.9E-02	2.9E-02	4.5E-01	6.4E-01	6.5E-02	1.3E-01	BDL	4.1E-02	1.3E-03
MW-10	2.3E-02	1.2E-01	1.2E-01	5.0E-02	7.3E-01	6.9E-01	TR	1.0E-01	3.2E-03	2.9E-02	1.7E-03
MW-11	3.1E-02	1.4E-01	1.3E-01	5.0E-02	9.8E-01	5.0E-01	5.0E-02	1.2E-01	1.3E-02	1.3E-02	1.0E-03
MW-14S	2.9E-02	5.3E-02	4.8E-02	2.7E-02	7.2E-01	4.7E-01	6.2E-02	9.1E-02	3.2E-03	BDL	8.5E-04
ML-143	8.8E-03	5.2E-02	5.0E-02	2.9E-02	6.8E-01	4.0E-01	TR	1.1E-01	4.8E-03	BDL	2.0E-02
MW-15S	5.4E-03	2.4E-02	2.4E-02	1.7E-02	4.8E-01	3.3E-01	5.4E-02	7.6E-02	1.6E-03	BDL	1.0E-03
MW-17	2.1E-03	2.3E-02	2.1E-02	1.8E-02	8.0E-01	3.4E-01	6.9E-02	1.1E-01	4.8E-03	BDL	4.8E-04
FS-1S	2.0E-02	7.8E-02	7.9E-02	4.2E-02	8.6E-01	4.3E-01	3.3E-02	1.0E-01	1.9E-02	4.5E-02	1.7E-03



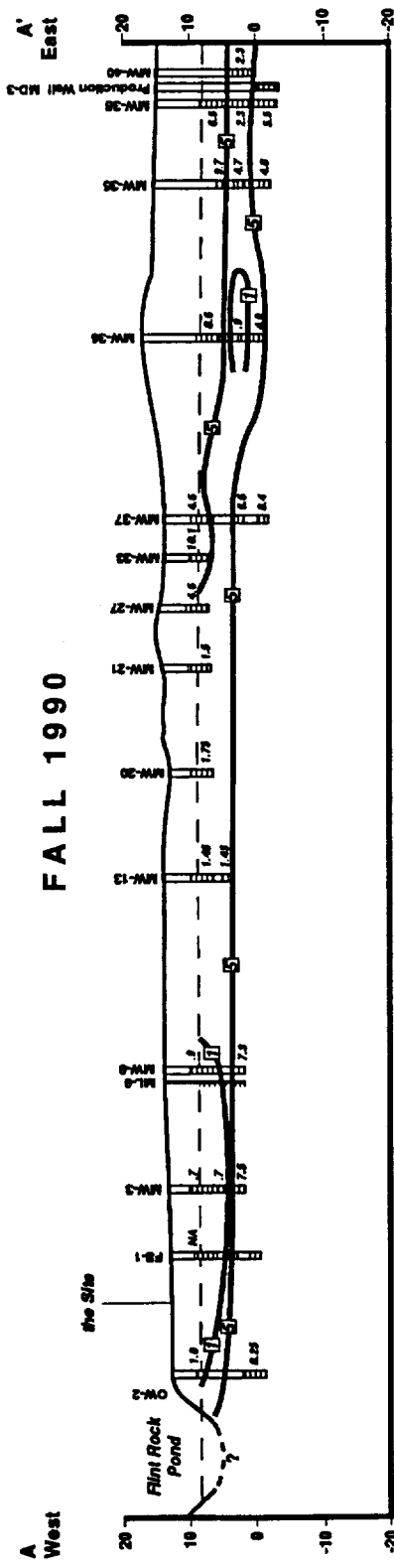
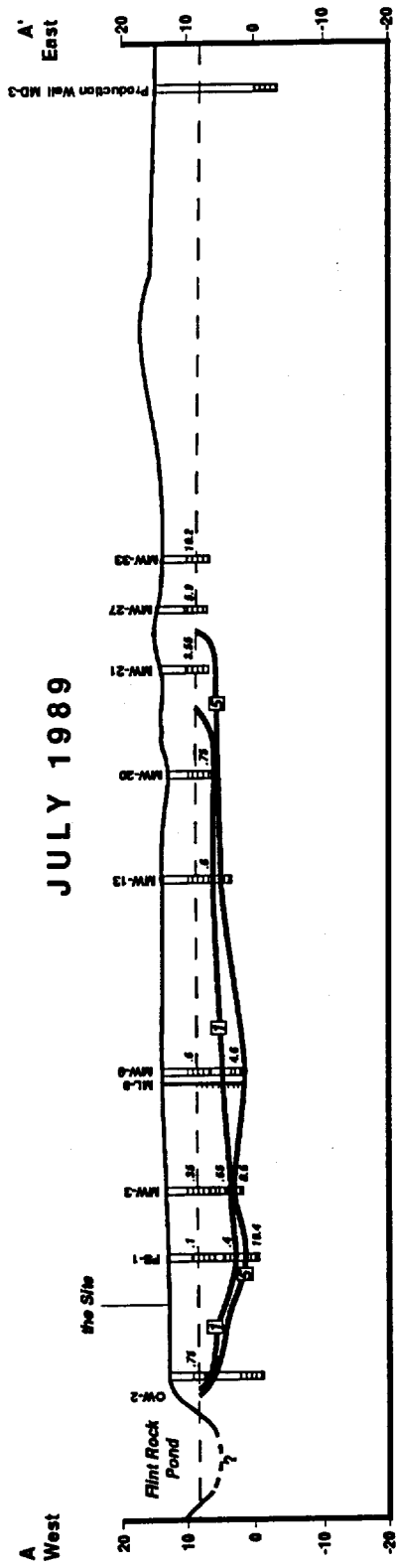


FIGURE 25. Dissolved Oxygen Concentrations in Ground Water
July 1989 and Fall 1990

4.6 Measured Dissolved Oxygen Concentration

— Line of Equal Dissolved Oxygen Concentration

Temperature, pH, and Eh

Measured groundwater temperatures ranged from 11.5 to 14.6 °C. The samples with higher temperature measurements may have been influenced by sunlight hitting the flow cell and warming the water as it moved through. This is especially true for well OW-2. There does not appear to be any significant correlation of temperature with the contaminant plume, although changes may be masked by the potential measurement errors.

Changes in pH and Eh correlate with dissolved oxygen concentrations. The pH values rise approximately 0.5 to 1.0 units within the plume, from 5.3 in well MW-15s (Figure 26) to 6.2 in a sample from ML-92. The background pH values are typical of the slightly acidic ground and surface waters on Cape Cod (LeBlanc *et al*, 1986). The quartz and feldspar sediments comprising most of the Cape provide little buffering capacity to mitigate acidic rainfall.

Background Eh values are over 300 mV, and drop to negative values within the plume. A slightly unstable connection in the Eh probe was discovered during the sampling of wells OW-2, MW-6, MW-7 and FS-1s. Also, the possibility of oxygen contamination reaching the Eh probe should be considered (Hem, 1970). While the reported values should be used cautiously, they show relative differences in Eh values throughout the plume and background areas that are useful in interpreting the groundwater chemistry.

Alkalinity

The alkalinity of the groundwater samples is a measure of its acid neutralizing capacity, of the amount of base that is present to neutralize the input of strong acid. It is a measure of the concentration of carbonate and bicarbonate present in the water, and the concentrations of other bases and weak acids. Alkalinities across the site ranged from 10^{-4} to 10^{-3} eq/l (Figure 26). This is typical for alkalinities on Cape Cod, as there is little buffering capacity in the groundwater, soils or subsurface sediments (Frimpter and Gay, 1979).

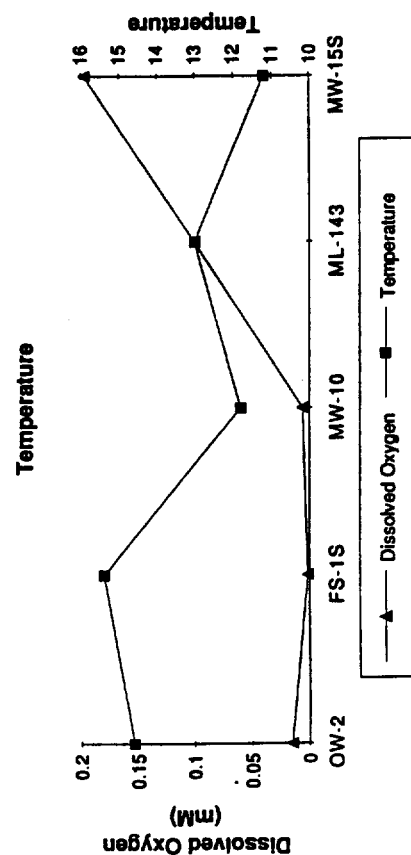
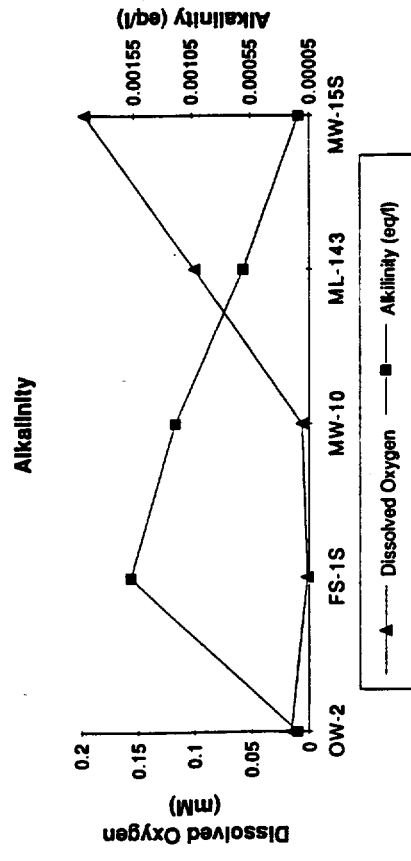
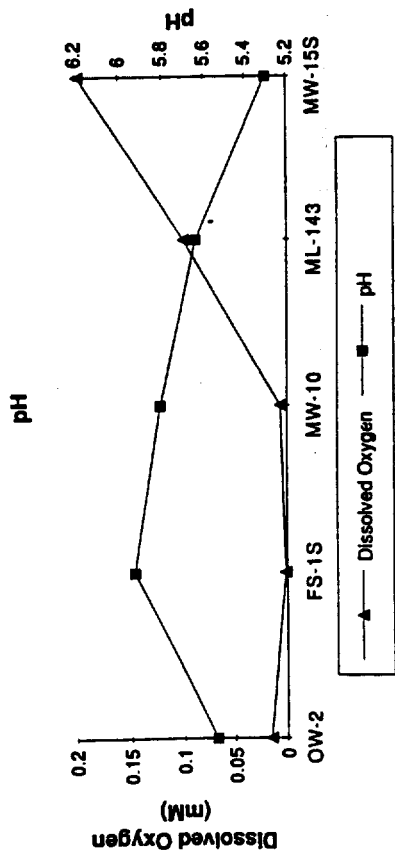
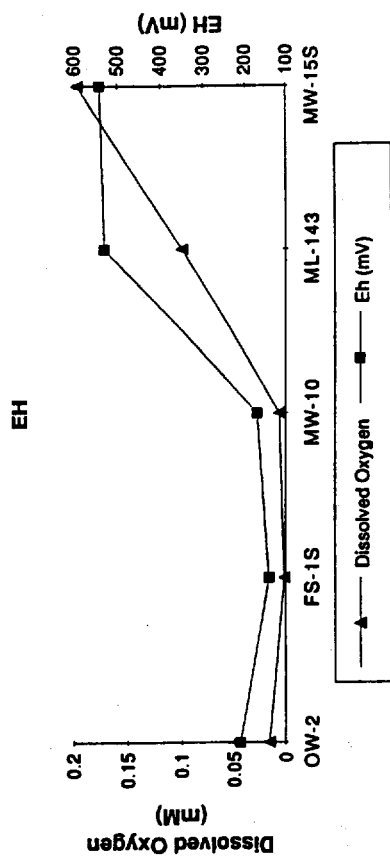


Figure 26: pH, Eh, Temperature and Alkalinity Longitudinally Through Plume

The alkalinities of the samples within the plume were higher relative to background areas. They were also elevated in samples from wells MW-6 and MW-7 downgradient from the concrete building and capped fire pit.

Calcium, Potassium, Magnesium, Sodium, and Chloride

Calcium, potassium, and magnesium concentrations are typically low in Cape Cod groundwater samples (Frimpter and Gay, 1979). The on-site samples confirm this, although they are elevated slightly within the plume above background levels (Figure 27). Much higher concentrations, however were found in wells MW-6 and MW-7, south of the main hydrocarbon plume. Potassium concentrations were eighty times higher than background in well MW-6. Calcium and magnesium levels were ten times and two times higher respectively. Well MW-6 and MW-7 are immediately downgradient of the concrete building in which straw is burned, and the capped concrete fire pit. Sodium concentrations across the entire site are slightly higher than typical background levels (Table 8, Figure 27). They are above the 20 mg/L EPA maximum contaminant level in wells MW-6, 7, 8, and 11. There does not appear to be any correlation between samples inside and outside the hydrocarbon plume.

Chloride concentrations are also highest in samples from well MW-6 and MW-7 (Figure 28). Chloride concentrations in background areas are typical for the area (Frimpter and Gay, 1979), and are slightly higher within portions of the contaminant plume.

Iron, Manganese and Sulfate

In typical oxygenated Cape Cod groundwater, iron and manganese concentrations are extremely low (Frimpter and Gay, 1979). In sediments these metals are usually found as oxides and oxyhydroxides. Iron and manganese concentrations within the plume are elevated relative to background concentrations (Figure 28). The highest iron concentration was 33 mg/L (0.59 mM) in a sample from ML-92. Manganese was detected in areas outside the contaminant plume, although iron concentrations were below the detection limits of the analytical method.

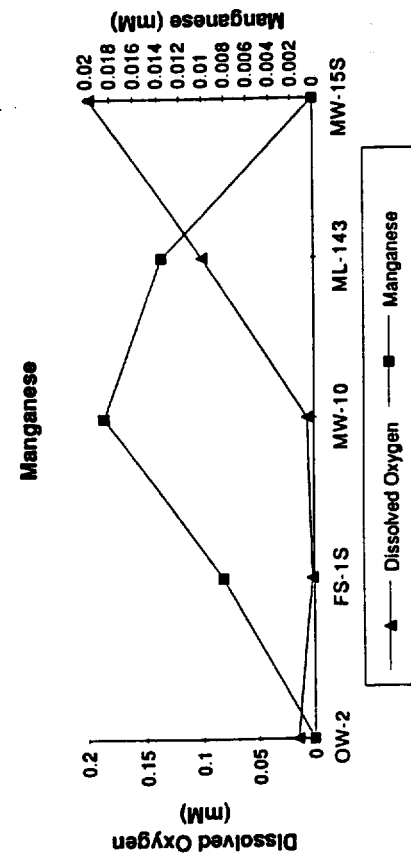
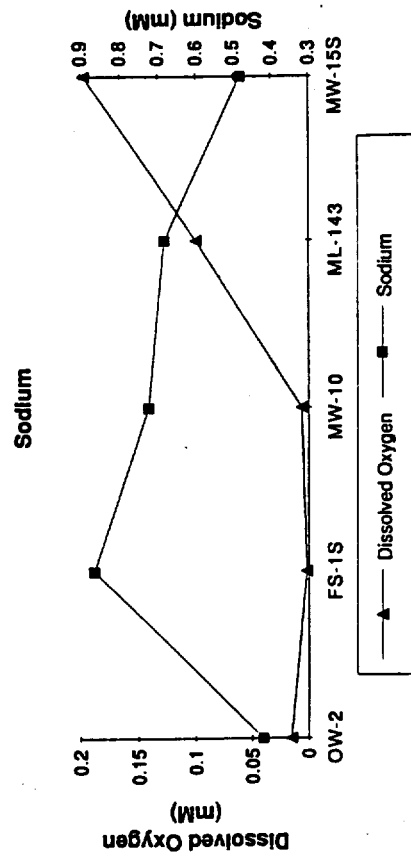
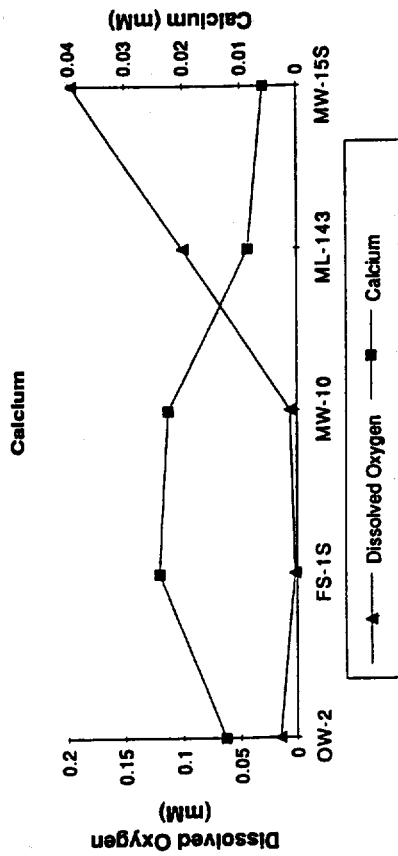
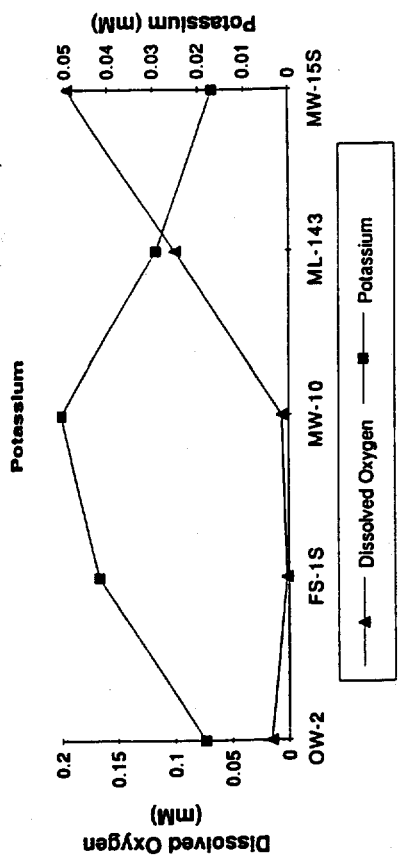


Figure 27: Calcium, Potassium, Magnesium and Sodium Longitudinally Through Plume

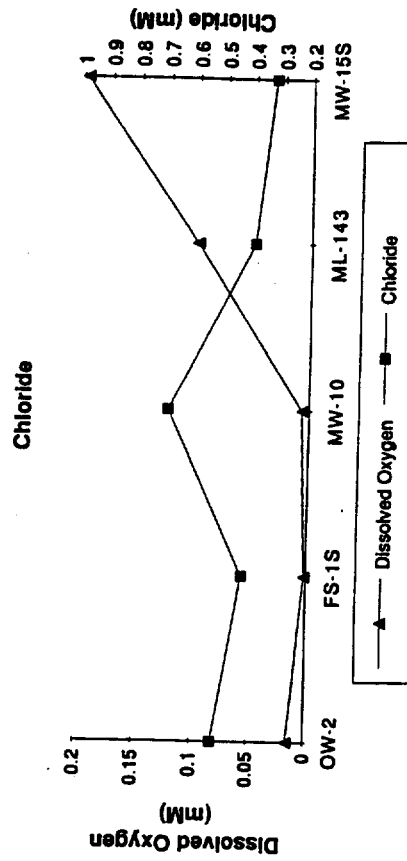
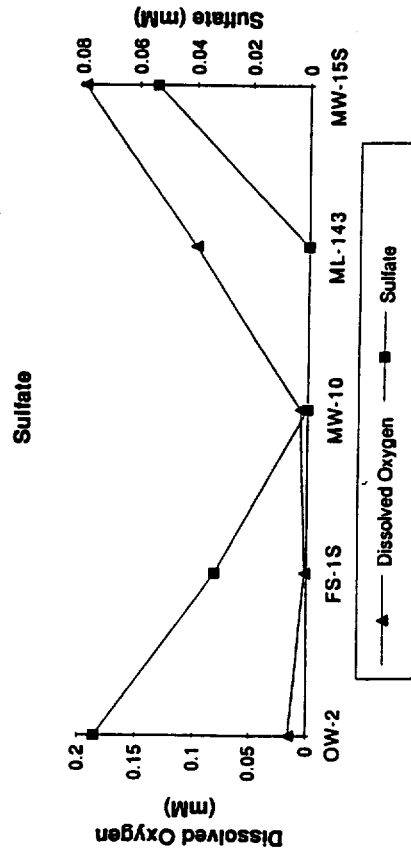
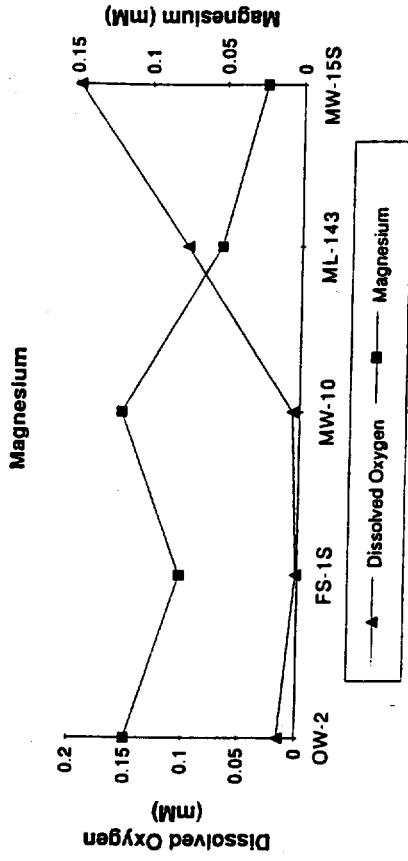
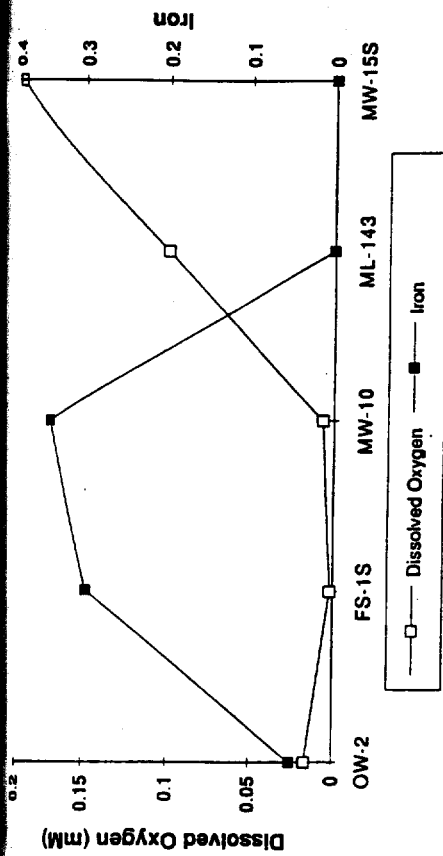


Figure 28: Iron, Magnesium, Sulfate and Chloride Concentrations Longitudinally Through Plume

Sulfate concentrations are highest in samples from well MW-6 and MW-7, similar to the calcium, potassium and magnesium concentrations. Within the hydrocarbon plume, the sulfate concentrations are lower than background areas (Figure 28).

Nitrate and Ammonia

Nitrate and ammonia concentrations are low across the entire site (Figure 29). While the total nitrogen concentrations do not vary significantly within the hydrocarbon plume, the relative concentrations of nitrate and ammonia do change. Nitrate levels are lower within the hydrocarbon plume, and ammonia concentrations are higher relative to background areas.

Aluminum and Silica

Silica concentrations are very consistent in all the samples (Figure 29). There is no noticeable difference within the contaminant plume. Aluminum concentrations are all low, with the highest concentrations found within the contaminant plume. Aluminum concentrations are all in the μM range, approximately three orders of magnitude below the other trace measured concentrations

DISCUSSION

Reduction Processes Within Plume

The reduction processes observed within the plume follow expected trends, and compare well with trends observed in similar environments. In a reducing environment, protons are consumed, thereby increasing pH and generating alkalinity. The decrease in protons and resulting increase in pH within the plume can be attributed to the oxidation of the hydrocarbons and other organic material by bacteria. As the bacteria oxidize the organic matter, they strip the aquifer of electron acceptors (O_2 , NO_3^- , Fe^{3+} , Mn^{3+} , and SO_4). The oxidation results in an increase of dissolved CO_2 , intermediate organic acid products, and metal ions which causes an increase in alkalinity.

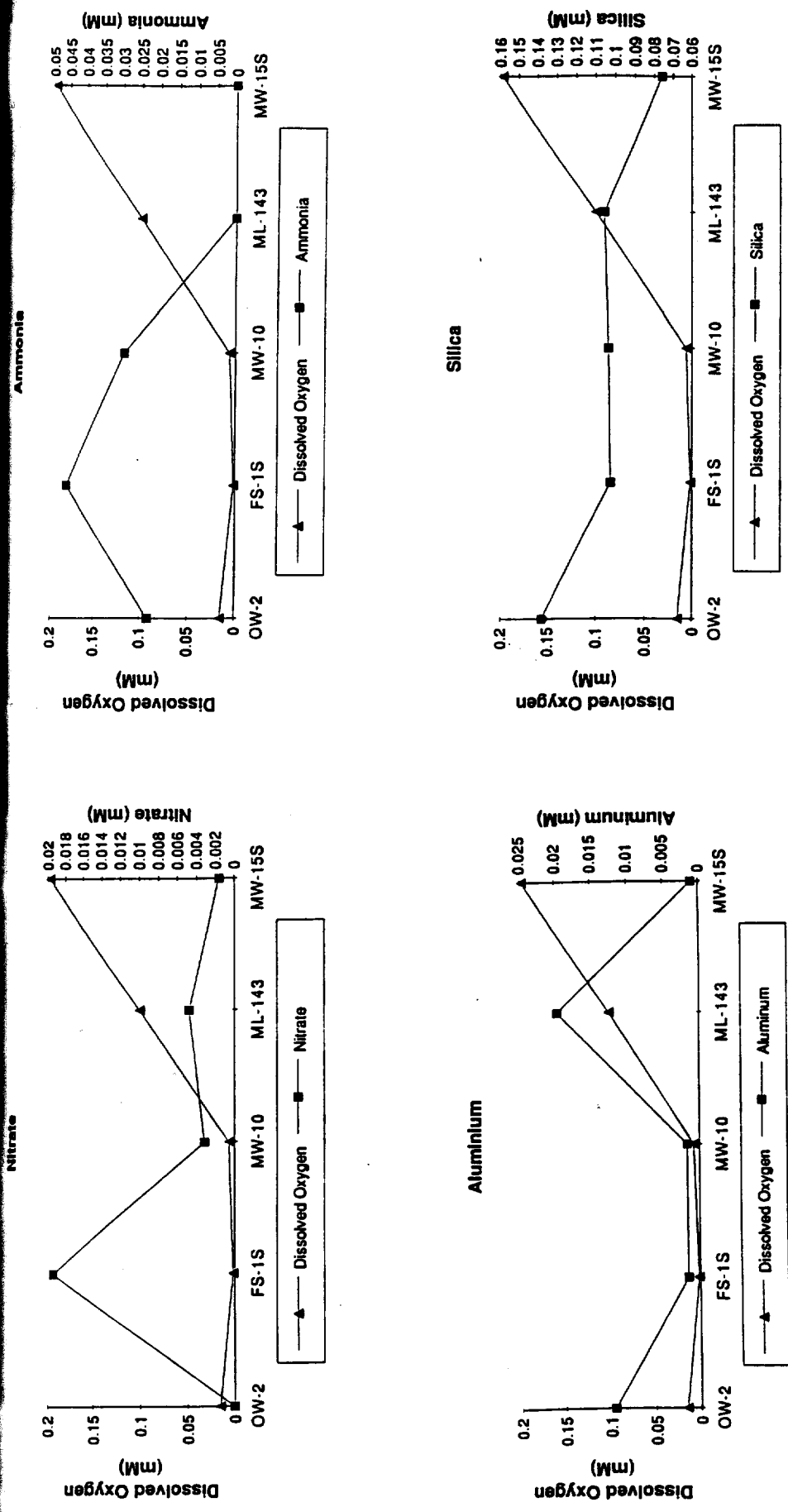


Figure 29: Nitrate, Ammonium, Aluminum, and Silica Concentrations Longitudinally Through Plume

These reductive processes have been observed in a number of groundwater systems where organic matter is being degraded by naturally occurring bacteria. Examples include the Lincolnshire limestone aquifer in Great Britain where the breakdown of organic matter consumes O_2 , Fe^{3+} , and SO_4 and results in increased pH, HCO_3^- , Fe^{2+} , and HS^- concentrations (Champ et al, 1979). Similar conditions have been observed at a creosote spill site in Pensacola, Florida (Cozzarelli *et al*, 1987), and in a sewage effluent plume at Otis Air Force Base, Massachusetts (LeBlanc, 1984).

The same processes are also observed within the plume at the Barnstable site. Little to no O_2 or NO_3^- is found within the plume (Figure 29), and both pH and alkalinity are increased within the plume relative to background areas (Figure 26). Concentrations of Fe^{2+} and Mn^{2+} are also elevated in the plume, as a result of reductive dissolution of their respective oxides. Measured Eh values are also lower in the plume relative to background areas.

Relative concentrations of nitrate and ammonia are reversed in the plume compared to outside the plume, again a result of the plume's reducing environment. In the plume, nitrate is most likely converted to N_2 gas through dissimilatory nitrogen reduction where nitrate is used as an alternate electron acceptor by respiring micro-organisms in the absence of oxygen. Ammonia may be produced by assimilatory nitrate reduction at the same time (Brock and Madigan, 1988). Both have a peak concentration in well FS-1s located in the plume source area.

Sulfate is an additional electron receptor that can be utilized by the bacteria degrading the hydrocarbons. This sulfate reduction results in decreased concentrations in the plume. Hydrogen sulfide odors have been detected during sampling in a number of the wells in the plume, indicating the reduced forms of sulfur are present.

Impacts of Iron and Manganese Dissolution

An integral component of the reduction processes within the plume is the dissolution of solid phase iron and manganese by bacteria degrading the hydrocarbons and using the metals as an electron acceptor in the respiration process. Both the groundwater

analyses and the extractable iron and manganese analyses indicate that considerable quantities of these two metals are available in the sediments to dissolve into groundwater. The mass of iron available in the aquifer sediments is greater than the amount of available manganese. This is consistent with the groundwater analyses which showed iron concentrations higher than manganese concentrations in all the samples.

Saturation indices were calculated using the WATEQ4F model (Plummer *et al*, 1978) to determine the potential for dissolution/precipitation reactions between aqueous and solid phases. Inputs to the model were the measured aqueous concentrations of the trace metals and other inorganic compounds that were measured, the dissolved oxygen concentrations measured in the field and the field measured Eh values corrected for the silver-silver chloride reference electrode (Nordstrom, 1977). The model showed that groundwater is supersaturated with respect to the iron minerals hematite and magnetite in all the samples. It is also supersaturated with goethite in each sample in which iron was detected, although not as supersaturated as the other crystalline minerals. The supersaturation of the crystalline minerals is due to their slow rates of precipitation relative to that for the amorphous form.

Groundwater is undersaturated with amorphous iron hydroxide upgradient of the plume, while slightly supersaturated near the toe of the plume (Well ML-143, Figure 30). This far downgradient of the source oxygen is diffusing back into the plume, causing precipitation of Fe^{2+} that dissolved from FeIII closer to the source in more reducing conditions. There is enough iron to precipitate that the amorphous iron becomes supersaturated. Downgradient of the plume, enough oxygen is present to force the precipitation of the remaining dissolved iron, as it is not detected in the sample from well MW-15. The water is again in equilibrium with solid phase Fe^{3+} . This data should be evaluated taking into account the location of the well screen relative to the contaminant plume. It likely includes clean water from above the plume, as dissolved oxygen measurements indicate the plume is moving below (Figure 25).

All the samples are undersaturated with respect to the manganese minerals (Figure 30). They are quite undersaturated with the manganese oxide minerals, although there is a slight trend of reduced undersaturation farther downgradient in the plume. The degree of undersaturation of the manganese carbonate (rhodochrosite) is less, although equilibrium is

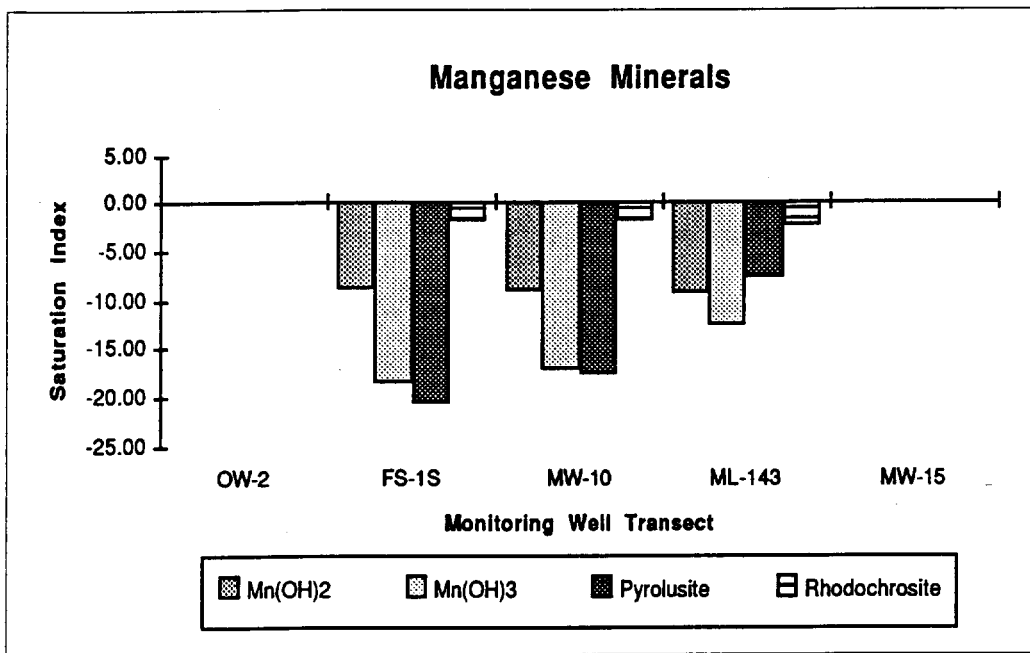
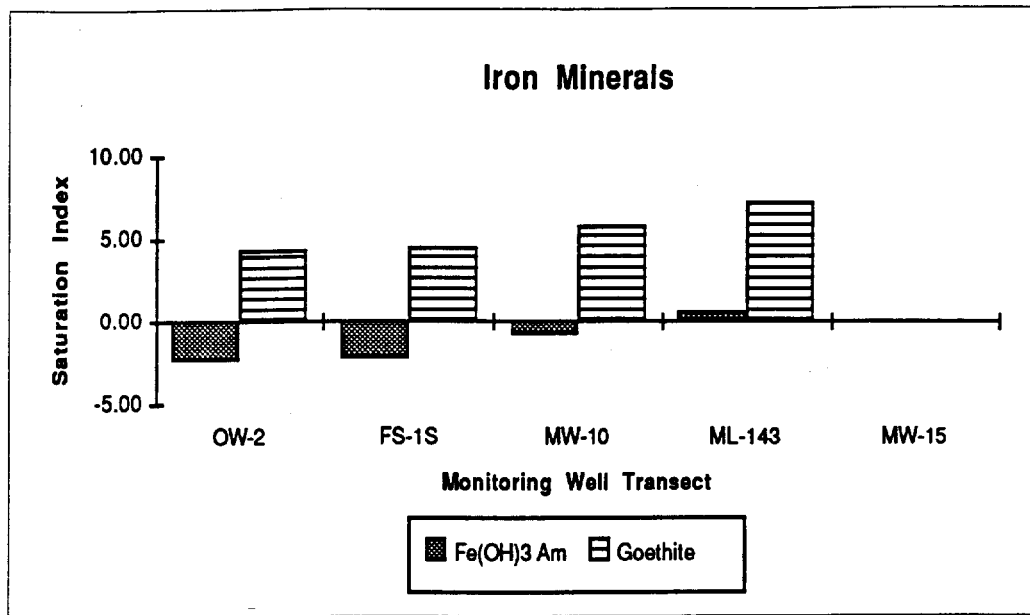


Figure 30: Saturation Indices of Iron and Manganese Minerals Longitudinally Through Plume

not reached in any of the samples. The mineral source of the dissolved manganese within the plume is not known. The fact that the manganese oxides and manganese carbonates are so undersaturated in all samples suggests that another mineral may be a source. One possibility is a silicate mineral, such as a amphibole or pyroxene, in which manganese is substituted for iron or another compound. Further analysis of the sediment composition is needed to determine the source of the manganese.

The presence of the metals in dissolved form has implications in plume remediation. If plume water is pumped by a recovery well, iron and manganese can precipitate out of solution onto the well screen, over time clogging screen openings and decreasing the efficiency of the well. If the metals pass through the screen, they can precipitate within an air stripper or within an activated carbon filter, thereby decreasing the efficiency of the treatment system. The proposed pump and treatment system for the site will need to include provisions to treat the iron and manganese expected to enter the system.

Iron and manganese mobilized by the hydrocarbon plume could move significantly distance through the aquifer. The dissolved oxygen hole created by the degradation of the hydrocarbons forces bacteria to use iron and manganese minerals as alternative electron acceptors resulting in an increase in dissolved metals concentrations in groundwater. Because the dissolved oxygen hole extends to the production well MD-3 and beyond, it is safe to assume that dissolved iron and manganese is also present throughout the length of the plume.

Dissolved iron and manganese could precipitate on the production well screen if the plume is pumped into the well. This would cause problems similar to those in recovery wells where the efficiency of the well is reduced. Aesthetic problems including poor taste and staining can also arise if the iron enters the water supply distribution system.

These metals problems, caused by the hydrocarbon spill, could be occurring even if the hydrocarbons themselves are not detected at the production well. Only trace VOC concentrations have been detected near the production well over the last five years. Most of the hydrocarbons are degraded while traveling through the aquifer from the plume source. The degradation, however, created the conditions that brought the iron and manganese into solution which then create their own impacts. The possibility also exists for the transport

of colloidal iron and manganese beyond the limits of the plume. The metals may precipitate at the toe of the plume where they react with oxygen diffusing into the plume from the surrounding area. The metal particles formed at the toe the hydrocarbon plume could travel to the production well and degrade the quality of the water supply. Such colloidal transport has been observed in the sewage disposal bed plume at Otis Air Force Base in Falmouth, Massachusetts where particulate transport of the iron/phosphorus mineral vivianite was observed (Gschwend, and Reynolds, 1987).

Aluminosilicate Weathering

As with the iron and manganese minerals, the equilibrium speciation of aluminosilicate compounds in the groundwater samples was modeled using WATEQ4F, and saturation indices were calculated. All of the samples were highly undersaturated with respect to carbonate minerals, including the rhodochrosite discussed above, suggesting that they are not present.

The aquifer sediments are composed primarily of quartz and feldspars. The dissolved solids detected in the aqueous samples are probably the result of the weathering of feldspar and other aluminosilicates (Freeze and Cherry, 1979; Drever, 1982; Hem, 1989). Quartz does not readily dissolve, and it is unlikely to contribute to the dissolved silica concentrations in the aqueous samples (Freeze and Cherry, 1979; Hem, 1989). The products of the aluminosilicate weathering will include dissolved components (Al^{3+} , H_4SiO_4 , K, Na, and Ca) and secondary mineral products. Secondary mineral products commonly identified include gibbsite ($Al(OH)_3$), SiO_2 , and kaolinite (Drever, 1982; Hem, 1989). The saturation indices data calculated with WATEQ4F has been used to evaluate these weathering processes at the Barnstable site.

Graphs showing changes in the saturation indices of silica minerals were prepared in longitudinal cross sections through the hydrocarbon plume. All the samples are supersaturated with respect to quartz, and undersaturated with respect to chalcedony and amorphous silica (silica gel and silica glass, Figure 31). There is no apparent trend through the plume.

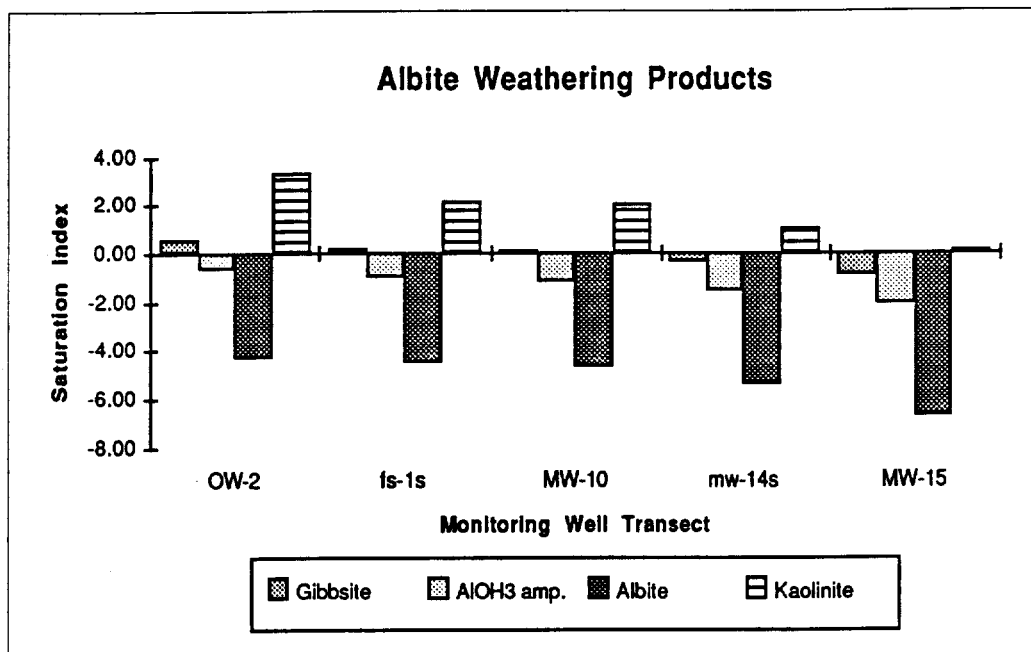
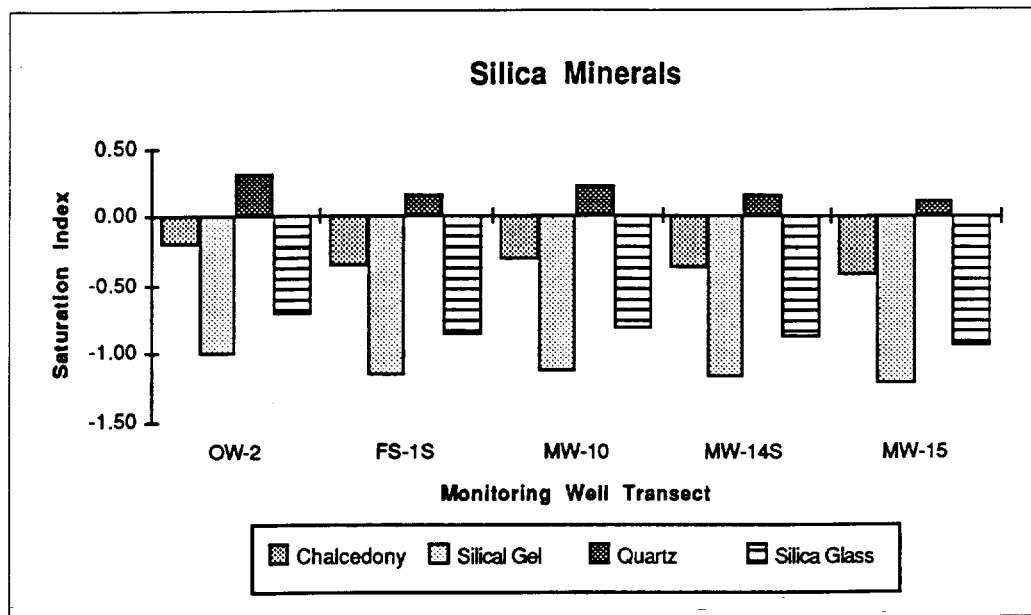


Figure 31: Saturation Indices of Silica Minerals and Albite Weathering Products Longitudinally Through Plume

The samples are all highly undersaturated with respect to parent aluminosilicate minerals such as albite, anorthite and muscovite (Figures 31 and 32). For each mineral, a trend of increasing saturation index from the plume center to the edge of the plume is observed. In the center of the plume (sample FS-1s), the parent mineral closest to equilibrium is muscovite. The samples are supersaturated with respect to gibbsite in the plume center (well FS-1s), while the rest of the samples are either at equilibrium, or slightly undersaturated. All the samples were within ± 1.0 log units from equilibrium. All the samples are undersaturated with respect to amorphous aluminum hydroxide, suggesting that if this phase is present, it could be dissolving into the water. A trend is also visible in the kaolinite saturation data, with samples in the plume supersaturated with respect to this secondary mineral, decreasing to near equilibrium in background water.

The mineral saturation indices for samples within the plume suggest that thermodynamic conditions favor the precipitation of kaolinite, gibbsite and quartz. A series of weathering pathway diagrams were prepared to further examine aqueous/solid phase interactions between these and other aluminosilicate minerals (Figure 33). The figures are identical to those used by Stumm and Morgan (1981), which were, in turn, taken from Garrels and Christ (1965) and Feth, Robersen and Polzer (1964). They plot the concentration of silica relative to either $\log(K/H^+)$, $\log(Na/H^+)$ or $\log(Ca/(H^+)^2)$, and show the stability fields of the parent and secondary or weathering product minerals.

All of the fourteen samples plot within the kaolinite stability field, consistent with their being supersaturated with respect to kaolinite. All of the samples fall close to a line within the field representing an H_4SiO_4 concentration of 10^{-4} M. Samples representing background conditions at the site plot at the lower end of the line, and samples from within the plume plot at the upper end of the line. The difference between plume and background samples is the amount of cations (Na, Ca and K); plume samples have greater cation concentrations making them plot higher in the kaolinite field. This implies that more weathering has occurred within the plume causing releasing more cations into groundwater.

The sample that plots the highest on the graph is from Well MW-6, downgradient of the concrete building where straw is burned. The burnt straw could be a source of potassium, calcium and sodium that could alter how this sample plots on the weathering diagrams.

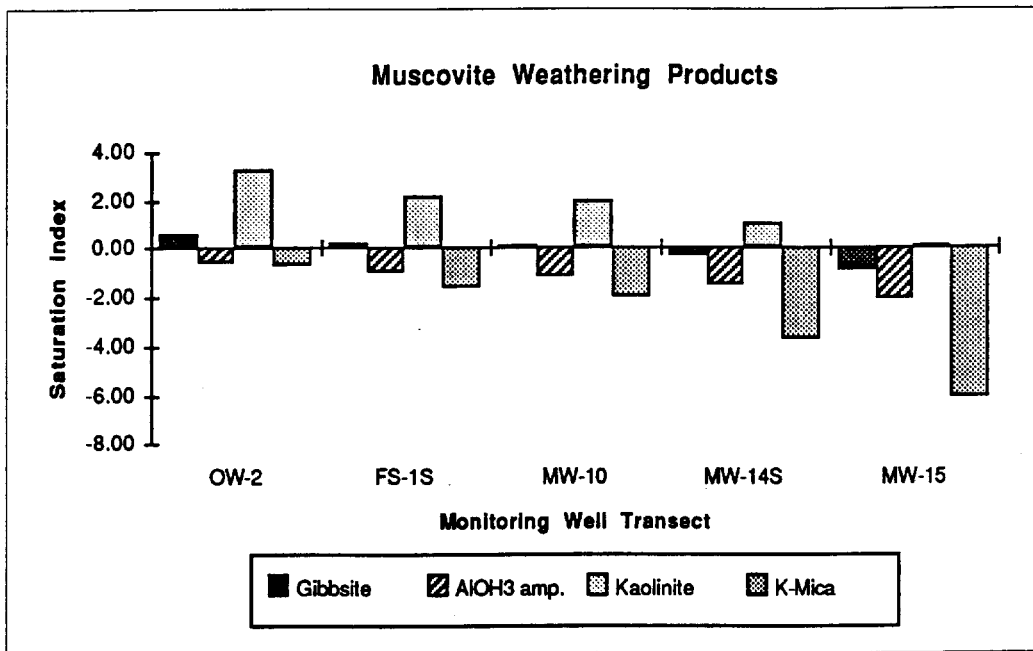
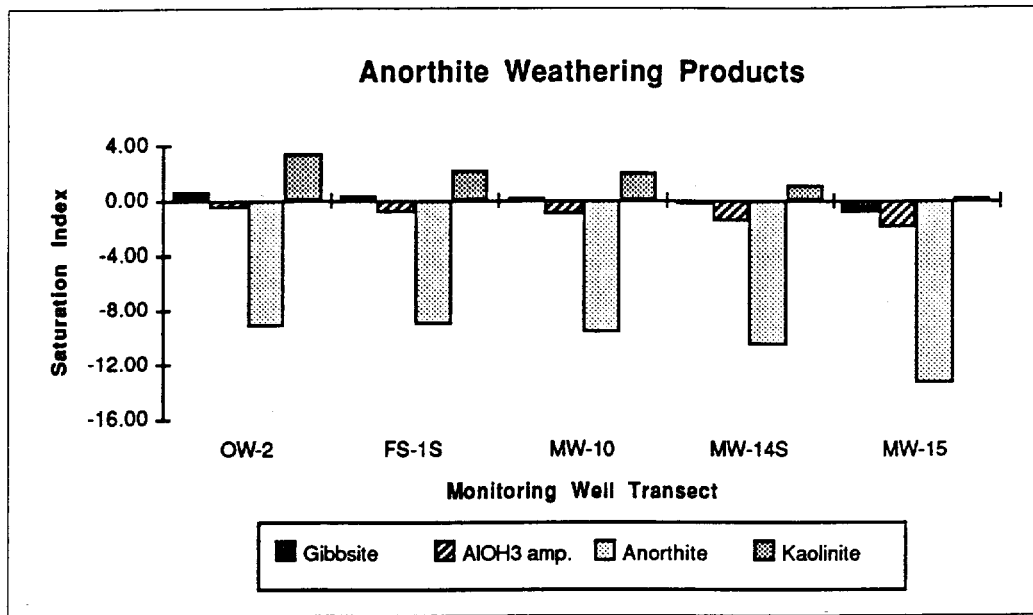
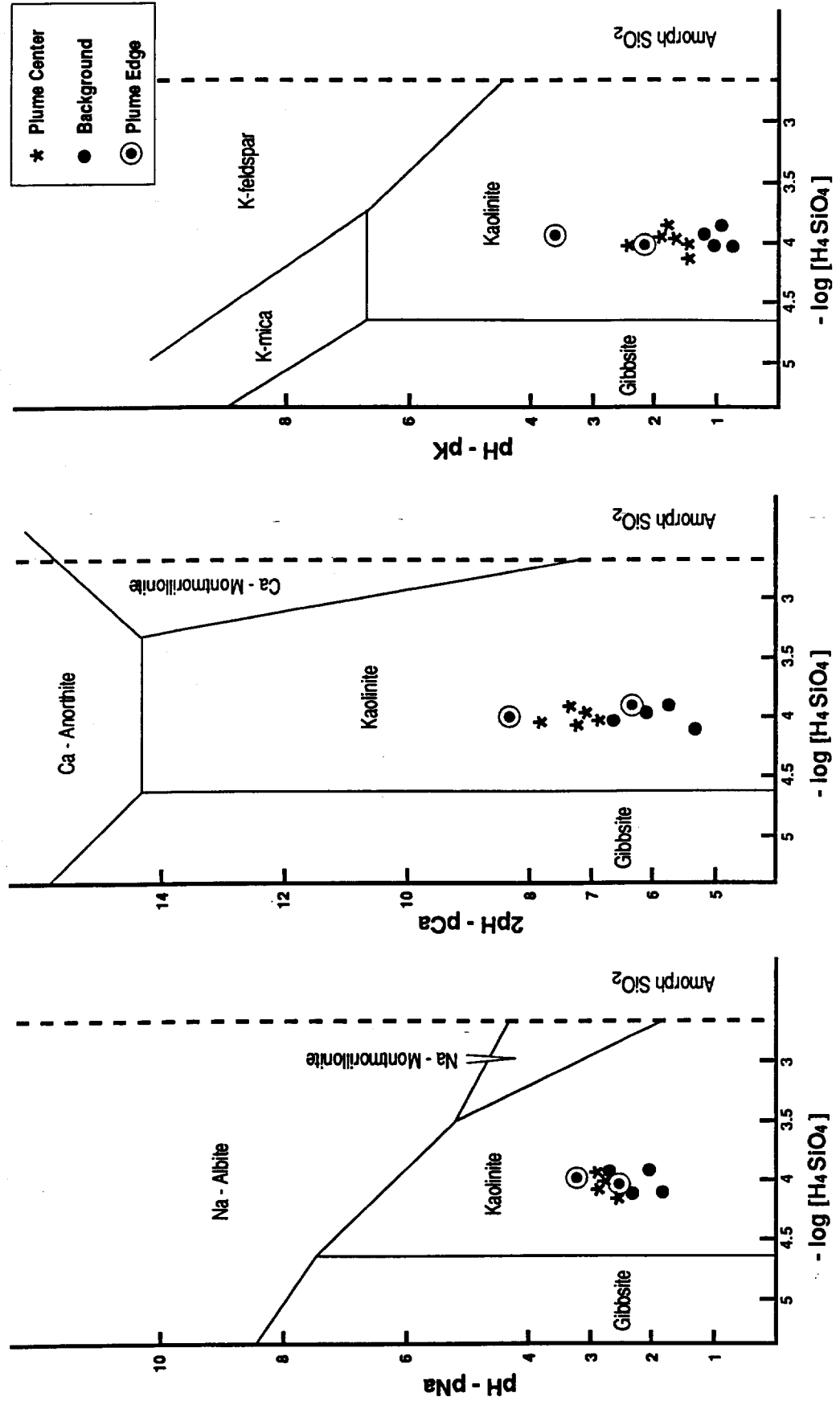


Figure 32: Saturation Indices of Anorthite and Muscovite Weathering Products Longitudinally Through Plume

FIGURE 33. Stability Relationships for Calcium, Sodium and Potassium Aluminosilicates with Water Quality Data from Barnstable Site (after Stumm and Morgan, 1981)



Several hypotheses have been considered to explain the straight line plot of the samples in kaolinite field. The hypotheses involve either the kinetics of dissolution/precipitation reactions, or solubility considerations. One possibility is that kaolinite is precipitating, but at a relatively slow rate. If this is occurring, the aqueous silica concentrations would increase with time, because the ongoing weathering of the parent minerals would be producing silica faster than it is lost to the kaolinite. The groundwater samples would plot in a diagonal line across the kaolinite field, from lower H_4SiO_4 concentrations on the left to higher concentrations on the right. This is not what is observed in the data for the Barnstable site.

Instead, the vertical line configuration made by the plotted samples suggests that there is solubility control regulating the silica concentrations. It is possible that the straight line is actually the equilibrium boundary between gibbsite and kaolinite that is offset from the boundary on the graph because of differences in temperature or uncertainties in the calculation of the equilibrium constants. The silica concentrations were taken from the WATEQ4F modeling results, and therefore, include corrections for temperature. The kaolinite saturation indices for the plume samples are greater than 2.0. Ball *et al* (1980) reports an uncertainty in the kaolinite gibbsite equilibrium constant of ± 0.88 . Even with this error, the samples are still supersaturated with kaolinite and fall within the kaolinite field.

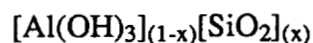
Another potential solubility control is quartz precipitation. All the samples plot on or near to the quartz saturation line reported by Nordstrom *et al* (1990) as $10^{-3.98}$. As Figure 31 shows, the samples are all supersaturated with respect to quartz, making its precipitation possible. The precipitation of quartz, however, is a very slow process at or near standard temperatures and neutral pH, and it is typically ruled out as a controlling phase in aluminosilicate weathering (Hem, 1989; Freeze and Cherry, 1979). Because of this, some other mineral's solubility is most likely controlling the dissolved silica concentrations.

Numerous investigators have hypothesized about, or identified a secondary mineral similar to kaolinite that is formed during weathering, and whose solubility controls aqueous silica concentrations. Rogers (1987) suggests that chalcedony precipitation is the reason

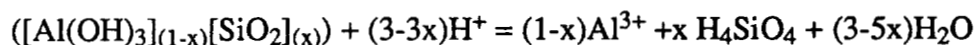
for near constant H_4SiO_4 concentrations found in a stratified-drift aquifer in Connecticut. Kenoyan and Bowser (1992a) suggest a secondary mineral phase controls silica concentrations in a sandy silicate aquifer in northern Wisconsin. In subsequent modeling, they propose that a gibbsite-kaolinite hybrid as the weathering product provides the best simulation of field data (Kenoyan and Bowser, 1992b).

Laboratory studies by Wollast (1967) involving the weathering of feldspars showed that silica concentrations reached a maximum even as weathering continued. The maximum was attributed to the precipitation of a hydrous, amorphous aluminosilicate. An amorphous aluminosilicate was also suggested by Paces (1973) as a feldspar weathering product during an analysis of groundwater samples taken in the Bohemian Massif of Czechoslovakia. Amorphous aluminosilicate and halloysite were also suggested as secondary minerals in column weathering experiments (Chou and Wollast, 1984, Chou and Wollast, 1985).

Paces (1972) suggests that the secondary mineral controlling the reactions he studied had the following composition:



and precipitated as an isoelectric amorphous aluminosilicate according to the following reaction:



The mole fraction (x) of H_4SiO_4 in the solid was found to vary with pH as shown below:

$$x = 1.24 - 0.135pH$$

The equilibrium constant for the reaction is based on an ideal solid solution between the gibbsite and amorphous silica. It varied as the composition varied, according to changes in pH:

$$\log K = -5.7 + 1.68pH$$

Paces plotted K vs pH and showed that samples from Sierra Nevada, and the Bohemian Massif of Czechoslovakia plotted at, or near the line, suggesting equilibrium with the aluminosilicate.

Allophane as Controlling Secondary Mineral

One possible aluminosilicate mineral that has been identified as a secondary weathering phase is allophane (Tait *et al*, 1978; Wada, 1989; Allen and Hajek, 1989). Allophane is a hydrous aluminosilicate consisting of hollow, irregularly shaped spherules with diameters ranging from 3.5 to 5 nm (Wada, 1989; Allen and Hajek, 1989). The formula for allophane is identical to that used by Paces (1972) to define the isoelectric amorphous aluminosilicate. Silica to aluminum ratios of 1:2 to 1:1, ($x = 0.5 - 0.67$) are typically determined from analyses of allophane collected from soil samples (Wada, 1989).

Allophane is considered an initial weathering product that eventually transforms into halloysite and kaolinite (Wada, 1989; Allen and Hajek, 1989). The transformation pathway is a subject of some disagreement although the final product is not disputed (Allen and Hajek, 1989). It is often found as a weathering product of volcanic ash (Wada, 1989), and has been identified as a weathering product in glacial rock flour (Funkert and Fieldes, 1968), glacial tills formed from granite, gneiss and schist (Tait, *et al*, 1978), and a variety of soils (Calvert *et al*, 1980b; Aomine and Wada, 1962; Eswaran and Sys, 1976; and Eswaran *et al*, 1973).

The possibility that allophane is controlling the weathering reactions at the Barnstable site has been evaluated using solid solution theory, incorporating the data available for allophane composition. An ideal solid solution between microcrystalline gibbsite and chalcedony was considered as the basis for allophane because of its microcrystalline structure described above.

Lippmann (1977, 1980, 1982a, 1982b) defines a total solubility product, $\Sigma\Pi$ representing the composition of a solid solution of A mixing with B and C as:

$$\Sigma\Pi = \{A\}(\{B\} + \{C\})$$

At equilibrium, the Lippmann total solubility product can be represented as:

$$\Sigma \Pi_{\text{eq}} = K_{\text{Al}} Y_{\text{Al}} X_{\text{Al}} + K_{\text{Si}} Y_{\text{Si}} X_{\text{Si}}$$

where:

K = Equilibrium constant for each component of the solid solution,

Y = Activity coefficients of each component of the solid solution,

X = Mole fraction of each component of the solid solution.

Using a solid solution between microcrystalline gibbsite and chalcedony,

$$\Sigma \Pi_{\text{eq}} = \{\text{Al}^{3+}\} \{\text{OH}^{-}\}^3 (Y_{\text{Al}} X_{\text{Al}}) + \{\text{H}_4\text{SiO}_4\} / (\{\text{H}_2\text{O}\}) (Y_{\text{Si}} X_{\text{Si}})$$

The solution is assumed to be ideal (activity coefficients = 1) and the range of mole fractions is taken from the allophane composition, of $X_{\text{Si}} = 0.5 - 0.67$ (Wada, 1989).

Using equilibrium constants provided by Nordstrom *et al.* (1990):

$$\log K_{\text{Al}} = -32.65 \quad \text{for microcrystalline gibbsite, and}$$

$$\log K_{\text{Si}} = -3.55 \quad \text{for chalcedony,}$$

then:

$$\log(\Sigma \Pi_{\text{eq}}) = -3.72 \text{ to } -3.85$$

for the mole fraction of silica ranging from 0.5 to 0.67. If the solubility product is corrected for the cooler temperatures at the Barnstable site (12.5 °C), using a ΔH_r for chalcedony of 4.72 kcal/M, and a ΔH_r for gibbsite of -24.5 kcal/M (Nordstrom *et al.*, 1990), the resulting total solubility product is:

$$\log(\Sigma \Pi_{\text{eq}}) = -3.88 \text{ to } -4.01$$

Under the slightly acidic conditions at the Barnstable site, the aluminum term in the total solubility product is negligible, both at, or far from, equilibrium with respect to microcrystalline gibbsite. As a result, the silica term dominates the total solubility product such that:

$$\Sigma \Pi_{eq} \approx \{H_4SiO_4\}$$

The calculated $\{H_4SiO_4\}$ values using the total solubility product closely match the measured values in Table 9. The median measured concentration is $10^{-4.00}$, at the upper end of the range of calculated values. The similarity of the calculated and measured values suggests that allophane is the secondary mineral controlling the silica concentrations in groundwater at the site. The fact that the measured values fall at the high end of the calculated concentrations suggests that the allophane is precipitating with roughly equal amounts of aluminum and silica, the same ratio found in the potential end products of the precipitation, halloysite and kaolinite. The allophane precipitation keeps the silica concentrations constant in the groundwater. Aluminum concentrations are controlled by a combination of gibbsite dissolution and allophane precipitation.

Table 9: Comparison of Calculated and Measured $\{H_4SiO_4\}$ values

	Barnstable Site	Northwest
Florida Aquifer		
No. Samples	14	42
Average Temperature (°C)	12.5	22
Calculated Range (log units)	-3.88 to -4.01	-3.76 to -3.89
Measured Range (log units)	-3.86 to -4.14	-3.79 to -4.00
Median (log units)	-4.00	-3.85

Silica concentrations in groundwater at a crude oil spill in Bemidjii, Minnesota were elevated within the plume (Bennett and Seigel, 1987). The elevated concentrations were attributed to weathering of quartz enhanced by organic acids formed as intermediate products during the degradation of the crude oil. Complexation of silica with organic acids was confirmed in the laboratory (Bennett *et al*, 1988). No analyses have been conducted to determine organic acid concentrations at the Barnstable site and their impact on enhanced mineral dissolution. However, the concentration of silica is consistent between the plume

water and background water, suggesting that organic acids do not significantly affect silica concentrations at the Barnstable site. If enhanced quartz weathering is occurring at the Barnstable site, it may be being masked by the precipitation of the allophane, which strips the silica out of solution.

Comparison to Alluvial Aquifer in Northwest Florida

Further evidence that the silica concentrations in the groundwater plume at the Barnstable site are not influenced by organic acids derived from petroleum products is the observation of similar water chemistry in an uncontaminated sand and gravel aquifer in the northwest corner of the Florida panhandle (Katz and Choquette, 1991). Groundwater samples were collected from 42 wells screened throughout a predominantly quartz aquifer with trace amounts of andesine, chlorite, calcite, kaolinite and illite. Silica concentrations ranged from 6.0 to 9.7 mg/L ($10^{-4.00}$ to $10^{-3.79}$ as H_4SiO_4). Like the Barnstable site, they plotted in a vertical line on a stability diagram for K-spar (Figure 34). The median silica concentration is $10^{-3.85}$, approximately 0.15 units greater than those for the Barnstable site. However, the average reported groundwater temperature in the Florida samples was 22 °C, 9.5 degrees higher than those in Barnstable. Applying the same temperature corrections used with the Barnstable data yields predicted silica concentrations that nearly match the measured concentrations (Table 9).

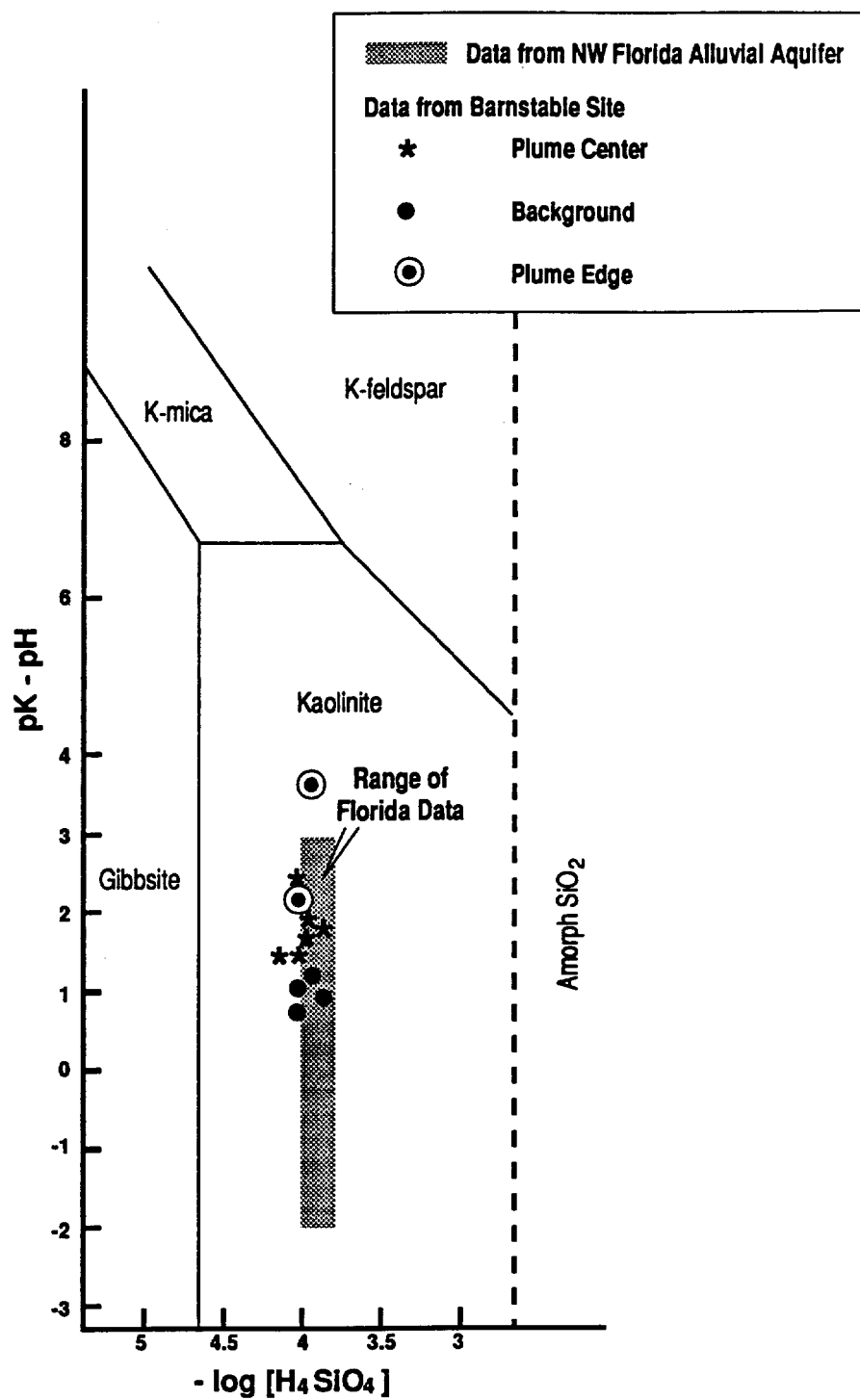
One problem with the theory of allophane precipitation is that the calculations assume an ideal solid solution between microcrystalline gibbsite and chalcedony. If the solution is not ideal, the activity coefficients for each end member would affect the results. This would be most important for chalcedony because the aluminum term in the total solubility product equation is so small. If the activity coefficients for the silica and the gibbsite varied from 0.9 to 1.1 the resulting changes in the predicted aqueous silica concentration would be ± 0.04 log units for any silica/aluminum. This variation is still within the range of the measured values.

Mass Balance Modeling

Mass balance calculations were applied using the results of the aqueous speciation modeling to determine the amount of mineral dissolution and precipitation in contaminated

FIGURE 34. Stability Relationships for Potassium Aluminosilicates with Water Quality Data from NW Florida Alluvial Aquifer

Source: Katz and Choquetts, 1991



areas of the site. The calculations allowed for effects of hydrocarbon degradation on mineral reactions, and also provided insights on sulfate reduction and nitrogen transformation.

The evaluation was conducted using the mass balance model BALANCE (Parkhurst, *et al*, 1982). Two key questions were addressed: 1) what are the increases in the mineral weathering that occur between the ground surface and the water table in the contaminated zone (well FS-1s) relative to the ground surface and water table under background conditions (MW-15), and 2) what additional weathering occurs as the groundwater flows downgradient from the source area.

Development of Feasible Weathering Reactions

The modeling was conducted using a set of feasible reactions that are believed to control the inorganic chemistry of the aquifer (Table 10). The reactions controlling water chemistry likely vary throughout the unsaturated zone and aquifer, because the composition of the sediments, and the amounts and types of hydrocarbons, vary. Despite these complications, one simplified set of reactions has been chosen that provides a reasonable representation of the compounds observed in the solid and aqueous phases. The aluminosilicate reactions were chosen based on sediment observations, literature data on similar aquifers, and thermodynamic data developed using the aqueous speciation model WATEQ4F (Plummer *et al*, 1978). Hydrocarbon reactions were chosen to represent the degradation of the residual petroleum products in the unsaturated zone, and the compounds dissolved in groundwater.

Visual observations of the sediments indicated they are composed primarily of quartz, with smaller amounts of feldspar and mica. The presence of a sodium rich feldspar was confirmed through the x-ray diffraction analyses described earlier. The presence of calcium feldspar as a source of Ca^+ was also assumed, based on data available for a similar aquifer approximately 20 km west of the site on Cape Cod (Barber *et al*, 1992). Individual reactions were used for the two plagioclase feldspar end members even though it is possible that one mineral with an intermediate composition is what actual exists at the site. This approach is supported by transmission electron microscopy of weathered feldspars, specifically labradorite, which show a micropertthitic structure where the Na-rich layers are

Table 10: Reactions Used in Balance Modeling

Gibbsite	$\text{Al}_2\text{O}_3 + 3\text{H}^+ = \text{Al}^{3+} + 3\text{H}_2\text{O}$
Muscovite	$\text{KAl}_2(\text{Si}_3\text{Al})\text{O}_{10}(\text{OH})_2 + 10\text{H}^+ = \text{K} + 3\text{Al} + 3\text{H}_4\text{SiO}_4$
Albite	$\text{NaAlSiO}_8 + 4\text{H}^+ + 4\text{H}_2\text{O} = \text{Na}^+ + \text{Al}^{3+} + 3\text{H}_4\text{SiO}_4$
Anorthite	$\text{CaAl}_2\text{SiO}_8 + 4\text{H}^+ + 4\text{H}_2\text{O} = \text{Ca}^{2+} + \text{Al}^{3+} + 3\text{H}_4\text{SiO}_4$
Chlorite	$\text{Mg}_5\text{Al}_2\text{Si}_3\text{O}_{10}(\text{OH})_8 + 11\text{H}^+ = 5\text{Mg} + \text{Al} + 3\text{H}_4\text{SiO}_4 + \text{H}_2\text{O}$
Allophane	$[\text{Al}(\text{OH})_3]_{(1-x)}[\text{H}_4\text{SiO}_4]_x + (3-3x)\text{H}^+ = (1-x)\text{Al}^{3+} + x\text{H}_4\text{SiO}_4 + (3-5x)\text{H}_2\text{O}$
Manganese	$3/2\text{O}_2 + 2\text{Mn}^{2+} + \text{H}_2\text{O} = 2\text{MnO}_2(\text{s}) + 4\text{H}^+$
Iron hydroxide	$\text{Fe}(\text{OH})_3 + 3\text{H}^+ = \text{Fe}^{3+} + 3\text{H}_2\text{O}$
CO ₂	$\text{CO}_2(\text{g}) = \text{CO}_2(\text{aq})$
Naphthalene	$\text{C}_{10}\text{H}_8 + 12\text{O}_2 = 10\text{CO}_2 + 4\text{H}_2\text{O}$
Benzoic Acid	$\text{C}_7\text{H}_6\text{O}_2 + 9\text{O}_2 = 7\text{CO}_2 + 6\text{H}_2\text{O}$
Oxygen Exchange*	$\text{O}_2(\text{g}) = \text{O}_2(\text{aq})$
Nitrification	$2\text{O}_2 + \text{NH}_4^+ = \text{NO}_3^- + 2\text{H}^+ + \text{H}_2\text{O}$
Denitrification	$\text{CH}_2\text{O} + 4/5\text{NO}_3^- = 2/5\text{N}_2(\text{g}) + \text{HCO}_3^- + 1/5\text{H}^+ + 2/5\text{H}_2\text{O}$
Sulfate reduction	$2\text{CH}_2\text{O} + \text{SO}_4^{2-} = \text{H}_2\text{S} + 2\text{HCO}_3^- + \text{H}^+$

* Oxygen exchange substituted for naphthalene in dissolved plume modeling

preferentially weathered (Inskeep *et al*, 1991). Muscovite was used as the source of potassium in the groundwater as micas were observed in the sediments. Chlorite was chosen as a magnesium source as it was identified in sediment samples from the aquifer at Otis Air Force Base (Barber *et al*, 1992).

Gibbsite is typically formed as an intermediate weathering product for these minerals (Hem, 1989; Drever, 1982), and was therefore included in the reactions. Allophane was chosen as the secondary weathering product based on the arguments presented earlier.

The aluminosilicate reactions are, in part, controlled by the amount of carbonic acid in the water, which is a function of CO₂ exchange with the atmosphere, degradation of naturally occurring organic matter in the unsaturated zone, and, within the contaminated areas, the degradation of hydrocarbons. These processes therefore need to be included in the modeling, and are represented using carbon dioxide exchange with the atmosphere, and hydrocarbon and organic acid degradation. Both the saturated and unsaturated zones are thought to be open to CO₂. Partial pressures of CO₂ in the unsaturated zone, which are typically above atmospheric values because of organic matter degradation, are increased further by the hydrocarbon degradation.

Naphthalene and benzoic acid were chosen to represent the degradation of the hydrocarbons in the unsaturated zone. With ten carbon atoms, naphthalene's composition is in the center of the range of hydrocarbon compounds found in No. 2 fuel oil, and has been used as a tracer compound for a similar hydrocarbon spill in Conroe, Texas (Bedient *et al*, 1984). Naphthalene degradation requires a 3:1 oxygen to carbon ratio, similar to that observed for most hydrocarbon degradation (Borden and Bedient, 1986). Benzoic acid was chosen as representative of the many organic acid breakdown products associated with hydrocarbon degradation.

Reactions were also included in the modeling to investigate sulfate reduction, nitrification and denitrification. These reactions do not significantly affect the aluminosilicate weathering processes but are additional reactions related to the hydrocarbon degradation for which data is available.

Thermodynamic data for the aluminosilicate reactions from the WATEQ4F modeling results indicate that the groundwater samples are undersaturated with respect to all the parent aluminosilicate minerals, and therefore have the potential to dissolve. An exception is allophane, which is precipitating. Naphthalene and benzoic acid are assumed to be degrading at all times. Within contaminated areas with reducing conditions, sulfate should be reduced to hydrogen sulfide, and nitrate should be reduced to nitrogen gas (nitrification). These constraints are used to evaluate the appropriateness of the reactions used in the modeling.

Unsaturated Zone Reactions

The first pathway examined with the mass balance model was recharge through the soil layer and unsaturated zone, down to the shallow portion of the aquifer. The additional weathering reactions in the contaminated portion of the unsaturated zone relative to uncontaminated areas was determined. In areas where contamination exists, it is assumed that recharge moves down towards the water table and passes through a zone of residual contamination. Oxygen in the water is consumed in the degradation of hydrocarbons. The degradation process produces carbon dioxide and organic acid products that, in turn, react with the aquifer sediments, accelerating the rate of weathering. The extent of residual saturation includes a 15 m by 30 m area in the center of the site (see Figure 15).

The additional weathering in the contaminated area was modeled using water quality data from wells FS-1s (at the source) and MW-15 (background). The differences in water quality in the samples from these two wells is assumed to be from the excess weathering caused by the hydrocarbon degradation at the plume source. It is also assumed the rate of transport through the unsaturated zone is the same for each site. The depth to water at well FS-1s is 1-2 m less than at well MW-15, so, if anything, the residence time in the residually contaminated zone is slightly less than in the area used for the background weathering. Therefore, the calculation of excess weathering because of the presence of the hydrocarbons may be conservative.

Based on the chosen set of reactions, a reasonable amount of additional weathering has occurred to create the water quality observed at the plume source (Table 11). More weathering of the parent minerals, muscovite, albite and anorthite, has occurred at the

Table 11: Mass Balance Reactions within Contaminated Vadose Zone

	Calculated Reaction* (μM)	5% Error Range (μM)
Dissolution Reactions		
Muscovite	25	(22 - 28)
Albite	380	(313 - 447)
Anorthite	15	(13 - 16)
Gibbsite	777	(650 - 906)
Chlorite	11	(11 - 12)
Manganese	4	(3.9 - 4.3)
Iron Hydroxide	300	(285 - 315)
Precipitation Reactions		
Allophane	-2535	(-2131 - -2951)
CO ₂ Exchange	3887	(3652 - 4308)
Napthalene Degradation	17.5	
Benzoic Acid	9.1	
Nitrification	-90	(-95 - -85)
Denitrification	-78	(-82 - -73)
Sulfate Reduction	21	

* Negative indicates reaction proceeding opposite to that specified in Table 10.

plume source than there is in background areas, producing greater concentrations of dissolved K, Na and Ca respectively. Albite is shown to dissolve more than the other aluminosilicate minerals. The only mineral precipitating is allophane. Varying the ratio of silica to aluminum in the allophane composition changes the amount of gibbsite and allophane reaction by $643 \mu\text{M}$, but does not significantly affect the amount of other mineral reactions.

Iron hydroxide and manganese dioxide are both dissolving as expected given the lack of oxygen and reducing conditions at the source. Sulfate is also being reduced because of the lack of oxygen. A relatively large amount of CO_2 ($3865 \mu\text{M}$) is brought into the water. The excess CO_2 accounts for degradation of hydrocarbons or organic compounds not attributed to the benzoic acid or naphthalene degradation. Given the wide range of organic compounds that exist in the residual saturation zone, it is likely that their interactions could be represented by a variety of organic reactions. Those used here are not unique, but represent one feasible combination of reactions that adequately simulate the observed water quality.

The results of the nitrogen modeling do not make sense given the known site conditions used in the modeling. Background sources of nitrogen include precipitation and upgradient groundwater impacted by anthropogenic nitrogen from septic system discharges, lawn fertilizers or road runoff. The background nitrogen is most likely in the nitrate form before it enters the hydrocarbon plume. In the plume the modeling suggests that nitrate is converted to ammonia, a process that could be occurring in the anoxic water near the hydrocarbon source. However, to balance the amount of ammonia production, the model converts nitrogen gas to nitrate, a process requiring oxygen that is not available. It is possible that there is another source of nitrogen not included in the modeling that would account for the observed transformations. Possible sources include organic nitrogen in the residual fuel oil, and nitrogen in the firefighting foams sometimes used at the site.

The sensitivity of the chosen reaction set to errors in the measurement of aqueous component concentrations was examined by varying the input concentration for each $\pm 5\%$. Model runs incorporating the assumed error were conducted, and a range of values for the individual phase reactions were determined. For the unsaturated zone modeling, the range of possible reaction amounts do not significantly effect the final results.

Plume Reactions

A second analysis was conducted to predict the weathering occurring in the hydrocarbon plume as it moves downgradient through the aquifer from well FS-1s to MW-10. The water from well FS-1s is assumed to represent the source area of the plume, with no mixing of background water. Water from well MW-10 is also assumed to represent plume water. Because it contains almost no dissolved oxygen, it is highly unlikely that mixing occurred during the sampling of this well. If mixing had occurred, both dissolved oxygen from the clean water, and iron from the plume water would have been detected.

Dissolved oxygen will not coexist for extended periods with the dissolved the Fe^{2+} in the plume water. If O_2 and Fe^{2+} are brought together the Fe^{2+} will be oxidized forming $Fe(OH)_3 (s)$. The rate at which the iron is oxidized varies with pH (Eary and Schramke, 1990). At the pH observed in the plume, Fe^{2+} has been found to have a half-life of approximately 1 day (Eary and Schramke, 1990). This translate to approximately 0.3 m of movement in the aquifer meaning that if oxygen is introduced to the plume it will be consumed before the plume moves any significant distance. However, during sampling, iron and oxygen can be mixed, and the reactions between them will not occur at a rate fast enough to prevent them from being detected in a sample of mixed water.

The mass balance modeling for the plume was conducted using most of the reactions used in the unsaturated zone analyses, with a few substitutions to better simulate the reactions expected to occur within the groundwater system. Oxygen exchange between the plume and background areas within the aquifer was substituted for naphthalene degradation as it has not been detected downgradient from the source. Sodium/magnesium exchange was included in the reactions, and the weathering of albite and anorthite was combined as one plagioclase mineral with equal amounts of sodium and calcium. These changes were made to provide for both calcium and sodium dissolution while balancing the reactions to account for the observed water chemistry within the plume. The sodium/magnesium exchange is needed to explain the loss of dissolved sodium between the source water (FS-1s) and well MW-10.

Overall, the model predicted less weathering in the plume than in the unsaturated zone (Table 12). The aluminosilicate reactions proceed as expected, with the exception of

Table 12: Mass Balance Reactions within Plume

Wells FS-1 to MW-10

	FS-1s to MW-10 Calc. Reaction (μM)	Error Range Minimum Error	Maximum Error
Dissolution Reactions			
Muscovite	8	3.4	12.6
Plagioclase	6	1.7	10.3
Na/Mg Exchange	67	25.7	107
Gibbsite	7	4.5	9.5
Chlorite	-5 *	1.1	-11.3 *
Manganese	5.4	4.7	6.1
Iron Hydroxide	50	17.5	82.5
Precipitation Reactions			
Allophane	-53	-37	-69.7
CO ₂ Exchange	-274	312	-913
O ₂ Exchange	129	166	160
Benzoic Acid	11	15.7	13.6
Nitrification	32	24.6	39.4
Denitrification	40	33.7	45.8
Sulfate Reduction	33	31.3	34.6

Negative number indicates reaction proceeding opposite to that specified in Table 10

* Dissolution/Precipitation reaction not thermodynamically possible

chlorite precipitation. When a 5% range of potential errors in the inorganic analyses is included in the reactions, the chlorite is shown to dissolve as would be expected. All the other aluminosilicate reactions proceed correctly, even when the errors are considered.

Oxygen is brought in from the surrounding aquifer, and benzoic acid is degraded in small amounts. Carbon dioxide is lost to the aquifer unless the range of error is considered. Under minimum error conditions, when the change in concentration between the two input waters is minimized, the model shows that CO₂ is brought into the system. This shows the sensitivity of the model to the redox-active species; a change of less than 5% can affect the direction in which a reaction proceeds. The sensitivity of the model in this scenario is most likely due to the small changes in concentrations that occur along the flowpath that is being modeled, and the interactions of the redox-active species. Without more detail on the specific hydrocarbons and organic acid species present in the water, it is not possible to accurately predict the degradation reactions that are occurring.

An attempt was made to simulate mass balance reactions further downgradient in the plume, from well MW-10 to well ML-143. However, the model did not provide reasonable results using the same reactions that were used in the upgradient portion of the plume. A number of changes to the feasible set of reactions were analyzed, substituting different hydrocarbons and organic acids for benzoic acid. Substitute compounds that were analyzed included toluene, xylene, benzene, formic acid, and acetic acid. None of these provided results that were reasonable and thermodynamically possible.

The simulations for this portion of the plume again showed how sensitive the model is to the choice of the hydrocarbon or organic acid that is used. This compound controls the redox reactions in the model, including CO₂ and O₂ exchange and reactions with iron, manganese, and sulfur. A change in redox state for the hydrocarbon or organic acid compound of ± 1 caused radically different model results, even reversing the direction of CO₂ and O₂ exchange between the plume and background water.

One potential reason for the difficulties in balancing reactions in the second half of the model could be the location of well ML-143 relative to well MW-10. Well ML-143 is not directly downgradient of well MW-10, and therefore the differences in water chemistry between these two wells may not be due to weathering and biodegradation reactions within

one streamtube in the aquifer. The water quality measured in the sample from well ML-143 is probably the result of different concentrations of hydrocarbons at a slightly different source location.

Aluminosilicate Weathering Rates

Rates of aluminosilicate weathering could not be determined for the unsaturated zone because the time for precipitation to move down to the water table was not determined. Using information for within the aquifer, estimates of anorthite and k-spar weathering were determined for the segment of the plume extending from well FS-1s to well MW-10. The rates were determined by calculating amount of silica dissolution from parent sediments in a unit volume of water as it migrated 35 m from the source (FS-1s) to well MW-10. Silica dissolution was determined from the increase in Ca^{2+} and K^{+} concentrations over time in the streamtube between the wells. Groundwater flows 0.32 m/day as calculated from the measured hydraulic gradient and hydraulic conductivity. With an assumed porosity of 35%, and assuming a uniform grain diameter of 1 mm based on the visual observations of the sediments, groundwater in a stream tube with a unit area of 1 m^2 and 35 m long comes in contact with 5.5×10^9 sand grains.

Of the total number of sediment grains, 1% are assumed to be anorthite and 1% to be k-spar, meaning 5.5×10^7 grains of each are present in the streamtube. The total surface area of the anorthite and k-spar grains is $6.9 \times 10^6 \text{ cm}^2$. The balance modeling predicted that $24 \mu\text{M}$ of anorthite dissolved between wells FS-1s and MW-10, resulting in a weathering rate of $2.5 \times 10^{-19} \text{ M/cm}^2/\text{s}$. $18 \mu\text{M}$ of k-spar dissolved in the same stream tube, resulting in a weathering rate of $2.8 \times 10^{-19} \text{ M/cm}^2/\text{s}$.

These rates are lower than measured laboratory rates for alkali feldspars and amphiboles of 10^{-13} to $10^{-16} \text{ M/cm}^2/\text{s}$ (Velbel 1992). Field weathering rates, however, are typically 3 orders of magnitude slower than rates measured in the laboratory (Velbel 1992). The rates measured for the Barnstable site compare well with the field measured rates for plagioclase of 10^{-17} to $10^{-19} \text{ M/cm}^2/\text{s}$ reported by Schnor (1990). More information on the composition of the aquifer sediments and the solid phase/aqueous phase reactions is needed to more accurately quantify the weathering rates.

CONCLUSIONS

A case study site with petroleum hydrocarbon contamination has been used to evaluate aluminosilicate weathering. The Barnstable, Massachusetts site consists of a sandy glacial aquifer with shallow depths to groundwater. A petroleum hydrocarbon plume resulting from spillage of oil at a fire training academy is migrating from the site and threatens two downgradient public water supply wells.

Weathering of aluminosilicate minerals was found to be accelerated in the plume relative to background waters, as indicated by increased concentrations of cations within the plume (Ca^{2+} , Na^+ , and K^+). While cation concentrations increase in the plume, silica concentrations are constant. This suggests that a secondary mineral phase is controlling the silica concentrations. Based on thermodynamic data for the site, allophane is proposed as the controlling secondary mineral. This is supported by literature references to secondary aluminosilicate minerals controlling water chemistry in other sandy aquifer, and by thermodynamic data for an alluvial aquifer in northwest Florida. Further information on the aquifer's mineral composition is needed to confirm the presence of allophane.

Mass balance reactions have been modeled for the site to quantify the extent of mineral weathering in the unsaturated zone and within a stream tube extending from the hydrocarbon source. Reactions of muscovite, albite, anorthite, gibbsite, chlorite iron hydroxide, manganese oxide, CO_2 and O_2 exchange, and naphthalene and benzoic acid degradation provide a reasonable simulation of the aquifer chemistry. Estimated weathering rates of 10^{-19} M/cm²/s for anorthite and k-spar compare well with reported field and laboratory measured rates for similar compounds.

Historical water quality monitoring at the site has been evaluated using a conceptual model of recharge to an unconfined aquifer through a zone of residual hydrocarbon saturation. Plume development in such an aquifer is controlled by the location of the source relative to recharge and discharge area. If the source is near the top of the aquifer mound, the plume will plunge deep into the aquifer. If it is near the discharge area, the

plume will remain near the water table. An understanding of the location of a plume source within an aquifer is needed to properly design a monitoring program.

Variations in the rate of groundwater causes fluctuations in the water table and, therefore, in the location of the plume relative to monitoring well screens. Changes in concentrations measured on-site in monitoring well samples correlate well with changes in water table elevations. These changes in water quality can be mis-interpreted if water-level fluctuations are not considered.

REFERENCES

- Allen, B.L., and B.F. Hajek. 1989. Mineral Occurrence in Soil Environments. IN: Minerals in Soil Environments, 2nd Edition. J.B. Dixon and S.B. Weed (Editors). Soil Science Society of America. Madison, Wisconsin. pp. 199-278.
- Aomine, S., and K. Wada. 1962. Differential weathering of volcanic ash and pumice resulting in formation of hydrated halloysite. *Am. Mineral.* v. 47, pp. 1024-1048.
- APHA -AWWA-WPCT. 1989. Standard Methods for Examination of Water and Wastewater. 17th Edition. APHA. Washington, D.C.
- Applin, K.R., and N Zhao. 1989. The kinetics of Fe(II) oxidation and well screen encrustation. *Groundwater* v.27 No.2, pp. 168-174.
- Ball, J.W., Nordstrom, D.K., and E.A. Jenne. 1980. Additional and revised thermochemical data for WATEQ 2, computerized model for trace and major element speciation in mineral equilibria of natural waters. U.S. Geological Survey Water Resource Investigations. Menlo Park, CA.
- Barber II, L.B., Thurman, E.M., and D.D. Runnells. 1992. Geochemical heterogeneity in a sand and gravel aquifer: effect of sediment mineralogy and particle size on the sorption of chlorobenzenes. IN: Chemical mediation of pollutant transport in aqueous systems. D.L. Macalady (Editor). *J. Contam. Hydrol.* v.9, pp. 35-54.
- Barnstable County Health and Environmental Department. 1987. Press release: Analysis of Volatile Organic Compounds in Water supplies - Barnstable County, Massachusetts.
- Bedient, P.B., Rodgers, A.C., Bouvette, T.C., Tomson, M.B., and T.H. Wang. Ground-water quality at a creosote waste site. *Groundwater* v.22, no. 3, pp. 318-329.
- Bennett, P.C. 1987. Solid phase studies of aquifer sediments, Bemidji, Minnesota. IN: U.S. Geological Survey Program on Toxic Waste-Ground-Water Contamination: Proceedings of the Third Technical Meeting, Pensacola, Florida, March 23-27, 1987.
- Bennett, P., and D.I. Siegal. 1987. Increased solubility of quartz in water due to complexing by organic compounds. *Nature.* v. 326, pp. 684-686.
- Bennett, P., M.E. Melcer, D.I. Siegel, and J.P. Hassett. 1988. The dissolution of quartz in dilute aqueous solutions of organic acids at 25 °C. *Geochim Cosmochim Acta.* v. 52, pp.1521-1530.
- Borden, R.C., and P.B. Bedient. 1986. Transport of dissolved hydrocarbons influenced by oxygen-limited biodegradation 1: Theoretical development. *Water Resources Research.* v. 22, no.13, pp 1973-1982.
- Brock, T.D, and M.T. Madigan. 1988. *Biology of Microorganisms*, Fifth Edition. Prentice Hall, Englewood Cliffs, NJ.

- Cambareri, T.C. 1986. Hydrogeology and Hydrochemistry of Sewage Effluent Plume in the Barnstable Outwash of the Cape Cod Aquifer, Hyannis Massachusetts. University of Massachusetts Masters Thesis.
- Calvert, C.S., Buol, S.W., and S.B. Weed. 1980. Mineralogical characteristics and transformations of a vertical rock-saprolite-soil sequence in the North Carolina Piedmont: II Feldspar alteration products - their transformation through the profile. *Soil Sci. Soc. Am.* v. 44, pp. 1104-1112.
- Cape Cod Planning and Economic Development Commission. 1978. Draft Environmental Impact Statement and Proposed 208 Water-Quality Management Plan for Cape Cod. Barnstable, Massachusetts.
- Cape Cod Commission, Water Resources Office. March 1991. Phase II Comprehensive Site Assessment - Barnstable County Fire Training Academy, Barnstable, Massachusetts.
- Champ, D.R., J. Gulens, and R.E. Jackson. 1979. Oxidation-reduction sequences in ground water flow systems. *Canadian J. of Earth Sci.* v. 16, pp. 12-23.
- Chou, L., and R. Wollast. 1985. Steady-state kinetics and dissolution mechanisms of albite. *Am. J. of Sci.* v. 285, pp. 963-993.
- Chou, L., and R. Wollast. 1984. Study of the weathering of albite at room temperature and pressure with a fluidized bed reactor. *Geochim. Cosmochim Acta.* v. 48, pp. 2205-2217.
- Coffin and Richardson, Inc. 1975. Pump Test for Barnstable Water Company Wells - MD-2, MD-3 and MD-4. Boston, Mass.
- Commonwealth of Massachusetts. 1987. Contamination in Municipal Water Supplies. Special Legislative Commission on Water Supply.
- Cozzarelli, I.M., M.J. Baedecker, and J.A. Hopple. 1987. Effects of creosote products on the aqueous geochemistry of unstable constituents in a surficial aquifer. IN: U.S. Geological Survey Program on Toxic Waste-Ground-Water Contamination: Proceeding of the Third Technical Meeting. Pensacola, Florida, March 23-27, 1987.
- Daugherty, S.J. 1991. Regulatory approaches to hydrocarbon contamination from underground storage tanks. IN: *Hydrocarbon Contaminated Soils and Groundwater*. Kostecki, P.T., and E.J. Calabrese (Editors). Lewis Publishers, Chelsea, MI. pp.23-64.
- Drever, J.I., 1982. *The Geochemistry of Natural Waters*. Prentice Hall, New Jersey.
- Eary, E., and J.A. Schramke. 1990. Rates of inorganic oxidation reactions involving dissolved oxygen. IN: *Chemical Modeling of Aqueous Systems II*. Melchior, D.C., and Bassett, R.L. (editors). American Chemical Society, Wash. D.C.
- Eswaran, H., Stoops, G., and P. de Paepe. 1973. A contribution to the study of soil formation on Isla Santa Cruz, Galapagos. *Pedologie.* v. 23, pp. 100-121.
- Eswaran, H., and C. Sys. 1976. Micromorphological and mineralogical properties of the Quoin Hill toposequence. *Pedologie.* v. 26, pp. 280-291.

Feth, J.H., Roberson, C.E., and W.L. Polzer. 1984. U.S. Geological Survey Water Supply Papers, no.1535I, Washington, D.C.

Freeze, R.A., and J.A. Cherry. 1979. Groundwater. Prentice Hall, Inc. New Jersey.

Frimpter, M.H., and F.B. Gay. 1979. Chemical quality of ground water on Cape Cod, Massachusetts. U.S. Geological Survey, Water Resources Investigation 79-65.

Funkert, R.J., and M. Fieldes. 1968. Allophane in New Zealand soils. Trans. Int. Congr. Soil Sci., 9th edition (Adelaid, S. Aust.). v. 3, pp. 133-141.

Garrels, R.M. and C.L. Christ. 1965. Solutions, Minerals, and Equilibria. Harper and Row. New York, NY.

Geschwind, P.M, and M.D. Reynolds. 1987. Monodisperse ferrous phosphate colloids in an anoxic groundwater plume. J. Cont. Hydrology. v.1, pp. 309-327.

Glynn, P.D., and E.J. Reardon. 1990. Solid-solution aqueous-solution equilibria: thermodynamic theory and representation. American Journal of Science. v. 2909, pp. 164-201.

Hem, J.D. 1989. Study and Interpretation of the Chemical Characteristics of Natural Waters, Third Edition. United States Geological Survey Water Supply Paper No.2254.

Horsley Witten Hegemann, Inc. 1991. Hydrogeologic and water quality investigation, Maher Wellfield, Hyannis, Massachusetts.

Horsley Witten Hegemann, Inc. 1992. Hydrogeological and Ecological Assessment of Mary Dunn Pond, Barnstable, Massachusetts.

Hult, M.F. 1987. Microbial oxidation of petroleum vapors in the unsaturated zone. IN: U.S. Geological Survey Program on Toxic Waste-Ground-Water Contamination: Proceedings of the Third Technical Meeting, Pensacola, Florida, March 23-27, 1987.

Hvorslev. M.J. 1951. Time lag and soil permeability in groundwater observations. U.S. Army Corps of Engineers Waterways Experimental Station Bulletin #36. Vicksburg, Mississippi.

IEP, Inc. 1986. Preliminary Site Assessment and Recommendations for Remedial Action at the Barnstable County Fire Training Academy, Barnstable, Massachusetts.

Inskeep, W.P., Nater, E.A., Bloom, P.R., Vandervoort, D.S., and M. S. Erich. 1991. Characterization of laboratory weathered labradorite surfaces using x-ray photoelectron spectroscopy and transmission electron microscopy. Geochim Cosmochim Acta. v. 55, pp. 787-800.

Katz, B.G., and A.F. Choquette. 1991. Aqueous geochemistry of the sand-and-gravel aquifer, northwest Florida. Groundwater v. 29, no.1, pp. 47-55.

Kaye, C.A. 1964. Outline of Pleistocene geology of Martha's Vineyard, Massachusetts. U.S. Geological Survey Prof. Paper 501-C, pp. C134-139.

- Kenoyan, G.J., and C.J. Bowser. 1992. Groundwater chemical evolution in a sandy silicate aquifer in northern Wisconsin, 1, Patterns and Rates of Change. *Water Resources Research*. v. 28, pp. 579-590.
- Kenoyan, G.J., and C.J. Bowser. 1992. Groundwater chemical evolution in a sandy silicate aquifer in northern Wisconsin, 2, reaction modeling. *Water Resources Research*. v. 28, pp. 591-600.
- Knott, J.F., and J.C. Olimpio. 1986. Estimation of recharge rates to the sand and gravel aquifer using environmental tritium, Nantucket Island, Massachusetts. U.S. Geological Survey Water-Supply Paper 2297. 26 pp.
- Kruseman, G.P., and N.A. DeRidder. 1990. Analysis and evaluation of pumping test data. Publication 47, 2nd ed. International Institute for Land Reclamation and Improvement. Wageningen, The Netherlands.
- LeBlanc, D.R. 1984. Sewage plume in a sand and gravel aquifer, Cape Cod, Massachusetts. U.S. Geological Survey Water-Supply Paper #2218. 28 pp.
- LeBlanc, D.R., Guswa, J.H., Frimpter, M.H., and C.J. Londquist. 1986. Ground-water resources of Cape Cod Massachusetts. U.S. Geological Survey Hydrologic Investigations Atlas HA-692.
- Lippman, F. 1977. The solubility product of complex minerals, mixed crystals and three-layer clay minerals. *Neues Jahrbuch fur Mineralogie Abhandlung* v. 130, no. 3, p. 243.
- Lippman, F. 1982a. Stable and metastable solubility diagrams for the system $\text{CaCO}_3 - \text{MgCO}_3 - \text{H}_2\text{O}$ at ordinary temperature. *Bulletin de Mineralogie*. v. 105, pp. 273-279.
- Lippman, F. 1982b. Nucleation and polymorphic precipitation of carbonate minerals. *Estudios Geoloigica* v. 38, pp. 199-208.
- Lippman, F. 1980. Phase diagrams depicting the aqueous solubility of binary mineral systems. *Neues Jahrbuch fur Mineralogie Abhandlung*. v. 139, no.1, pp. 1-25.
- Ludvigson, P.J., D.H. Chen, C.C. Stanley, and D. Draney. 1991. Petroleum release decision framework (PRDF). IN: *Petroleum Contaminated Soils, Volume 3*. Kostecki, P.T., and E.J. Calabrese (Editors). Lewis Publishers. Chelsea MI. pp. 19-27.
- Makay, D.M., and J.A. Cherry. 1989. Groundwater contamination: pump-and-treat remediation. *Env. Sci. and Tech.* v. 23, no. 6, pp 630-636.
- Montgomery, J.H., and L.M. Welkom. 1990. *Groundwater Chemicals Desk Reference*. Lewis Publishers. Chelsea, MI.
- Nelson, M.E., S.W. Horsley, T.C. Cambareri, M.D. Giggey and J.R. Pinnette. 1988. Predicting nitrogen concentrations in ground water - an analytical model. IN: *Proceedings of the FOCUS Conference on eastern regional ground water issues*. National Water Well Association. 23-27 September 1988.

Nordstrom, D.K. 1977. Thermochemical redox equilibria of ZoBell's solution. *Geochim Cosmochim Acta*. v. 41, pp. 1835-1841.

Nordstrom, D.K., L.N. Plummer, D. Langmuir, E. Busenberg, H.M. May, B.F. Jones, and D.L. Parkhurst. 1990. Revised chemical equilibrium data for major water-mineral reactions and their limitations. IN: *Chemical Modeling of Aqueous Systems II*, D.C. Melchior and R.L. Bassett (Editors). American Chemical Society Symposium Series 416. pp. 398-413.

Oldale, R.N. 1974. Geologic map of the Hyannis Quadrangle, Barnstable County, Cape Cod Massachusetts. U.S. Geological Survey Geologic Quadrangle Map GQ-1158.

Oldale, R.N. 1984. Notes on the Generalized Geologic Map of Cape Cod. U.S. Geological Survey, Preliminary Open File Report.

Ostendorf, D.W., and D.H. Kampell. 1991. Biodegradation of hydrocarbon vapors in the unsaturated zone. *Water Res. Res.* v. 27, no.4, pp 453-462.

Paces, T. 1972. Chemical characteristics and equilibration in natural water-felsic rock-CO₂ systems. *Geochim Cosmochim Acta*. v. 36, pp. 217-240.

Paces, T. 1973. Steady-state kinetics and equilibrium between ground water and granitic rocks. *Geochim. Cosmochim. Acta*. v. 37, pp. 2641-2663.

Palmer, C.D., 1977. Hydrogeologic implications of various wastewater management proposals for the Falmouth area of Cape Cod, Massachusetts. Woods Hole, Massachusetts, Woods Hole Oceanographic Institution Technical Report WHOI-77-32 (Appendix), 142p.

Pamukcu, S., Hijazi, H.M., and H.Y. Fang. 1990. Study of possible reuse of stabilized petroleum contaminated soils as construction material. IN: *Petroleum Contaminated Soils*, Volume 3. Kostecki, P.T., and E.J. Calabrese (Editors). Lewis Publishers. Chelsea, MI.

Parkhurst, D.L., Thorstenson, D.C., and L.N. Plummer. 1982. BALANCE - A computer program for calculation of chemical mass balance. U.S. Geological Survey Water Resources Investigations 82-14.

Plummer, L.N., Jones, B.F., and A.H. Truesdell. 1976. WATEQ4F- a Fortran IV version of WATEQ, a computer program for calculating chemical equilibrium of natural waters. U.S. Geological Survey Water Resources Investigations 76-13.

Potter, T.L. 1991. Fingerprinting petroleum products: unleaded gasolines. IN: *Petroleum Contaminated Soils*, Volume 3. Kostecki, P.T., and E.J. Calabrese (Editors). Lewis Publishers. Chelsea MI. pp. 83-92.

Pye, V.I., Patrick, R., and J. Quarles. 1983. *Groundwater Contamination in the United States*. Univ. of Pennsylvania Press. Philadelphia, PA.

Rogers, R.J. 1987. Geochemical evolution of groundwater in stratified-drift and arkosic bedrock aquifers in north central Connecticut. *Water Res. Res.* v. 23, no.8, pp. 1531-1545.

Ryan, B.J. 1979. Cape Cod aquifer, Cape Cod, Massachusetts. U.S. Geological Survey Water-Resources Investigations 80-157.

- Schnor, G.L. 1990. Kinetics of chemical weathering: a comparison of laboratory and field values. IN: Aquatic Chemical Kinetics. W. Stumm (Editor) Wiley Interscience. New York, NY.
- Siegal, D.I. 1987. Geochemical facies and mineral dissolution, Bemidji, Minnesota, research site. IN: U.S. Geological Survey Program on Toxic Waste-Ground-Water Contamination: Proceedings of the Third Technical Meeting, Pensacola, Florida, March 23-27, 1987.
- Strack, O.D.L. 1989. Groundwater Mechanics. Prentice Hall, Englewood Cliffs, NJ. 732 pp.
- Stumm, W., and J.J. Morgan. 1981. Aquatic Chemistry. John Wiley and Sons. New York, NY.
- Tait, J.M., Yoshinaga, N. and B.D. Mitchell. 1978. The occurrence of imogolite in some Scottish soils. Soil Sci. Plant Nutr. v. 24, pp. 145-151.
- Theis, C.V. 1935. The relation between the lowering of the piezometric surface and the rate and duration of discharge of a well using ground-water storage. Trans. Amer. Geophysical Union. v. 16, pp. 519-524.
- Thiem, G. 1906. Hydrologische Methoden. Gebhardt, Leipzig.
- Thorntwaite, C.W., and J.R. Mather. 1957. Instructions and tables for computing potential evapotranspiration and the water balance. Drexel Institute of Technology, Centerton, NJ. Publications in Climatology. v. 10, no.3, 311 pp.
- Todd, D.K. 1980. Groundwater Hydrology, 2nd ed. John Wiley & Sons.
- U. S. Environmental Protection Agency. 1982. Cape Cod aquifer determination. Federal Register, v. 47, no. 134, pp.30282-30284.
- U. S. Environmental Protection Agency. 1987. Health Advisories for 25 Organics. National Technical Information Service #PB87-235578.
- U. S. Environmental Protection Agency. 1991. WHPA, An Integrated Semi-Analytical Model for the Delineation of Wellhead Protection Areas. Office of Ground Water and Drinking Water. Wash., D.C.
- Wada, K. 1989. Allophane and Imogolite. IN: Minerals in Soil Environments, 2nd Edition. J.B. Dixon, and S.B. Weed (Editors). Soil Science Society of America. Madison, Wisconsin. pp.1051-1087.
- Walkley, A., and I.A. Black. 1934. An examination of the Degtjareff method of determining soil organic matter and a proposed modification of the chromic acid titration method. Soil Science. v. 37, pp. 29-38.
- Wise, W.R., Chang, C., Klopp, R.A., and P.B. Bedient. 1991. Impact of recharge through residual oil upon sampling of underlying ground water. Ground Water Monitoring Review. v. 11, no. 2, pp. 93-100.
- Wollast, R. 1967. Kinetics of the alteration of K-feldspar in buffered solutions at low temperature. Geochim. Cosmochim. Acta. v. 31, pp. 635-648.

**APPENDIX A:
PETROLEUM HYDROCARBON PLUME DEVELOPMENT IN
UNCONFINED AQUIFERS RECEIVING CONSTANT OR PERIODIC
RECHARGE**

To predict the movement of hydrocarbon spills and design cost effective sampling and remediation systems, it is important to understand the processes controlling plume development and migration. Of the many processes controlling plume development, two that are interrelated, infiltration of recharge and water-level fluctuations, are described. Their effects will be evaluated for hydrocarbon plumes resulting from residual contamination in the unsaturated zone in an unconfined aquifer receiving both constant and periodic recharge.

Plume formation affected by infiltrating recharge is controlled by the location of the plume source relative to the recharge and discharge areas in the aquifer. The closer the source is to the upgradient boundary or "top" of the aquifer, the deeper the plume will plunge into the aquifer. If infiltration is not constant, the resulting water table fluctuations can change plume size as well as its depth in the aquifer.

The effect of recharge on BTEX concentrations in groundwater below a zone of residual hydrocarbon contamination has been examined at a aviation fuel oil spill site in Traverse City, Michigan (Wise *et al*, 1991). A positive correlation between increased recharge and increased BTEX concentrations in groundwater directly below the residual zone was observed. These data, and the data from the Barnstable site, highlight the need for a better understanding of how recharge processes affect plume development. These processes, in turn affect the installation of monitoring wells and the interpretation of sampling data for a hydrocarbon plume.

For most hydrocarbon investigations, monitoring wells are constructed with 1.5 to 3.0 m screens placed across the water table. If a plume moves downward through the aquifer, these types of wells can provide misleading information on how far the plume is moving. If water levels fluctuate during investigations, the depth and strength of the plume can change. The location of monitoring wells relative to the changing water table must

therefore be considered when interpreting sampling. If ignored, improper predictions can be made on the location and strength of the plume, information needed for health risk assessments and remedial action planning.

A conceptual model of an unconfined aquifer receiving recharge has been developed to describe plume formation. Differences in plume development under constant and variable recharge conditions will be described. The model will be used to demonstrate how, in many situations, "typical" monitoring well design will provide misleading data on plume location and movement.

The effects of these hydrologic processes will then be examined for the data developed for the Barnstable site. They will be shown to overshadow other physical and chemical processes controlling plume movement such as dispersion, diffusion, adsorption/retardation and, potentially, biodegradation. None of these processes can be properly understood until the effects of recharge and water-level fluctuations are known.

Plume Development With Constant Recharge

Under steady-state conditions, recharge water enters the aquifer at a constant rate, and a balance is reached between recharge and groundwater discharge out of the aquifer. The water table reaches a steady elevation and does not change unless affected by pumping or injection wells. Groundwater will not only move horizontally throughout the aquifer but will be forced downward by the infiltration of recharge from above. Vertical and horizontal groundwater velocities will vary with location in the aquifer. These variations need to be understood to predict plume movement and plan sampling networks.

Using the conceptual aquifer model described in Figure A-1, downward vertical gradients are the largest at the top of the groundwater mound. Horizontal gradients are low relative to the vertical gradients as most of the water is moving downward. The flow line at the upper (left) boundary of the aquifer would move directly downward to the aquifer base before moving horizontally through the aquifer (Figure A-1, line A). A plume formed from a source in this location will move deep into the aquifer because of the dominant vertical gradient.

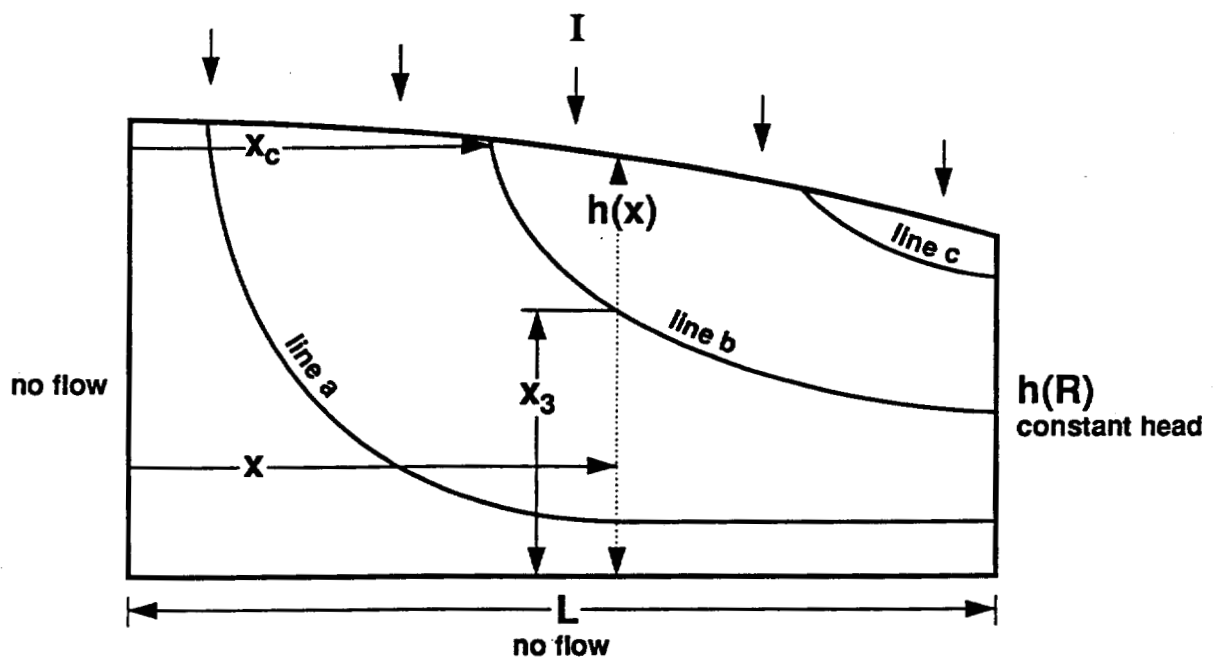


FIGURE A-1. Conceptual Unconfined Aquifer Receiving Constant Recharge

In the center of the aquifer system, infiltrating recharge continues to create a downward vertical gradient. The horizontal gradient, however, is increased relative to the vertical gradient. Water recharging this portion of the aquifer must stay above the water that was recharged further up in the aquifer. Recharge entering this part of the aquifer will plunge below the water table (Line B, Figure A-1), but not as deep as line A.

Recharge still enters the aquifer near the discharge point (Line C, Figure A-1), but remains shallow, and discharges soon after entering the aquifer. A plume formed in this area will not move down into the aquifer, but will flow near the surface towards the discharge point. For this reason these areas are often considered as appropriate locations for the siting of potentially hazardous land uses, such as landfills. If any leakage occurs, the potential for groundwater contamination is less than if the site was located higher up in the aquifer.

An analytical solution for the stream lines in the system depicted in Figure A-1 is given by Strack (1989). Each stream line can be plotted using:

$$X_3 = \frac{h(x)X_0}{X}$$

where:

- X_3 = the height of the streamline off the base of the aquifer,
- X = the horizontal distance from the upgradient boundary (left hand side) of the aquifer,
- X_0 = the horizontal distance of the source from the upgradient boundary (left hand side) of the aquifer, and
- $h(x)$ = the water table elevation at point X.

The water table elevation, $h(x) = [h(r)^2 + (L^2 - X^2) I/K_x]^{1/2}$

where:

- $h(r)$ = The water table elevation at the constant head boundary on the right side of the aquifer,
- L = The overall length of the aquifer,
- K_x = hydraulic conductivity in the x direction, and
- I = the recharge, or infiltration rate.

The height of a streamline above the aquifer base decreases as it moves towards the discharge point. At any point in the aquifer, the height is a function of the water table elevation and distance of the source from the top (left hand side) of the aquifer. Using the calculated streamlines as approximations of plume location, it is possible to illustrate hydrocarbon plume development from sources at each of the three locations discussed previously; at the top of the groundwater mound (plume A), in the center of the aquifer (plume B), and near the discharge point (plume C).

Plume configurations have been developed using the hydrologic conditions measured at the Barnstable site, including the average recharge rate (46 cm/yr, 18 in/yr), saturated thickness (15 m) and the average hydraulic conductivity (55 m/d). As expected, plume A plunges deep into the aquifer, plume C stays near the water table, and plume B descends to an intermediate depth (Figure A-2). The hydrogeologic setting at the Barnstable site is similar to that of plume B, as it is located in the center of the aquifer system that encompasses the town.

To evaluate the effectiveness of water table monitoring wells in detecting the contaminant plumes, several wells with uniform screen lengths are placed across the water table at identical distances from each plume, and relative contaminant concentrations expected from samples from each of the wells are calculated (Figures A-3, A-4, and A-5). Very different sample results are obtained for each type of plume.

Samples from wells near the plume A would indicate a short, concentrated plume (Figure A-3). The plume delineated by the wells downgradient of plume B is slightly longer but still shorter than the actual plume that is moving underneath the wells (Figure A-4). This is in contrast to the sample results for the plume near the discharge point (Plume C), where the plume is detected in wells located 700 m from the source (as opposed to 300 m for plume B, Figure A-5). The use of water table wells to analyze this plume is more appropriate than for the other two scenarios.

Besides well location, the choice of screen lengths can also cause problems in interpretation. For example, consider the differences in the two screen lengths used to calculate relative contaminant concentrations for plume B (Figure A-6). Samples from

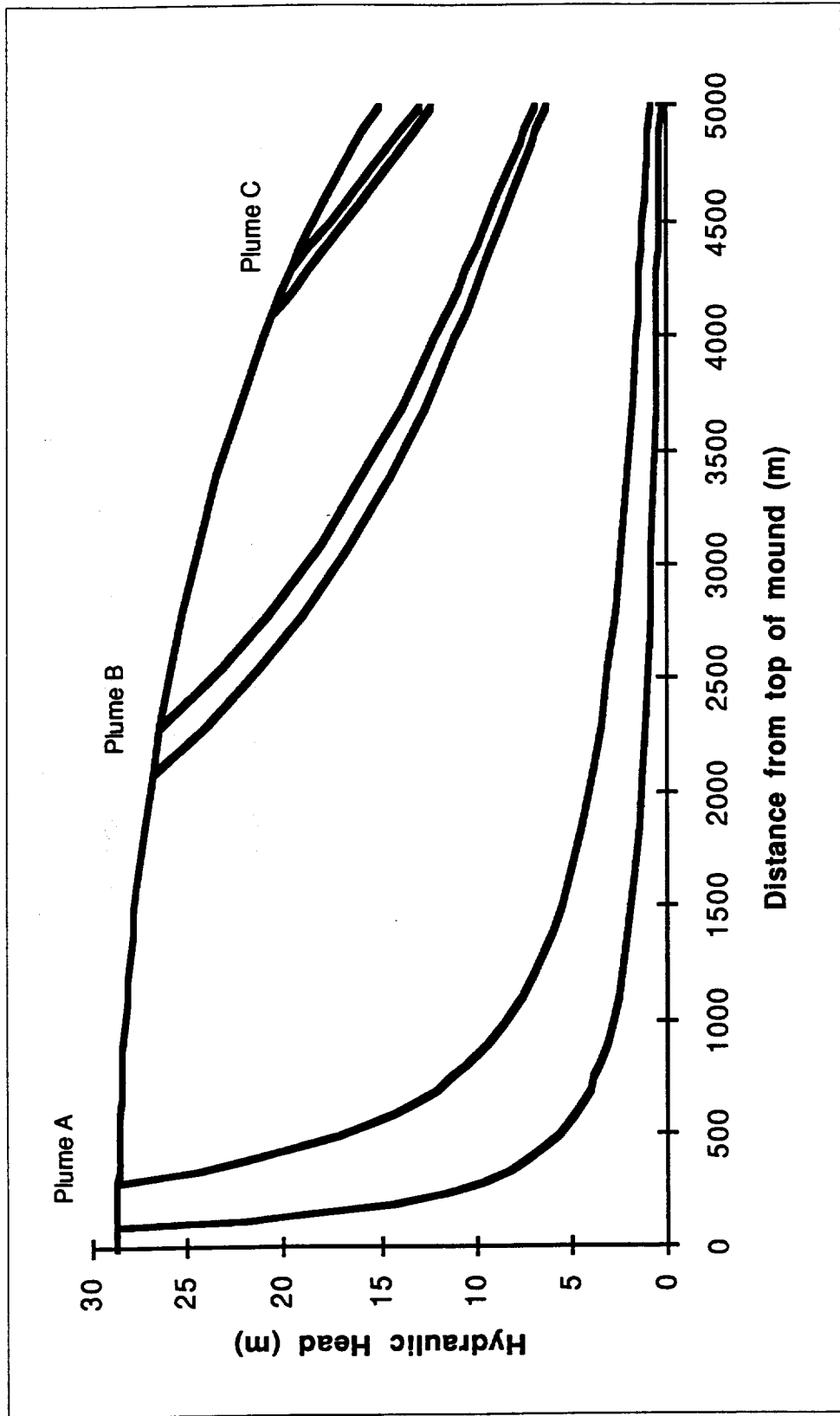


Figure A-2: Comparison of Plume Development with Varying Source Locations

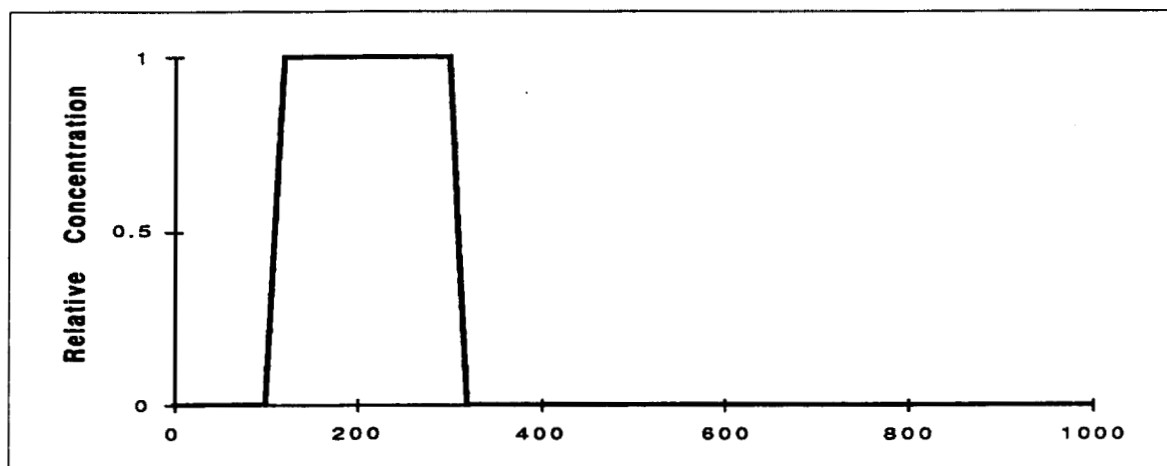
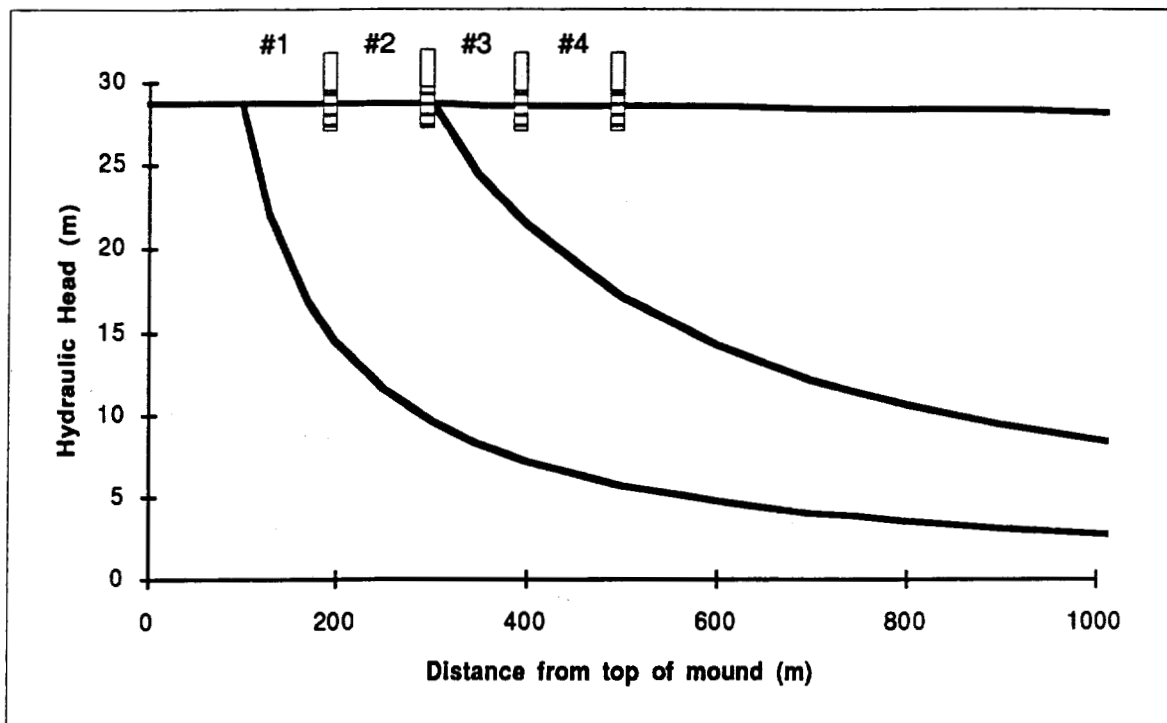


Figure A-3: Well Placement Relative to Plume Location - Plume A

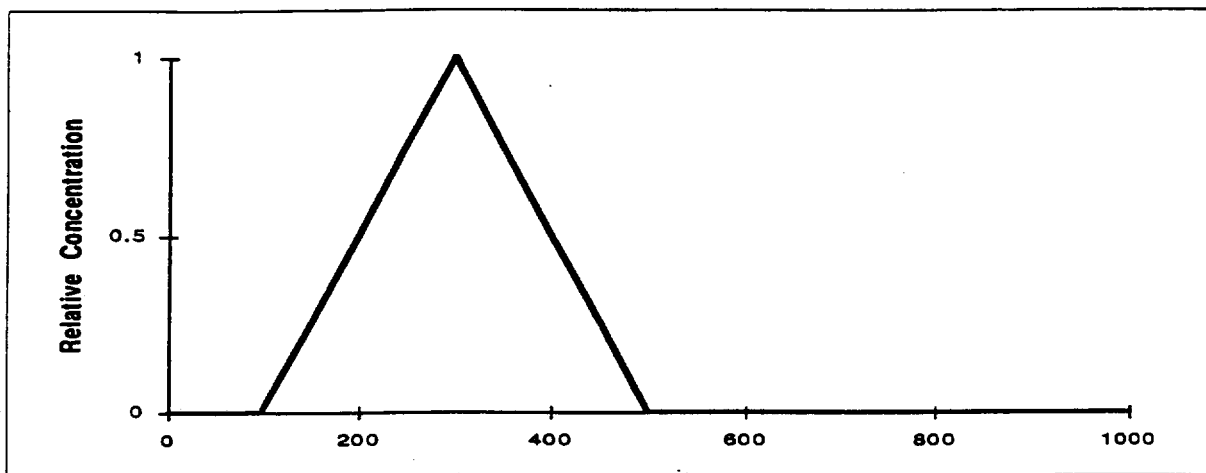
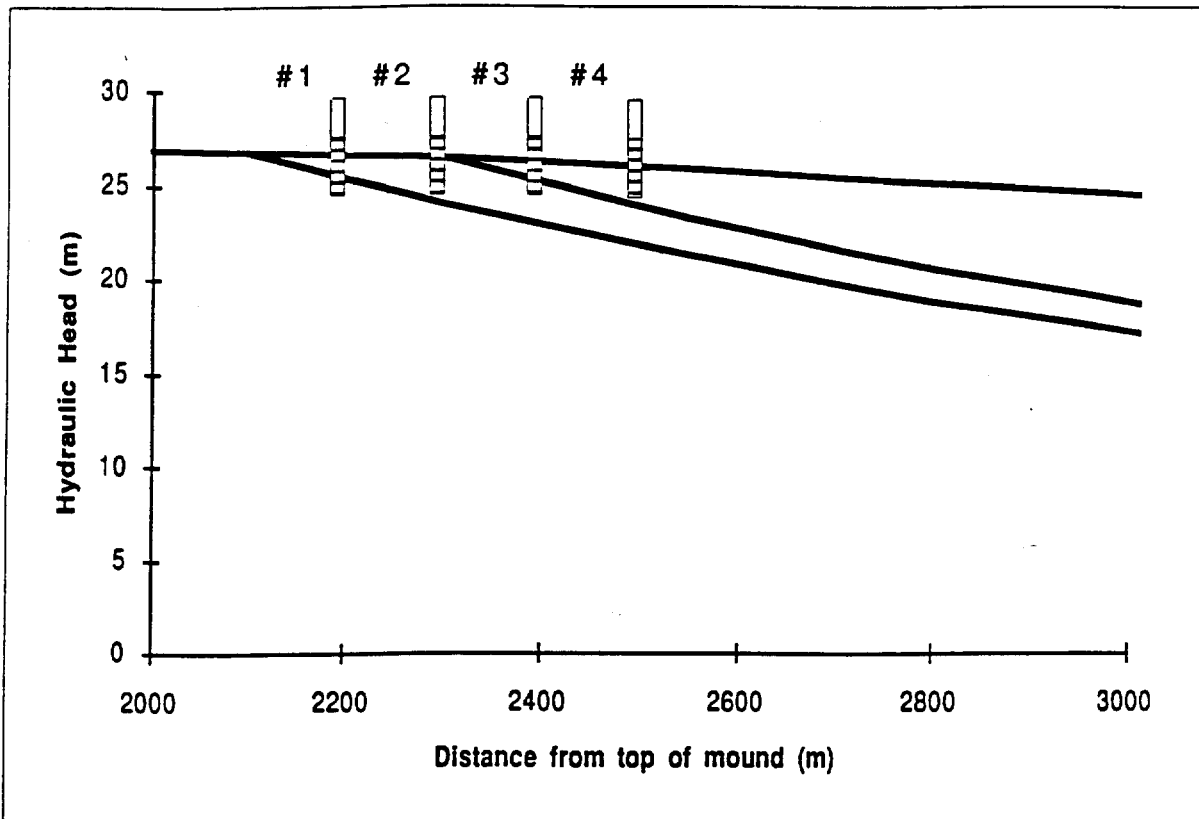


Figure A-4: Well Placement Relative to Plume Location - Plume B

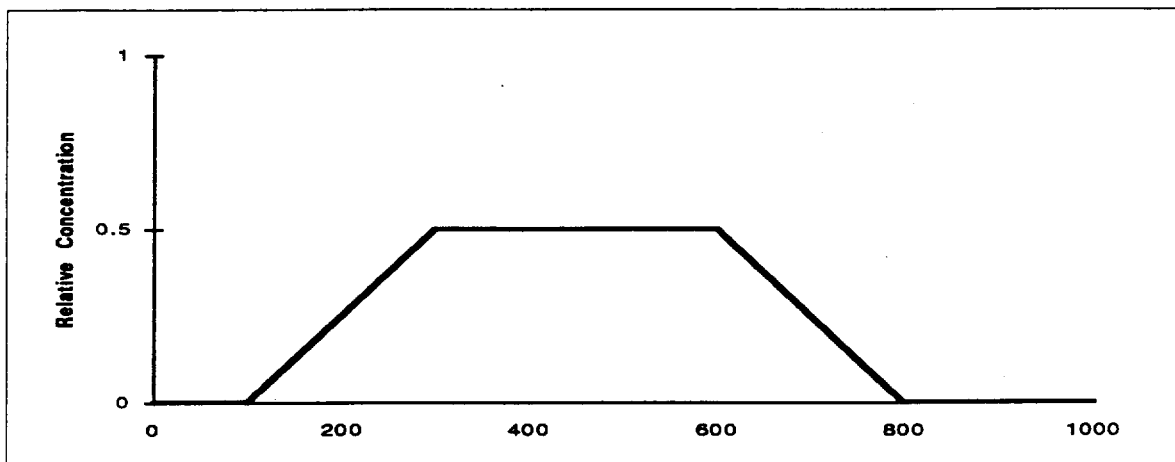
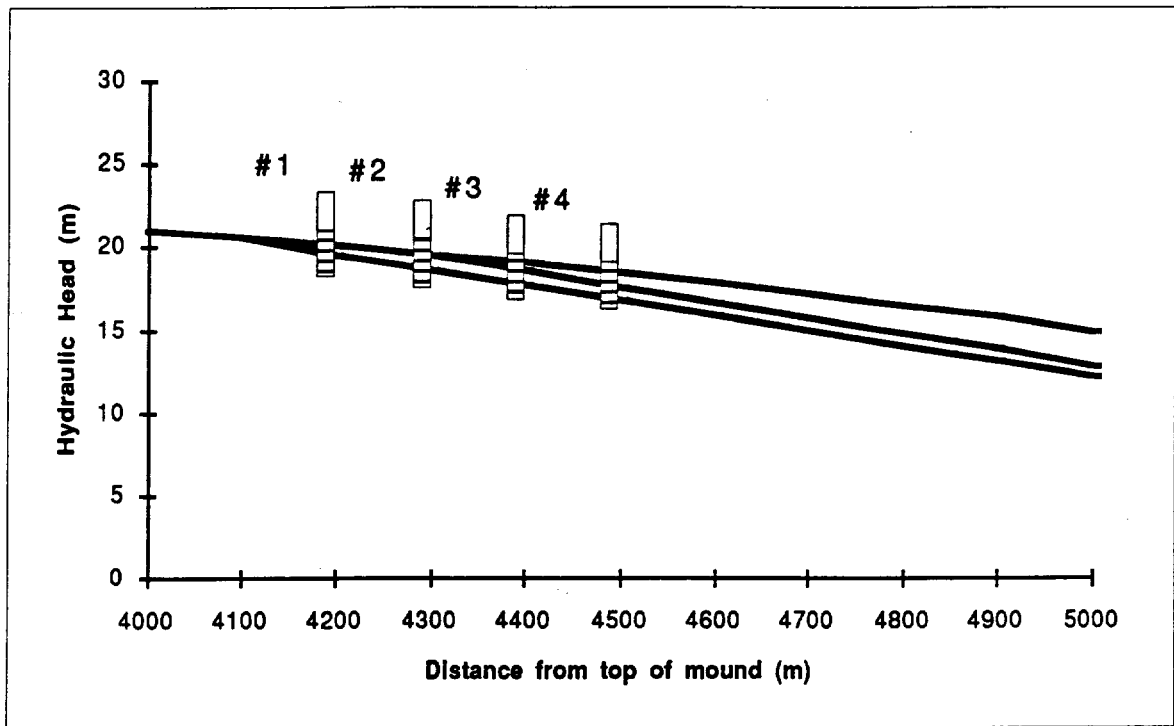


Figure A-5: Well Placement Relative to Plume Location - Plume C

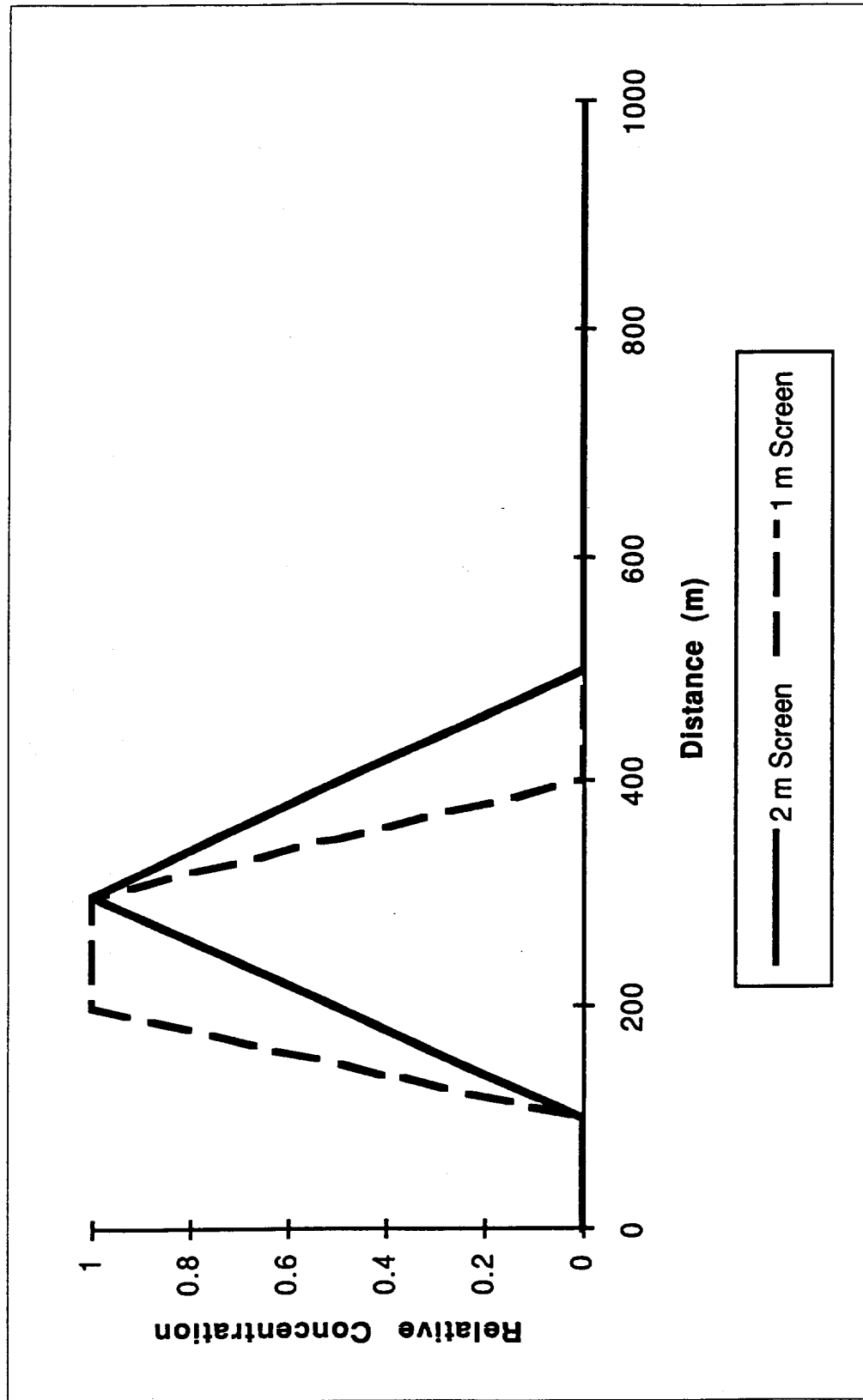


Figure A-6: Changes in Measured Concentrations With Varied Screen Length - Plume B

wells with the shorter of the two types of screen show the plume to be shorter but more concentrated, with the toe 300 m from the source, as opposed to 400 m for the longer screened wells. A different interpretation of the plume is made because of different well construction.

For example, most of the wells at the Barnstable site have 3.3 m (10 ft) screens which were installed to allow sampling of a relatively large cross-section of the aquifer. However the plume is only 4-5 ft thick. The dilution of the contaminated water within the well during sampling results in an erroneously low estimate of the plume strength. If the plume does not completely intersect the well screen but flows partially above or below, the sample result will be even further below the actual plume concentration.

Variable Recharge Effects at Plume Source

Most contamination sites do not receive recharge at a uniform rate. Instead recharge varies, both seasonally and over longer periods of time. This periodic recharge causes fluctuations of the water table which affect the thickness of the plume. The thickness of the plume (if density considerations are not included) is also partially controlled by recharge moving down through contaminated sediments and causing the underlying contaminated water to sink as it moves past the residual saturation zone.

At the site of plume A, water-level fluctuations have a minimal effect on plume thickness. The plume is moving downward with very little horizontal flow, and changes in recharge rate will not significantly affect its flow path.

The changes in plume thickness with water-level fluctuations are similar for plume B and plume C. An increase in recharge causes a water table rise which increases the thickness of a contaminant plume, as groundwater is in greater contact with the source in the previously unsaturated sediments (Figure A-7). The plume thickness decreases during periods of low water levels, as less groundwater is in direct contact with the source contamination, and there is little or no recharge moving through the source and down into the aquifer. At extremely low water levels, groundwater is not in contact with the residual contamination. Contamination only enters the system with recharge moving through the source in the unsaturated zone. During periods of low water, this recharge is minimal.

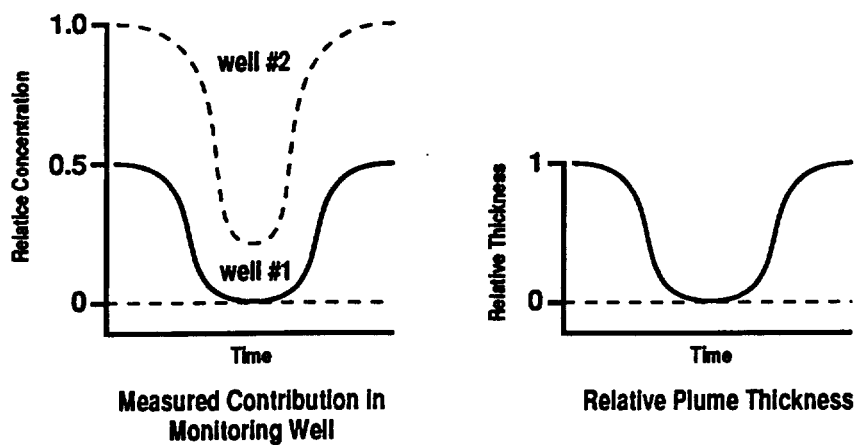
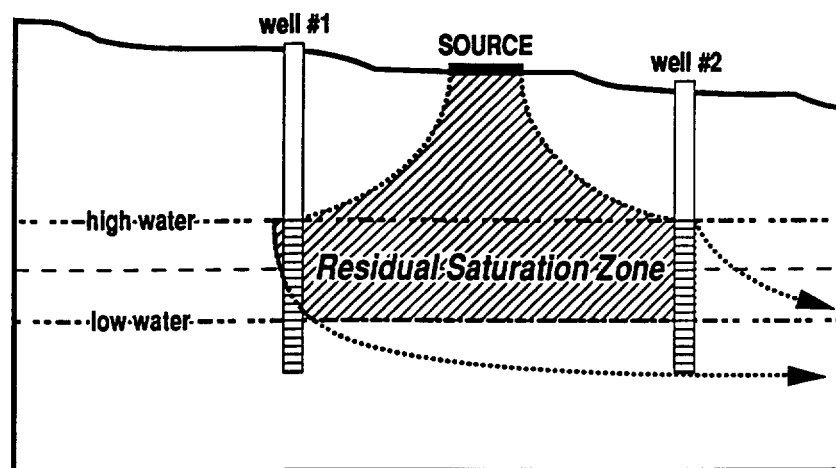


FIGURE A-7. Fluctuations in Plume Thickness and Measured Concentrations at Source Unconfined Aquifer with Periodic Changes in Recharge Rate

The range of water-level fluctuations will be smaller for the area around plume C because it is closer to the constant head boundary imposed on this side of the aquifer in the conceptual model. As a result, the variations in thickness will be less here than at the location of plume B.

Monitoring wells are typically screened partially in and partially below the residual saturation zone in order to prevent them from going dry. In the areas of plumes B and C, when the water table rises, a sample from a well at the upgradient end of the zone of residual saturation would show an increase in contaminant concentration, because there is an increase in the relative proportion of contaminated water being sampled (Figure A-7, well #1). If this change is not detected between sampling rounds, then one could interpret that the plume concentration has increased, when in fact less clean water is mixing with the plume.

When water levels decrease, less contamination is detected in the monitoring well. The plume thickness decreases, as there is less water in contact with the residual saturation zone, and the proportion of clean water mixing with the plume water increases. Again, if the water level change is not recognized, one can make an improper interpretation of the status of the plume, in this case concluding that concentrations are decreasing, when, in fact, the plume thickness is decreasing.

A plume is thicker at the downgradient end of the zone of residual contamination because the contaminated water from further upgradient is forced downward by recharge as it moves downgradient. The thickness can again be calculated using Strack's approach for plotting streamlines. Under average recharge conditions for the Barnstable site, the thickness of the plume increases 1.2 meters across a 100 m long zone of residual contamination. Because the plume is thicker at the downgradient end of the source, a higher concentration should be detected in a well here relative to one at the upgradient end of the source (Figure A-7, well #2). This will be true regardless of how the water table fluctuates. If the 1.2 m increase is accurate, at high water table elevations, the screen of well #2 is completely within the contaminated zone. The thickening of the plume at the downgradient end of the source has also been shown in evaluations of plumes B and C where wells in the center of the plume provide lower concentrations than those at the downgradient end (Figures A-4 and A-5).

Variable Recharge Effects Downgradient of Plume Source

Given the conceptual model that has been used above, the only portion of the aquifer where effects of varying recharge will change measurements in downgradient monitoring wells is the center (plume B). At the top, plume A will continue to plunge nearly straight down into the aquifer, regardless of the recharge rate. No water quality changes will be observed in downgradient wells. Near the discharge point, plume C will not sink very far into the aquifer, and, again, downgradient wells will not be as affected by varying recharge rates.

The range of plume configurations under varying recharge conditions for the area of plume B have been plotted using conditions for the area around the Barnstable site. Recharge rates of 58 cm/yr (23 in/yr) under maximum conditions and 43 cm/yr (17 in/yr) under minimum conditions were used based on measured precipitation data in Hyannis from 1985 to 1991 (HWH, 1992). The mean precipitation during this period was 1.02 m/yr. The maximum and minimum precipitation values are calculated using ± 1 standard deviation from this mean (0.15 m), and the recharge rate was determined assuming a 50% evapotranspiration rate.

The variation in water table elevation is approximately 2 m at the top of the mound and drops to zero at the constant head boundary on the discharge side of the aquifer (Figure A-8). Two wells have been placed downgradient from the source; one across the upper water table (well #1), and one across the lower water table (well #2). Well #1 just intersects the plume during maximum recharge conditions. During times of less recharge, the well would be above the plume and no contaminants would be discovered. If a sample is taken at this time, one could improperly interpret the results, thinking the water is clean, when, in fact, the plume is underneath the well. At minimum recharge conditions the well could potentially go dry.

Well #2 intersects the plume under minimal recharge conditions, and, as the water table rises, the concentration in the well will rise as more of the plume intersects the well. Again, if this rise is not detected, one could think the plume is getting stronger. Further downgradient from the source the effects of water-table fluctuations are dampened. The plumes under each recharge condition become closer together and discharge from the

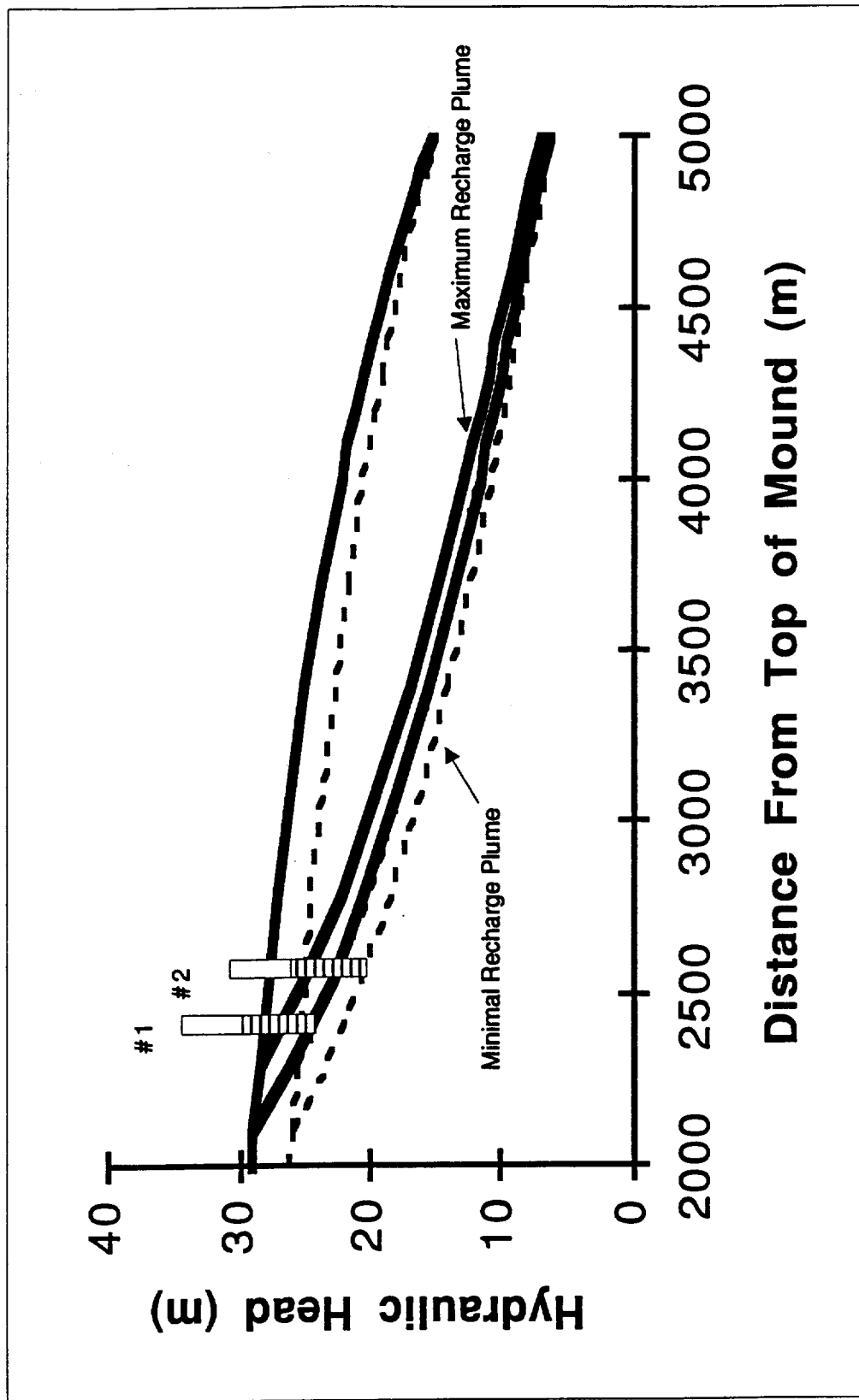


Figure A-8: Development of Plume B at High and Low Recharge Rates (43 - 58 cm/yr)

aquifer at the same depth. The depth of the plume at the discharge point is controlled by the horizontal location of the source in the aquifer. The water table elevation does not control the final plume depth.

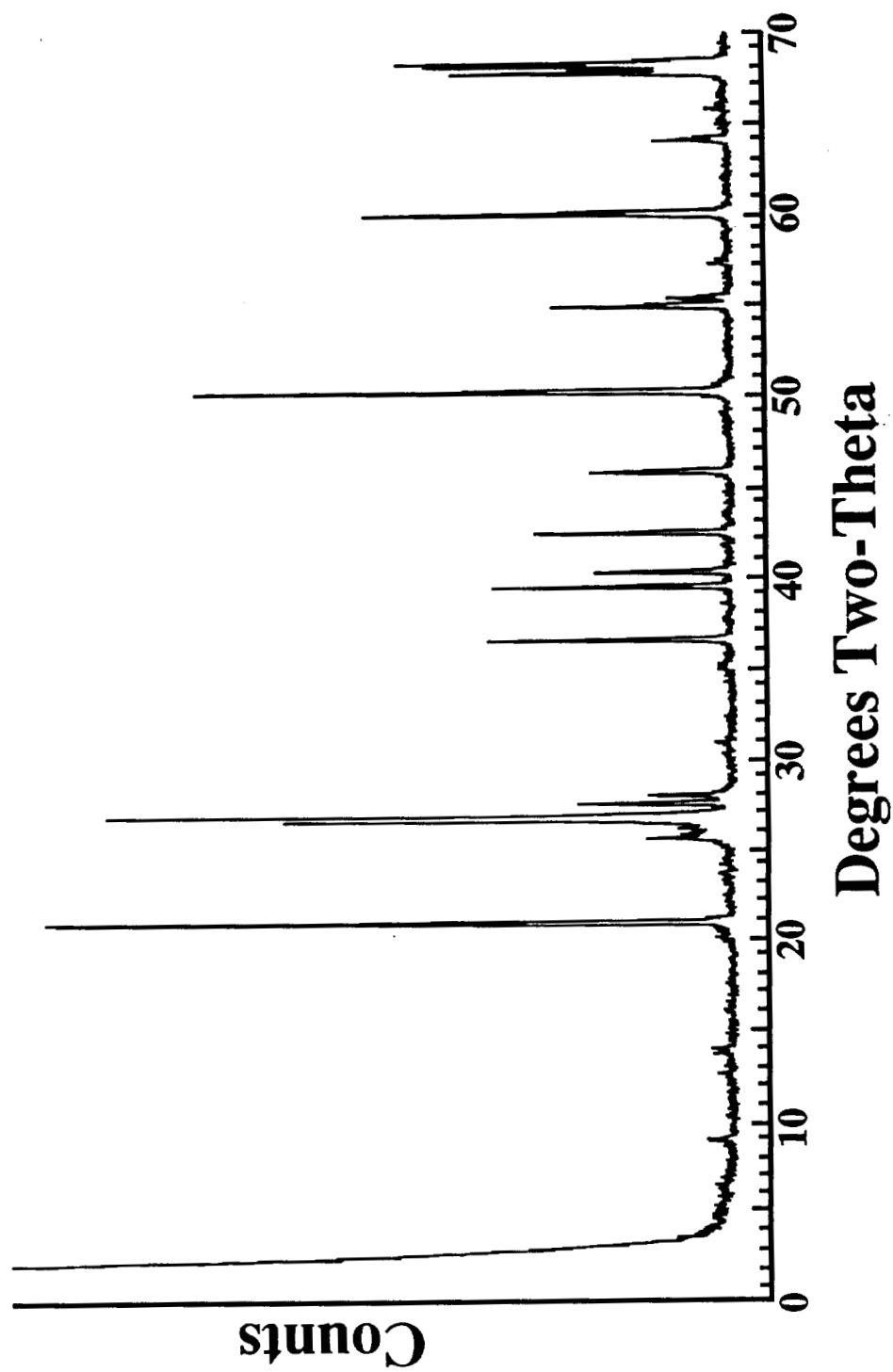
Because the model depicts steady-state conditions it overestimates the fluctuations of the water table with varying amounts of recharge. In real-life, transient conditions, the fluctuations will be dampened by water entering and being released from storage. As a result the effects on downgradient monitoring wells will be minimized.

Summary

Water quality samples from monitoring wells used to evaluate plumes in all of the conditions described above must be interpreted based on knowledge of local recharge rates and groundwater flow patterns, both of which contribute to the plunge of a plume. If recharge varies spatially, for example if a site is covered with asphalt or concrete, the migration of the plume will be controlled by factors other than recharge. The size of the residually contaminated zone that forms the source of the plume will affect plume thickness and therefore alter the most appropriate well design.

The size and migration of a contaminant plume is also controlled by other physical and chemical transport processes. Retardation will affect the rate at which each hydrocarbon compound moves through the aquifer. The plume will spread and thicken as a result of molecular diffusion and heterogeneities in the aquifer causing mechanical dispersion. These processes will help to smooth out differences in plume thickness caused by recharge fluctuations at the source. While these processes are occurring, the scale of changes they cause are small relative to those caused by mounding and water-level fluctuations, suggesting their role is not as significant in controlling the eventual depth and thickness of the plume.

Appendix B: X-Ray Diffraction Pattern for Sediment Sample B-25



Biographical Sketch

Mark E. Nelson was born on 7 August 1962 in Davenport, Iowa. He lived there for four years, and then spent the remainder of his cavity prone years in Waterbury, Connecticut and West Barnstable, Massachusetts. He attended Brown University in Providence, Rhode Island, graduating in 1984 with an Bachelor of Science degree with honors in Geology. Following Brown, Mark worked for three years with an environmental consulting firm on Cape Cod, focusing on the delineation of water resource protection areas and the investigation and cleanup of sites with contaminated groundwater. In 1988, he began his planned "1-year Masters program" at the Oregon Graduate Institute, which now comes to an end five years later with the completion of this thesis. In the interim, Mark has been a Senior Hydrogeologist with Horsley & Witten, Inc. in Barnstable, Massachusetts where he continues to manage a variety of groundwater projects including the delineation of wellhead protection areas, and investigations of groundwater contamination incidents. He also serves as an instructor for the US Environmental Protection Agency at workshops pertaining to groundwater protection and groundwater quality.